The sedimentation pattern of the last deglaciation and postglacial phase in a high-Arctic valley: Endalen, Spitsbergen

Stian Soltvedt

Thesis for
Candidatus Scientiarum Degree
in Sedimentology

Bergen
2000

Geological Institute
University of Bergen

UNIS

The University
Courses on Svalbard

ABSTRACT

The present study, focused in the valley-side gravel fans in the eastern part of Endalen and the adjoining side-slope of Adventdalen, has contributed to an understanding of the spatial pattern of the late Weichselian deglaciation and associated meltwater drainage in a 3rd-order and a 2nd-order valley and adjacent mountain plateau in central Spitsbergen, Norwegian high-Arctic. The author's fieldwork in 1998 was focused on the following main topics: (1) the mapping and chronology of postglacial sediment accumulations, with special emphasis on the development history and depositional processes of the valley-side gravel fans; (2) the snow-cover conditions on the valley-side slopes during the winter to autumn season 1998, including comparative photographic documentation and fixed-point snow thickness measurements; and (3) the assessment of the intensity, routes and controlling factors of the downslope transfer of sediment and water, including the recognition and spatial pattern of meltwater palaeoflow scours and their significance for the reconstruction of the ice-sheet retreat.

The analysis of infrared aerial photographs has proved to be very useful in deciphering the areal pattern of meltwater palaeodrainage and in the recognition of other glacial/postglacial geomorphic features. Arrays of surficial palaeochannels are recognizable on the eastern plateau of Endalen, trending NW and lacking any obvious water catchment today. These scours are attributed to the meltwater runoff during the early Holocene deglaciation. The morphological mapping revealed also relict late-glacial deposits in the form of a lateral moraine and several raised beach terraces near the mouth of Endalen, but no preserved glacigenic diamicton deposits have been recognized on the adjacent eastern plateau. Erratic cobbles and boulders have been found on western plateau, directly outside the Endalen drainage basin, which indicates that the mountain plateaux were covered by the glacier. Some long-transport erratics, derived probably from the eastern part of Spitsbergen, have also been identified in Endalen and on the valley's eastern slope. Based on the aerial photographs and direct field observations, a tentative spatial model has been suggested for the deglaciation of the Adventdalen area.

The valley-side gravel fans whose formation involved meltwater flow from the plateau are larger, associated with well-incised ravines and show two stories of deposits recognizable in geomorphic terms: a broad mound of older, vegetated base-of-slope deposits (alluvial fan), distinguished as sedimentation stage I, and a smaller, steeper accumulation of relatively fresh younger deposits (colluvial fan) superimposed onto the upper/apical part of the former and distinguished as sedimentation stages II and III. The three stages of deposition are interpreted as: (I) an early Holocene, early postglacial stage dominated by the meltwater runoff from the plateaux and coeval high-viscosity debrisflows on the mountain slopes between the ravines; (II) a middle Holocene stage dominated by rockfall processes and minor debrisflows; and (III) the late Holocene stage dominated by the more mobile, watery or slush-laden debrisflows. The low-viscosity debrisflows of stage III have commonly caused strong incision in the fan apex and upper segment, with channels up to a few metres deep and the associated intersection-point deposits making the fan prograde in a "telescoping" style and aggrade in the lower segment. The tripartite stratigraphy of the valley-side fans is thought to reflect the Holocene regional climatic changes.

The snow cover in the study area is generally sparse, due to the low precipitation in the Arctic desert, but the predominance of strong and variable winds renders them a key agent controlling the thickness distribution and local excessive accumulation of snow in Spitsbergen. In Endalen, the winter winds are capable of filling ravines with several metres of snow and forming large snow cornices, although no snow avalanches (nor any other active slope-waste processes) have been observed on the valley slopes during the weekly visits in 1998. Slope-waste processes are infrequent and highly episodic. Most of the snow cover seems to disappear due to the processes of sublimation and gradual melting, with the main phase of melting in the early June. The meltwater runoff from the mountain plateau is very limited and incapable of removing large amounts of debris from the ravines, except for the fine-grained sediment, rarely coarser than sand or perhaps granule to fine-pebble gravel. However, the percolating water almost certainly has the capacity to infiltrate the coarse, ravine-entrapped gravel with fine sediment, and this watery matrix might then lubricate the gravel mass and turn it into a debrisflow. The presence of slush in the ravines may have a similar lubricating effect on the cobbly to bouldery rockfall gravel that tends to accumulate in the steep bedrock ravine.

ACKNOWLEDGEMENTS

Bergen, 21.03.2000

Stian Soltvedt

CONTENT

1. INTRODUCTION

The present study, co-supervised by Dr. Ida Lønne and Prof. Dr. Wojciech Nemec, has been completed by the author within the framework of scientific co-operation between The University Courses on Svalbard (UNIS) and the University of Bergen (UoB). This thesis is a contribution to UNIS's regional project "Sediment transport during and after the last deglaciation and its effects on the development of a high-arctic landscape, Svalbard", led by the first supervisor.

The aim of this regional project is to study the dynamic relationships between landform evolution and sediment distribution in a high-Arctic drainage basin, the Adventdalen and tributary valleys (Fig. 1.1), with an emphasis on the physical processes and spatial pattern of
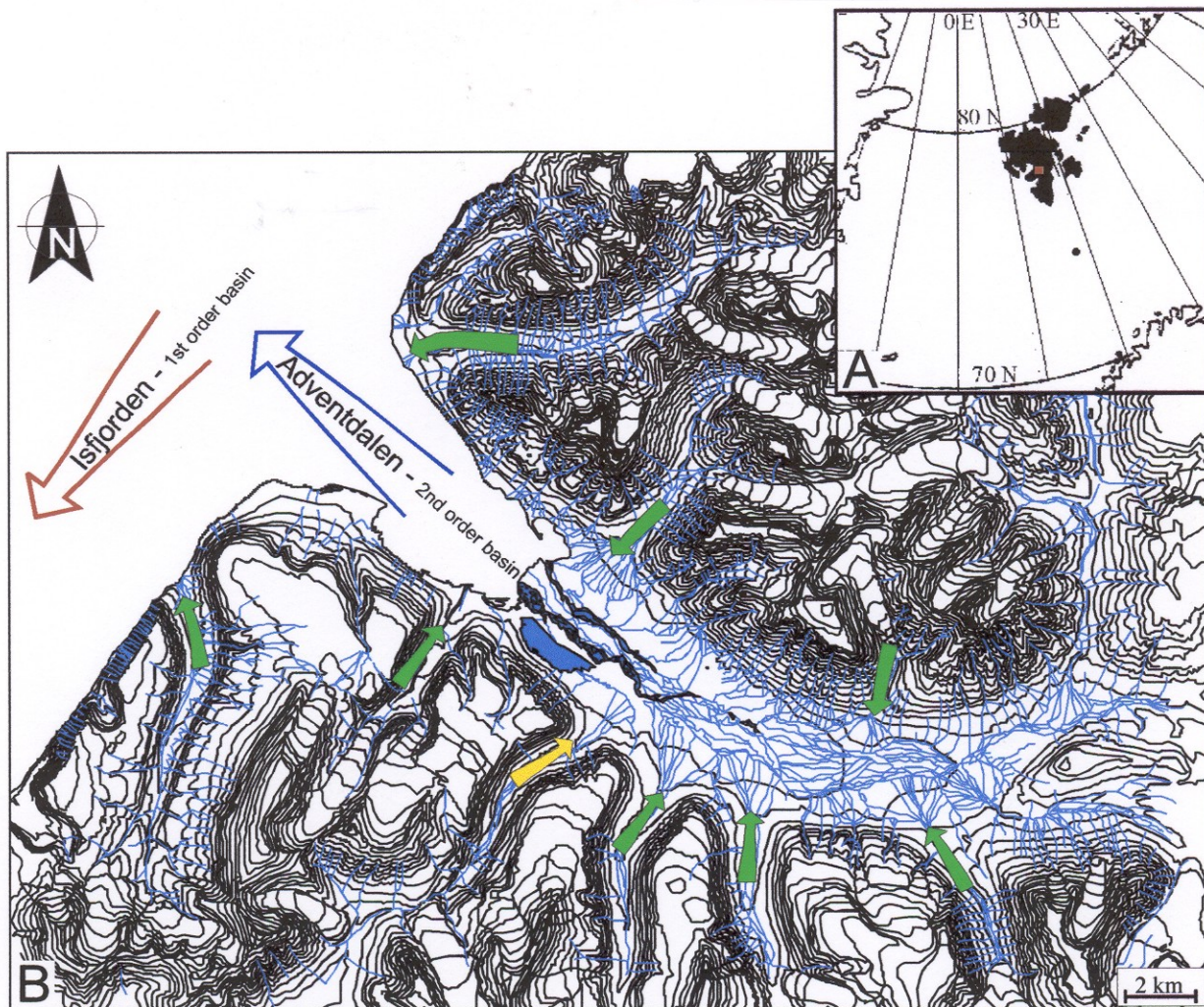
Fig. 1.1: **(A)** Locality map of the study area (show by red square) in the Svalbard archipelago, Norwegian high Arctic. **(B)** Details from the digitalized topographic map of Adventdalen, sheet C9 (Norsk Polarinstitut), showing the 1st- 2nd- and 3rd-order basins in the study area. The green arrows indicate the drainage direction from the 3rd-order basins. The yellow arrow represents the drainage from Endalen, whose eastern side has been studied by the present author. Contour intervals of the map is 50 m.

downslope sediment transfer during the postglacial period, and the relationship between these processes and the distribution and preservation of glacial landform features at high-Arctic latitudes.

Several decades of research on the west coast of Svalbard have yielded conflicting data and no conclusive evidence of glaciers having reached the shelf edge during the Late Weichselian maximum are found in terrestrial data (see review by Landvik *et al.,* 1998). Only recently, offshore studies have demonstrated, with the aid of seismic data and sediment cores, that the glaciers during the Late Weichselian maximum did occupy the large fjord basins of Svalbard and extended to the shelf edge, where large submarine outwash fans were deposited. The large 1st-order basins, such as Isfjorden (Fig. 1.1), were rapidly deglaciated between 15 and 10 ka BP. Although the regional pattern of the Late Weichselian to Holocene deglaciation of Svalbard is broadly known, the spatial-dynamic relationship between the deglaciation of the main, 1st-order basins and the smaller 2nd- and 3rd-order fjords and valleys is poorly understood. The aim of the aforementioned UNIS project is to improve our knowledge in this area.

The present thesis reports on the results of a detailed study of the syndeglaciational and postglacial sediment transport in Endalen, a 3rd-order tributary valley of Adventdalen (2nd-order basin) in west-central Spitsbergen (Fig. 1.1). The author's study was focused on the eastern side of Endalen, but included direct co-operation with Lægreid (1999), who studied concurrently the valley's western side. The field work included a number of systematic measurements and was carried out in March-September 1998, with a special emphasis on:

1. The mapping and chronology of the sediment distribution, downslope transfer routes and landforms, with the aid of aerial photographs.

2. The recognition and spatial pattern of meltwater palaeodrainage traces, and their significance for the reconstruction of the last deglaciation.

3. The development and depositional processes of the valley-side gravel fans, based on direct geomorphic and sedimentological observations combined with the analysis of aerial photographs.

4. The snow-cover conditions on the valley-side slopes during the whole melting to freezing season of 1998, including comparative photographic documentation and fixed-point snow thickness measurements.

5. The qualitative differences in the postglacial sediment dynamics in a semiarid high-Arctic valley and a morphologically similar sub-Arctic terrain, such as the southwestern Norway (studied by others).

2. THE STUDY AREA AND METHODS

2.1. Geographical setting

Spitsbergen is the main island of the Svalbard archipelago, Norwegian Arctic, and the present study has been focused on the area around Endalen in west central Spitsbergen (Fig. 2.1). Endalen is a NE-trending glacial valley, 300 to 400 m deep and ca. 6 km long. The valley floor spans an altitude range from 20 m (outlet) to 250 m (head zone), and is drained axially by Endalselva, a braided river collecting meltwater from three upvalley glaciers as well as the snowmelt water from the surrounding plateaux. The drainage area of Endalselva is ca. 30 km^2.
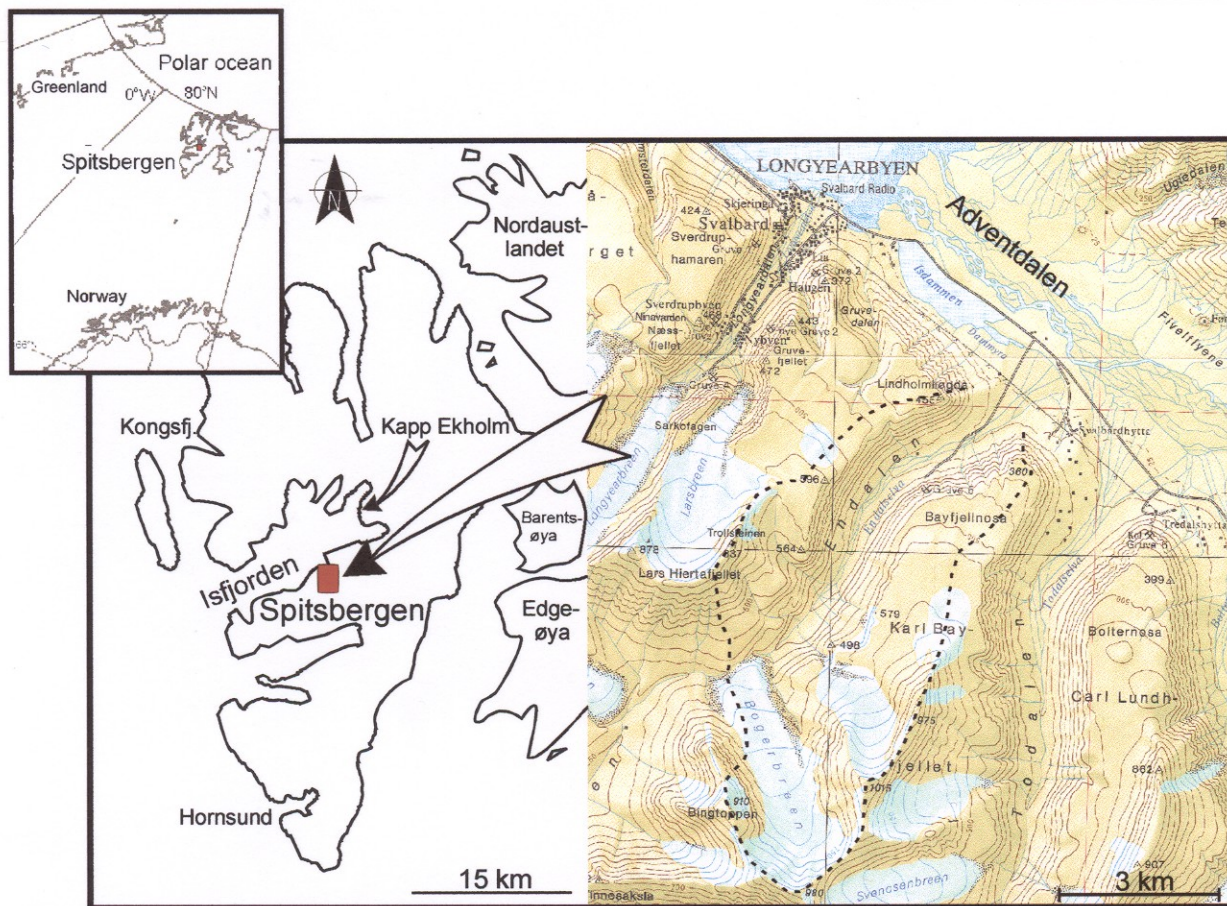
Fig. 2.1: Localitymap of Spitsbergen and a thopographic map of Endalen and it's surroundings in west-central Spitsbergen. The Endalen drainage basin is marked with a black stippled line.

The studied part of the basin has been divided into four areas (see labels A-D in Fig. 2.2). Area A is the adjoining side-slope of Adventdalen, north of Bayfjellnosa, between the outlets
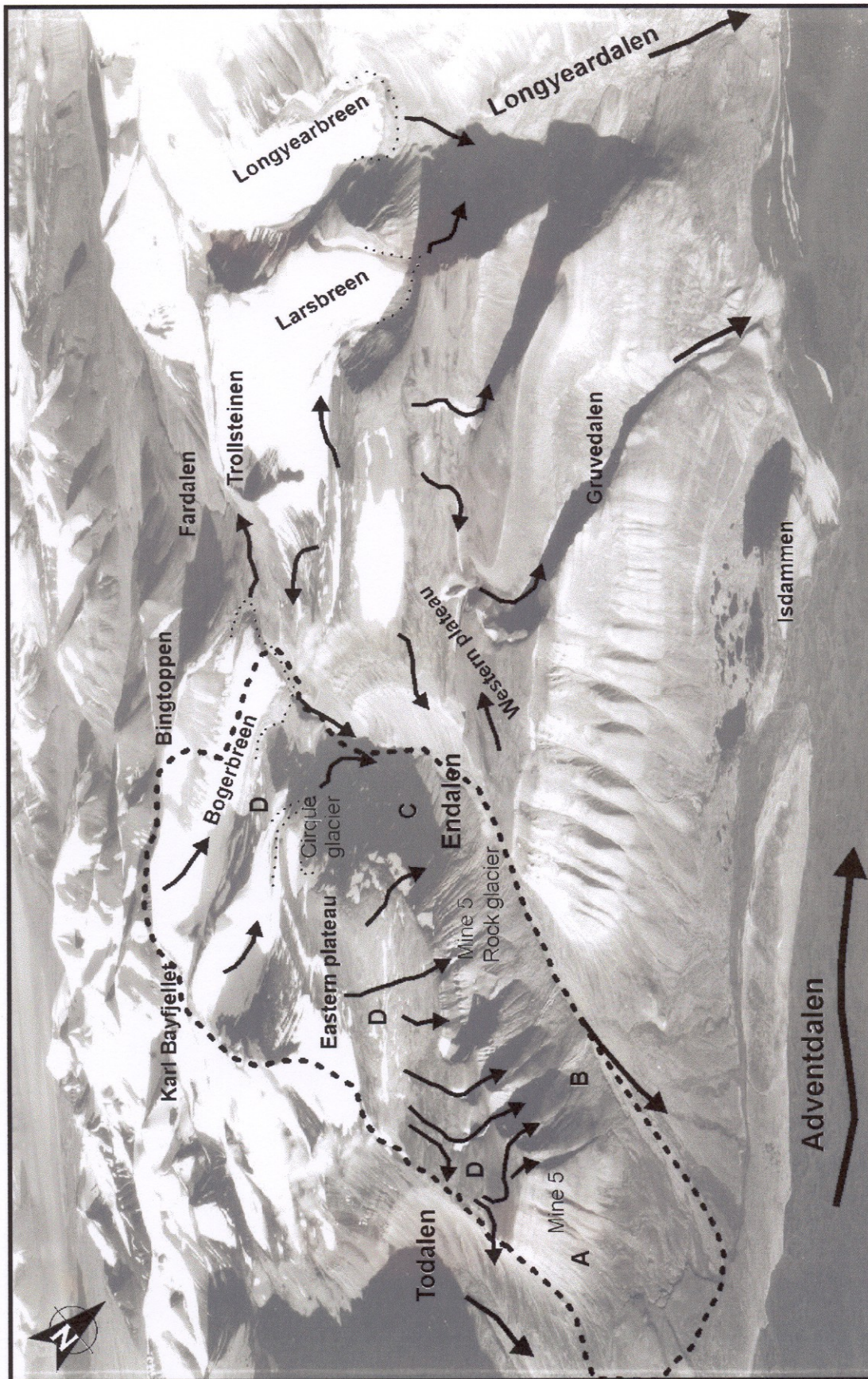
Fig. 2.2: Oblique aerial photograph, Norsk Polarinstitutt S-36 nr 2296, showing the study area (stippled), the present day drainage (arrows) and the terminal moraines of the Little Ice Age (fine-dotted lines). Labels A, B, C and D indicate areas referred to in the text.

of Endalen and Todalen. The gravel fans on this slope are referred to as fans A1 to A5 in further text. Area B is the eastern side-slope of Endalen, between the valley outlet and Coal Mine 5. The gravel fans associated with this outer part of the valley-side slope are referred to as fans Ee1 to Ee6 in further text. Area C is the inner valley-side slope of Endalen, between Coal Mine 5 to the Bogerbreen glacier in valley-head zone. Area D is the adjoining mountain plateau on the eastern side of the valley, between Endalen and Todalen. The plateau is at an altitude of ca. 500 m, and the surrounding valley-side slopes have mean inclinations in the range of 20 to 40 degrees.

2.2. Bedrock geology

Endalen is a U-shaped valley scoured in the subhorizontal succession of Cretaceous and Tertiary sedimentary rocks (Table 2.1). The fluviodeltaic sandstones of the Helvetiafjellet Fm. occur at the outer valley-floor level, whereas to the sandstone-rich Aspelintoppen Fm. constitutes the highest mountain peaks. The Carolinefjellet Fm. consists of marine mudshales intercalated with sandstone tempestites, and is separated from the overlying Palaeocene rocks by a large stratigraphic gap and slight angular unconformity (Major & Nagy 1972). The Palaeocene Firkanten Fm. is coal-bearing in the lower part, but dominated by quartz-rich arenitic sandstones in the upper part, which forms steep rocky slopes and cliffs. The mudshales of the Basilika Fm. are weathering into small prismatic chips and form gentler slopes (30-35º), whereas the overlying sandstones of the Grumantbyen Fm. form steep slopes and rockwalls. A similar topographic relationship is shown by the Eocene Frysjaodden Fm. and Battfjellet Fm. in the higher mountains south of the present-study area (Larsson, 1982).

Table 2.1: Stratigraphy of pre-Quaternary bedrock stratigraphy in Spitsbergen region (modified from Dallmann in press).

Age		Lithostratigraphic units	Rokcs and origin
TERTIARY	Oligocene		Alternating light grey to greenish sandstones, grey siltstones and darker shales of fluvial, lacustrine and estuarine origin.
		Aspelintoppen Fm.	
	Eocene	Battfjellet Fm.	Sandstones interbedded with shallow-marine to estuarine shales and siltstones.
		Bjørnsonfj. Mb. / Gilsonryggen Mb. / Marstranderbreen Mb. / Frysjaodden Fm.	Black and dark-grey silty marine shales weathering with sandstone wedges.
		Grumantbyen Fm.	Greenish- and grey marine sandstones.
	Paleocene	Basilika Fm.	Black marine shales.
		Kolthoffberget Mb. — Endalen Mb. / Firkanten Fm. / Todalen Mb.	Coal-bearing deltaic/eustarine shales, silt-stones and sandstones passing uppwards into waveworked deltaic sandstones
EARLY CRETACEOUS		Unconformity	
		Carolinefjellet Fm.	Marine shales with interbedded sandstones, tempestites
		Helvetiafjellet Fm.	Coal-bearing fluviodeltaic sandstones and subordiante mudstones

2.3. Modern climate

2.3.1. Climatic conditions

Svalbard's climatic conditions are classified as a high-Arctic semiarid desert, with a mean annual precipitation of 190 mm reported from the Longyearbyen airport area in 1961-1990 (Førland *et al.*, 1997). The same meteorological station, ca. 9 km west of Endalen, has reported a mean annual summer temperature of 4.3°C for June-August and a mean annual winter temperature of -14°C for December-February period (Førland *et al.*, 1997).

Glaciers cover about 60% of the Svalbard land-surface area, and the ground is perennially frozen. The permafrost layer is largely continuous and its thickness varies from 100 m to locally more than 400 m (Hagen *et al.,* 1993). The surficial active layer, subject to freeze-thaw cycles, is 30 to 150 cm thick (André, 1994). Permafrost features, such as stone rings, pingos and rock glaciers, are common. The vegetation cover is a typical tundra assemblage of mosses, flowers and grass, with sporadic occurrences of dwarf birch (*Betula nana)* in Spitsbergen. Due to the catiabatic effect of the glaciers and the deep, long and relatively narrow valleys, the winds here are generally strong. From October until March, some 15 to 20 days a month have wind with a power of 6 or more in the Beaufort scale. The strong winds cause major snowdrift, even though the overall precipitation is low. The average thickness of snow cover in March-May time is 19.2 cm (Førland *et al.*, 1997). The air temperature, wind and precipitation vary to some extent with the topography and valley trend, but the meteorological data from the Longyearbyen airport can serve as a reasonable approximation of the weather conditions in Endalen.

Relatively little is known, thus far, about the magnitude and variation of water runoff in this high-latitude region, and about the effects of flowing water on the sediment movement and landscape development. The surficial runoff in the high-Arctic is due to direct precipitation, the melting of glaciers and snowpack, and the melting of the active layer (Lønne, 1998a). The precipitation is generally low and rather difficult to measure due to the prevailing windy weather. Most of the precipitation in the Arctic occurs in the form of winter snowfall, when the high-speed easterly winds from the Barents Sea prevail and the conventional gauges are able to collect little more than a small fraction of the "true" ground-level precipitation (Førland *et al.*, 1997). The effect of late-summer rainstorms on the sediment movement on mountain slopes is better known, and is well-recognized in Longyeardalen and some of the adjacent valleys. The summer melting of the glaciers boosts the water and sediment discharge of the valley-axis rivers and affects the deltas, but does not seem to play any significant role in the sediment transport on the mountain slopes. However, the conditions were probably quite different during the last deglaciation, when the meltwater runoff must have been enormous and the fluvial drainage was extensive and poorly confined.

The snow cover in the modern climatic conditions is thin and discontinuous, and the bulk of the snow melts within a couple of weeks. The snowmelt thus has a short-lived effect and does not contribute much to the landscape changes. The permafrost and bouldery talus debris generally hinders deep erosion. However, the runoff effectively washes fine grained sediments, possibly up to granule gravel, into the mountain slope ravines, causing its transient

storage, and the wind-drifted snowpack in the ravines may often be thick and trigger debrisflows. The melting of the active layer contributes little to the sediment transport as such, but in combination with rainstorms, can cause slope failures and debrisflows. The latter processes seem to be most important in the geomorphic evolution of the valley-side slopes and the general transfer of sediment to the valley floor. In short, the effects of meltwater runoff as well as the impact of rainstorms may vary in a valley, depending upon the time of occurrence and the type and state of substratum.

2.3.2. Modern glaciers

The most dominating glaciers on Svalbard are the large continuos ice masses divided into separate ice streams by mountain ridges and nunataks. Several large ice caps are located in the eastern flat parts of Svalbard at Edgøya, Barentsøya and Nordaustlandet (see Fig. 2.1), but numerous smaller valley and cirque glaciers are present in the more alpine western parts of Spitsbergen. Ice shelves do not occur on Svalbard because all glacier fronts terminating in the sea are grounded (Hagen *et al.*, 1993).

Most of the present-day glaciers in the Svalbard region belong to the subpolar or polar category, and many of them are surging glaciers (Hagen *et al.,* 1993). Although Hagen *et al.* (1993) have suggested that 90 % of the Svalbard glaciers are subject to surging, the more recent estimate by Hamilton & Dowdeswell (1996), based on 615 glaciers (30 % of the total population), indicates only 36.4 % are probably surge-type glaciers. Glacier surging may be an important factor contributing to the sediment transfer from the mountains to the valleys and fjords, playing a major role in the development of modern glacial landforms.

As recognized by Lehman & Forman (1992), the subpolar and polar glaciers can override valley-floor deposits without eroding much sediment or depositing a till mantle (see also Landvik *et al.,* 1998). In contrast, a surging glacier commonly incorporates large amounts of substratum debris in the basal ice. The debris becomes concentrated and progressively transferred to the surface along the internal thrusts, forming transverse ridges at the glacier surface. The development of such debris-rich thrusts may explain the hummocky moraine ridges commonly formed by melting surging glaciers (Hambrey *et al.*, 1996).

2.3.3. The Quaternary glaciation of Svalbard

Three major glaciations have been recognized in the Svalbard region, based on the Kapp Ekholm outcrop section in Billefjorden area (Mangerud & Svendsen, 1992; Mangerud *et al.*, 1998; Landvik *et al.*, 1998). The ice-cap is thought to have reached the continental shelf west of Spitsbergen during the shorter maxima of these three stages (Fig. 2.3). There are few other extensive stratigraphic sections of glacial deposits in onshore Svalbard. The majority of the valleys have their floors covered with glaciofluvial deposits and the sides mantled with slope-waste aprons, which means that the glacial deposits and landforms have been strongly obliterated or virtually erased by erosion. In practice, only the youngest features of the last glaciation are recognizable and only in a few areas.
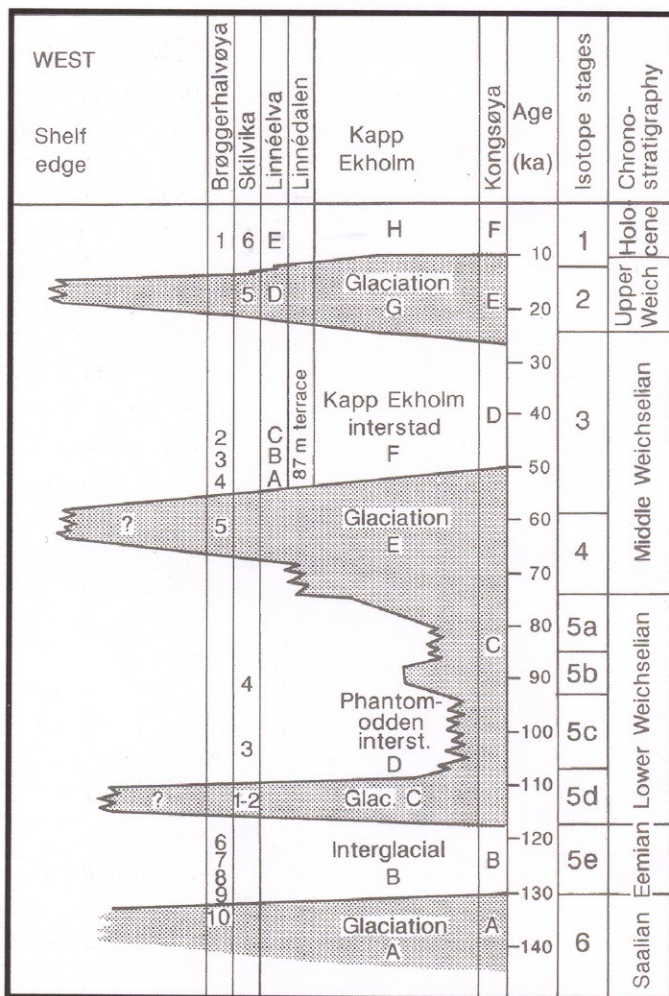
Fig. 2.3: The glaciation curve from the Northern Barents Sea and Svalbard, based on onshore sections in Svalbard (Mangerud *et al.*, 1998).

The regional reconstruction of the last glacial stage is based chiefly on the Kapp Ekholm section (Mangerud & Svendsen , 1992), but supported by data from other areas (see Landvik *et al.*, 1998; Mangerud *et al.*, 1998). Svalbard is thought to have been covered by the Barents

Sea ice-sheet, about 800 m thick in western Spitsbergen and as much as 1500-2000 m thick in the eastern part of Svalbard (Lambeck, 1995). Although it is widely accepted that the ice-sheet extended to the shelf break west of Isfjorden, the thickness of the ice is still debated and some researchers argue that the late Weichselian glacier could only reach the shelf through the large fjords (Andersson *et al.*, 1999). The latest studies concerning the eastward extent of the late Weichselian ice-sheet suggest that the latter terminated in the Pechora Sea and Kara Sea region, with much of the Russian Arctic remaining ice-free (Astakhov, 1999; Mangerud *et al.*, 1999; Svendsen *et al.*, 1999; Tverranger *et al.*, 1999). The lack of reliable dating methods extending beyond the resolution of the conventional radiocarbon technique is a major problem, although some newer techniques, such as the cosmic radiation analysis of rocks, seem to be promising and may possibly be utilized in the near future.

The Barents Sea region was covered with a large ice-sheet that extended westwards over Svalbard and reached the continental-shelf margin west of Spitsbergen during the Late Glacial Maximum (LGM) ca. 22 to 19 ka BP, until the onset of the deglaciation ca. 15 ka BP Landvik *et al.*, 1998). The deglaciation of the Barents Sea region was relatively rapid, probably due to the glacier calving in the deepest parts, and the region is thought to have already been ice-free by 12 ka BP (Fig. 2.4).
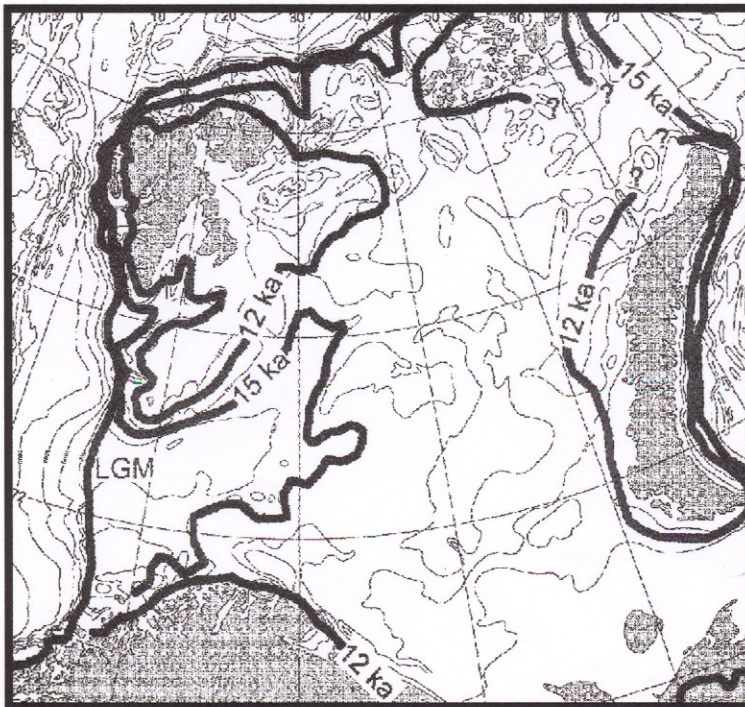
Fig. 2.4: Reconstruction of the Late Weichselian ice-front positions of the Barents Sea Ice Sheet. LGM= Late Glacial Maximum (Landvik *et al.*, 1998).

The deglaciation of the western margin of Spitsbergen was interrupted by a local readvance culminating shortly after 12.4 ka BP. During the Younger Dryas, outlet glaciers draining the

remnants of the ice-sheet still occupied the inner fjords (Landvik *et al.*, 1998), which were then rapidly deglaciated around 10 ka BP (Svendsen *et al.*, 1996).

The glaciation and climatic changes in the Svalbard region are generally correlative with the glacial history of northwest Europe. The deglaciation occurred in a stepwise fashion, accelerated by two episodes of climatic warming around 12.5 ka and 10 ka BP. No field evidence of a major cooling or glacier readvance in the Younger Dryas time has thus far been found, but Svalbard is located north of the latitude where the oceanographic changes in the North Atlantic regime caused the largest Allerød/Younger Dryas temperature amplitudes (Fig. 2.5). The thermal maximum occurred in conformity with the climatic change in the northern Europe, from 10 ka to 4.4 ka BP, and so did the subsequent cooling that began around 4 ka BP and culminated in the Little Ice Age. This youngest advance is represented by the fresh-looking ice-cored moraine ridges fronting the modern glaciers (Svendsen & Mangerud 1992; 1997; Birks *et al.*, 1994).
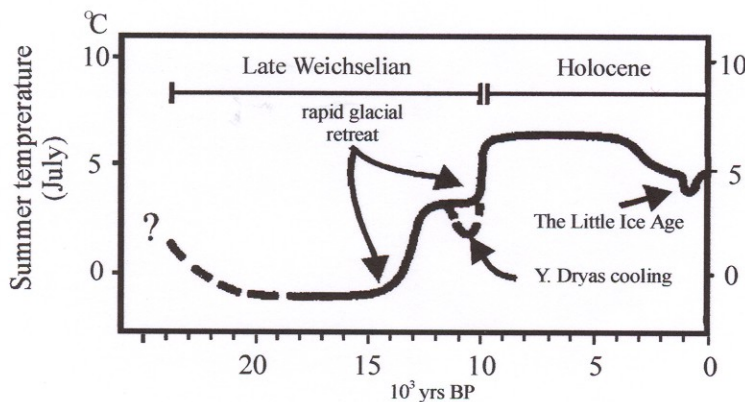
Fig. 2.5: Estimated summer air temperatures in Isfjorden, Western Spitsbergen during the last 20,000 years (Svendsen & Mangerud, 1992).

2.4. Methods and terminology

2.4.1. Mapping

The study area has good aerophotographic coverage, and this extensive documentation, made available by Norsk Polarinstitutt, has been examined in detail prior to the fieldwork and used further for the mapping of surficial features. The Svalbard 1990 aerial photograph series has mainly been used, including black-and-white and infrared pictures in 1:50 000, 1:15 000 and

1:7000 scale (in the infrared aerial photographs, red colors indicate a vegetation cover). In addition, oblique aerial photographs from 1936 have been studied for comparative purpose.

The aerial photographs have been scanned on a HP desk-scanner with a resolution range of 300-600 dpi (dot per inch) and further processed using CorelDraw-8 software. Enlarged prints of these images have been used for the detailed mapping of surficial features during the field season.

Due to the lack of a good age curve for lichens, lichenometric observations are only mentioned to give an impression of the relative age of the deposits in the form of old or fresh. A more extensive mapping, like in André (1986) is needed to be able to use lichenometry as a dating method in the area.

2.4.2. Measurements of snowpack thickness and mountain-slope profiles

In order to assess the snow accumulation and melting conditions on the valley slopes in the study area, the thickness of the snow cover has been measured systematically at a number of fixed points during the winter season (March-May) in 1998. The thickness of the winter snowpack on two selected valley-side fans, one in Endalen (fan Ee3) and the other on the adjoining slope of Adventdalen (fan A5), has been measured with a scaled iron rod at 10 m spacing along a fixed downfan profile. The measurement points for week-by-week observations were fixed, with the accuracy of a 50 cm radius, using bamboo sticks and a 10 m rope. Despite this limited accuracy of the measurement point location, the data are considered to be representative in general terms and satisfactory as a basis for the recognition of possible downslope trends in snowpack thickness.

The morphometric profiles of the valley-side fans and mountain slopes are difficult to derive from the existing topographic maps, whose scales range from 1:100 000 to 1:1 000 000 and the elevation differences shown are no more detailed than 50 m contour lines. The gradient of the lower part of the valley-side slope was thus measured directly in the field, using a portable Sokkia Electronic Total Station (SETS). The longitudinal morphometric profiles of several valley-side fans and the mountain slope between some of them have been measured. The SETS data have been electronically processed and displayed graphically with the use Microsoft Word Excel and CorelDraw-8 software. The accuracy of SETS data depends upon the number of the measurement points used to establish a profile (smoothed curve), but the scale of data display in the present cases renders the error negligible. Some

morphometric profiles have been measured also manually, by walking an upslope traverse and using a Silva compass, Suunto clinometer, a 50 m measuring tape and a digital altimeter.

2.4.3. Clast fabric measurements

Clast fabric is a useful criterion for distinguishing deposits of cohesive high-viscosity debrisflows, characterized by internal "rigid-plug" regime (Johnson, 1970), from those of low-viscosity debrisflows, rich in watery matrix or containing wet snow/slush (Lawson, 1982; Blikra & Nemec, 1998). The latter tend to have an orderly, much better organized fabric, in addition to the characteristic scour-and-tongue morphology and possible upslope fining of debris.

The fabric, or spatial orientation, of gravel clasts has been measured in several of the fresh debrisflow deposits on the valley-side fans. The measurements were limited to the surficial part of the gravel lobe, and the local "samples" consisted of the azimuthal orientation of the long (*a*) axis of 50 randomly selected clasts, 10 to 50 cm in size, measured with a Silva compass within a small sampling area (ca. 3-4 m^2). Each sample was summarized in the form of a rose diagram (circular histogram) for comparative purposes. The dip direction and angle of the clast *a-b* planes was not taken into account, because the fan slopes are fairly steep and the clasts are often subvertical and their dip direction apparently accidental.

Another, more rapid technique used to measure the clast fabric of debrisflow lobes involved an orthogonal photographing of the portions of a lobe surface from a 4 m high two-arm (standing) ladder. The azimuthally oriented photographs were scanned and processed semi-manually on the computer screen with the use of CorelDraw-8 software, and the digitalized data sets (30-50 clasts per ca. 4 m^2 area) were plotted as rose diagrams using EZ-Rose software (Baas, 2000). The processing procedure was relatively simple: on the screen image of a photograph, straight-line segments were drawn electronically to represent the clast *a*-axes, whose azimuthal orientation was automatically recorded and the whole data set automatically processed for graphical display (rose diagram) and statistical evaluation. The latter included the calculation of vectorial statistics and a statistical test for preferential (non-isotropic) fabric.

2.4.4. Clast roundness analysis

The roundness of clasts is an important aspect of the textural maturity of sediment. For example, a well-sorted gravel comprised of rounded clasts typifies beaches. Gravel with subrounded to rounded clasts and moderate sorting may likely be fluvial, or represent glacial outwash. A poorly sorted gravel comprised of both angular and (sub) rounded debris indicates "textural inversion" (*sensu* Folk, 1968) and may be a product of resedimentation, or mixing by slope-waste processes.

The roundness of debris in a range of gravelly deposits in the study area have been studied on the basis of samples comprised of 100 clasts, 16-32 mm in size (*a*-axis length), and using Krumbein's (1941) semi-quantitative visual scale of roundness. The so-called "half-rounds" (broken rounded clasts), when encountered, where categorized as if they were unbroken, because the fragmentation in the present case is mainly secondary, due to frost shattering. The samples included fresh debrisflow gravel, a presumed moraine gravel and an inferred palaeobeach gravel.

2.4.5. Terminology

The descriptive terminology used by the author for gravel characteristics, including clast fabric notation, is after Blikra & Nemec (1998).

Colluvium is a general term for slope-waste deposits, which are typically coarse grained and texturally immature, but may involve resedimentation of some pre-existing rounded debris. Colluvial fans and aprons are associated with mountain slopes of 15-45°, dominated by avalanches. An *avalanche* is a rapid movement of a wet or dry rock debris, snow, or their mixture, occurring on a steep slope. Colluvial avalanches include rockfalls, debrisflows (possibly snow-bearing), snowflows and occasionally some slides of rock or debris (Blikra & Nemec, 1998).

Rockfall is the gravitational movement of clasts that fall from a steep headwall and proceed downslope by bouncing, sliding and rolling. Rockfall debris is typically very angular, but may show some sorting, or size segregation, in the downslope direction. Larger bedrock failures may in some cases form cohesionless debrisflows, rather than rockfalls, if the concentration of debris is high and clast collisions are important (Blikra, 1994; Blikra & Nemec, 1998).

Debrisflow is a plasticoviscous rheological type of sediment-gravity flow, defined as a gravitational movement of a shearing, highly concentrated, yet relatively mobile, mixture of debris and water. Some debrisflows may be dry, whereas some others may involve an admixture of wet snow or slush.

For the convenience of description and easier reference, a colluvial fan is divided into *segments* (upper, middle, and lower) as well as *sectors* (Fig. 2.6). The *left-hand* and *right-hand* sectors are distinguished with respect to the downfan, or downflow, direction.
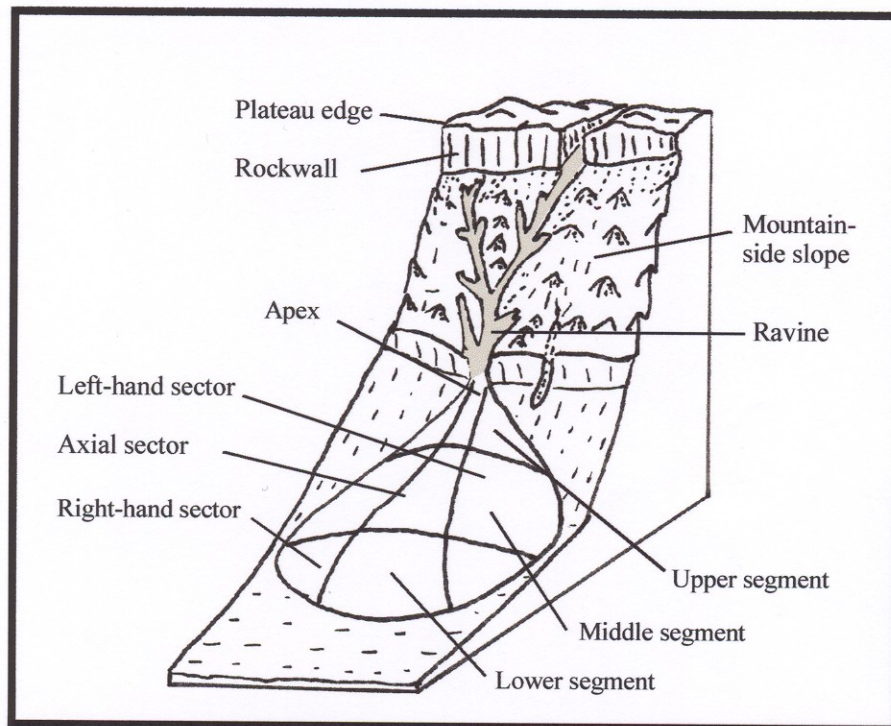
Fig. 2.6: Explonatory sketch for the descriptive terminology used in the present study. Note that the fan sectors are defined relative to the sediment transport direction (Modified after Eisbacher & Clague, 1984).

3. MORPHOLOGY AND SEDIMENTARY DEPOSITS

OF THE EASTERN SIDE OF ENDALEN

This chapter is a review of the main geomorphic features and sedimentary deposits recognized on the eastern side of Endalen (Fig. 3.1A), based on the author's field study combined with an extensive analysis of the aerial photographs, including infrared images.

3.1. The Endalen drainage basin

The Endalen drainage basin has an area of about 30 km^2. Nearly a third of this area (ca. 8 km^2) is covered by the three glaciers located in the head part of the valley (Fig. 3.1A), and the remaining part comprises large portions of the adjoining mountain plateaux to the east and west (ca. 8 km^2) the steep valley-side slopes (ca. 11 km^2) and the gently N-NE-inclined valley floor (ca. 3 km^2). These different parts of the drainage basin and their specific elements are discussed in the following sections. The geomorphological details are summarized in the photogrametric sketch-map of the present drainage pattern shown in Figure 3.1B, compiled from a hand-tracing study of 14 aerial photographs and verified by direct field observations.

3.2. The eastern plateau

The area of the eastern-side mountain plateau that is drained into Endalen and the adjoining Adventdalen is referred to broadly as **area D** (Fig. 2.2), but divided further into three subareas, labelled **DI, DII** and **DIII** (Fig. 3.2), for the purpose of describing morphological variation of the plateau.

3.2.1. Subarea DI

This part of the plateau is drained into the Endalen basin, with the exception of the narrow marginal zone at the plateau's northeastern edge, drained into Adventdalen (Fig. 3.1B & Fig. 3.3). The bedrock are sandstones of the Firkanten Fm. overlain by the Basilika Fm. shales (see Table 2.1), all fractured and heavily shattered by frost. The surficial sediment varies from
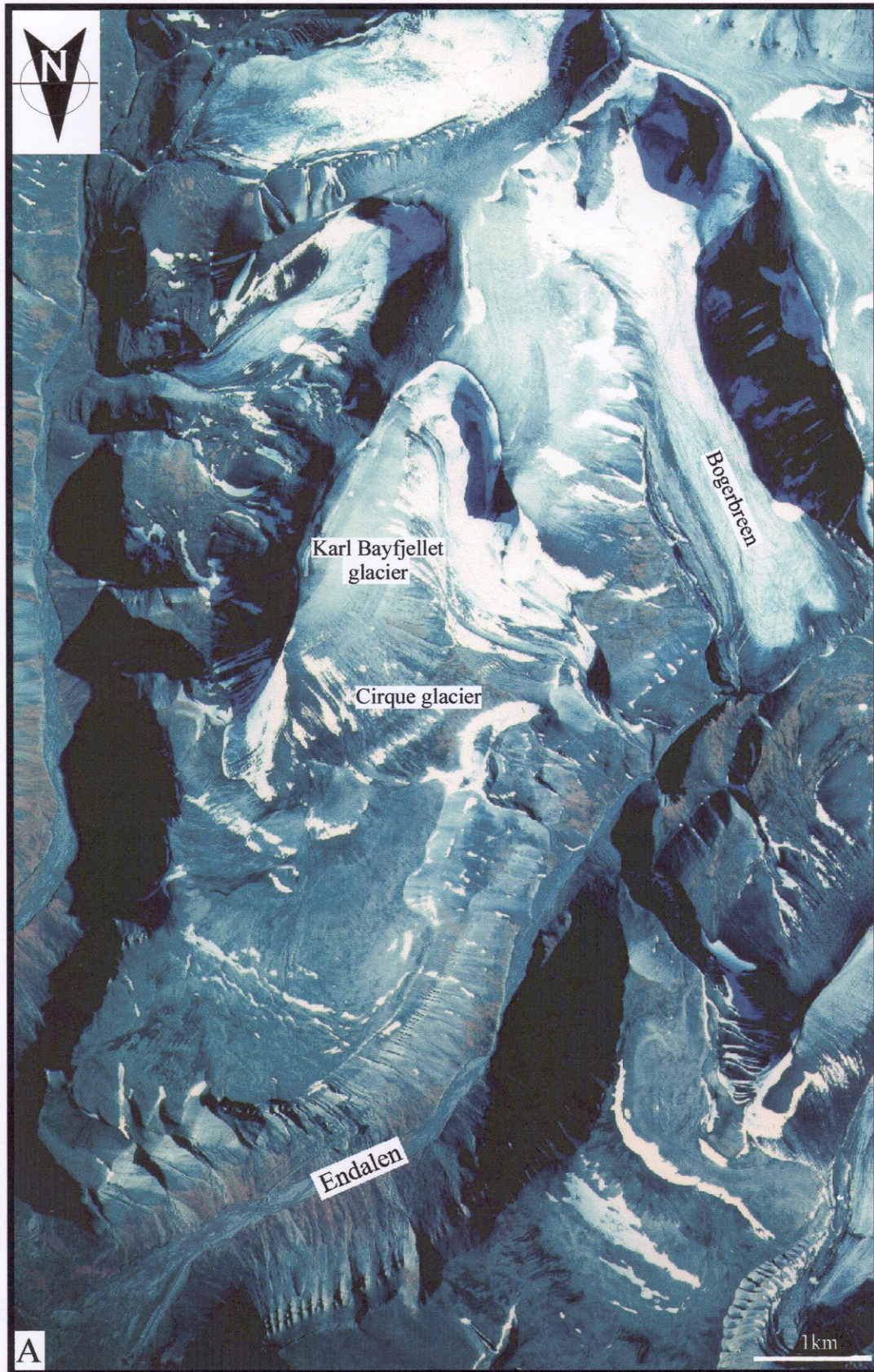
Fig. 3.1A: Aerial photograph S-90 3430 (1:50000), showing the Endalen drainage basin with adjacent glaciers.

Fig. 3.1B: Photogrammetric sketch of the Endalen drainage basin, based on a mosaic of 14 aerial photographs with approximate scale 1:15000 (S-90 5337, 5338, 5339, 5407, 5408, 5409, 5410, 5411, 5412, 5469, 5470, 5471, 5472 and 5473, Norsk Polarinstitutt). Made in co-operation with A.K. Løgreid and modified from Løgreid 1999. The postglacial sediment transport is in this figure illustrated by tracing of the meltwater drainage pattern from the plateaux, over the plateau edge, into the ravines and further out into the 3rd-order Endalen basin, where deposited as gravel fans or further transported out in Endalselva. The plateau drainage pattern controls the mountainside morphology where drainage enter the valley in ravine escarpments. Few remnants of late glacial morphological features are visible today, but an attempt has been made to color this sketch combining a rough geomorphological interpretation of the main surface sediments with the sediment transport.
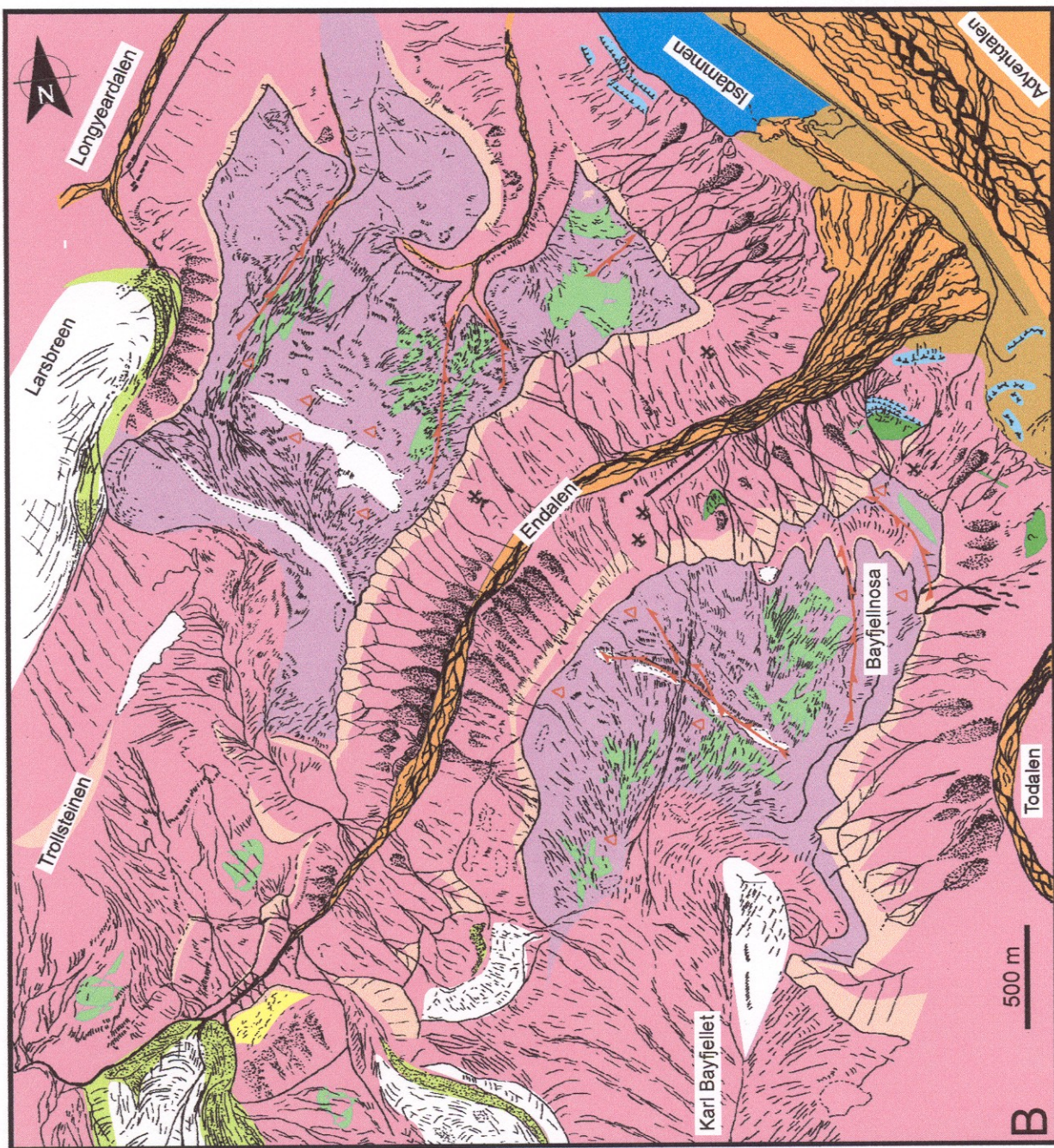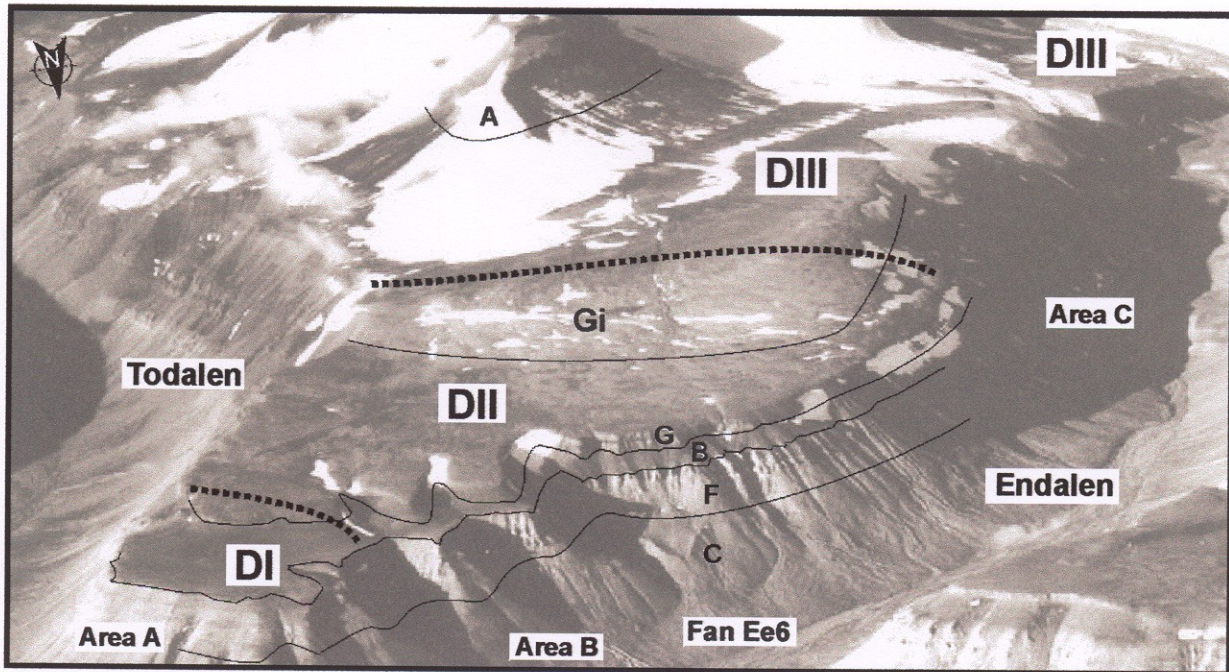
Fig. 3.2: The eastern mountain plateau in Endalen divided into subareas DI, DII and DII by dotted lines. The bedrock stratigraphy units are separated by black lines: C= Carolinefjellet Fm.; F= Firkanten Fm.; B= Basilika Fm.; G= Grumantbyen Fm.; Gi= Gilsonryggen Mb. of the Battfjellet Fm.; A= Aspelintoppen Fm. Area A, B and C pertain to the valley-side slope. Oblique aerial photograph (Norsk Polarinstitutt S-36 2296).

"block fields" of openwork angular sandstone debris of cobble to boulder size, characteristic of the plateau margin, to a mixed assemblage of sand- or mud-supported gravel, rich in subrounded to rounded pebbles and cobbles along the SE-trending topographic ridge which constitute the water-shed in the more central part of the plateau (Fig. 3.3A). The lower-lying, subhorizontal portions of subarea DI are thinly covered with tundra vegetation, but locally show a frost-shattered barren bedrock, notably in the catchment "crown" parts of the adjoining steep slope's ravines.

The plateau is perennially swept by strong winds and has little potential to accumulate any thick snowpack during the winter, as confirmed by the present author's field observations in 1998 (next chapter). The block-field edge zone is slightly higher than the adjoining part of the plateau to the south, and there is no morphological indication of any pronounced surficial drainage across this zone. The coarse openwork gravel entraps some snow in the winter, but the meltwater apparently percolates through the gravel without establishing any surficial conduits.

The winds sweep also rock cliffs and often carry abundant silt and fine sand, in addition to ice crystals. However, the roundness of gravel in large parts of the plateau cannot be attributed to surficial aeolian abrasion, because: (a) the clasts have clearly been abraded all around, not just at their exposed upper surfaces, ventifact fashion; (b) the rounding is by no
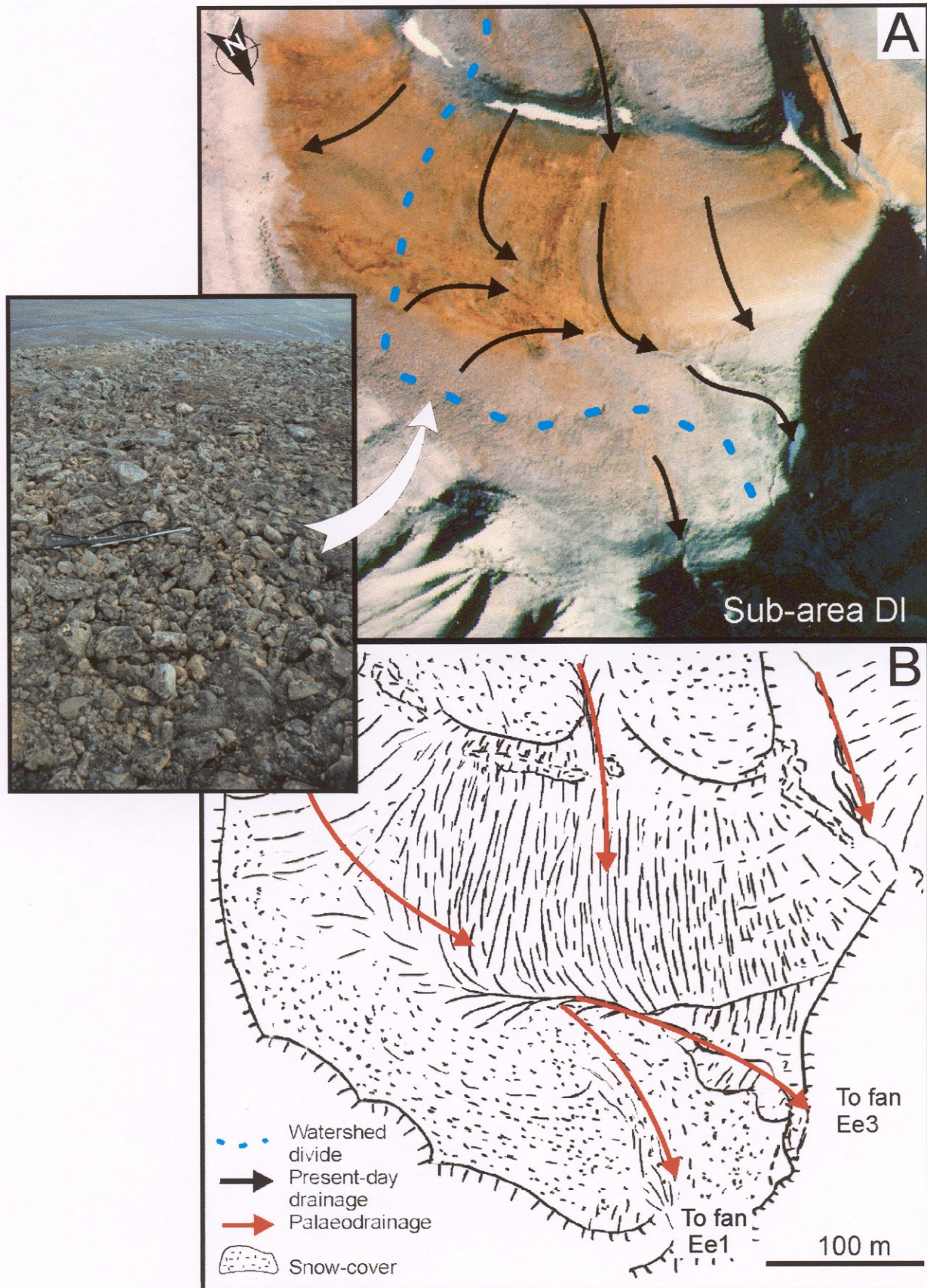
Fig. 3.3:(A) Aerial photograph (Norsk Polarinstitutt, S-90 5409), showing the present day drainage (black arrows) and the water-shed divide (dashed blue line). Note the ridge that defines the water divide. The insert photo shows the surface sediments comprising rounded pebbles and cobbles. **(B)** Interpretation of the drainage pattern based on the aerial photograph with the red arrows indicating the inferred paleodrainage pattern.

means limited to the protruding surficial clasts, but shown also by the sheltered and subsurficial clasts; and (c) no similar rounding is shown by the block-field debris, although the latter is far more predisposed to wind abrasion. Furthermore, the bedrock is practically devoid of gravel component, which implies that the rounded gravel must have been derived from elsewhere, especially since the debris are mainly bedrock fragments. The surficial patches of rounded gravel are thus interpreted to be the subglacial or proglacial depositional relicts of the last glaciation, with the roundness of clasts due to the associated waterflow processes.

The plateau surface in subarea DI is generally smooth and shows few signs of scouring by flowing water, except for one isolated NW-trending abandoned channel in the central part (Fig. 3.3B), apparently formed at an earlier stage of abundant meltwater runoff. At the north-western corner of the plateau, a couple of channel-like gullies can be traced to the slope-ravine catchments of fans Ee1 and Ee3 in subarea DII (Fig. 3.3B), although these low-relief features are admittedly easier to recognize in the aerial photographs, than in the field. No similar drainage features are recognizable at the Adventdalen margin of the plateau (Fig. 3.3). The relatively flat and vegetated surface of the inner part of the plateau shows little evidence of significant modern runoff, as is indicated also by the local development of weak soil polygons and stone stripes due to the perennial thawing of the active layer.

3.2.2. Subarea DII

The plateau surface in the northeastern part of subarea DII consists mostly of *in situ* frost-shattered shale partly covered by vegetation (Fig. 3.4). The Tertiary rocks are dipping at a low angle towards the southwest, whereas the plateau surface is gently inclined towards the north. About 200 m away from the northern edge of the plateau, the Firkanten Fm. is overlain by the Basilika Fm. and Grumantbyen Fm., consisting of shales interbedded with siltstone and sandstone (Major & Nagy, 1972). These interbeds form topographic steps at the surface. Poorly developed tor-like features are recognizable in this area. Similar larger features are commonly also observed on the mountain side slope between ravines and on the mountain ridges between several valleys in the Adventdalen area. Tors are not previous described in Svalbard, and due to the high erosion rate in the Tertiary sandstones on Spitsbergen, they are interpreted to have been formed in postglacial time.

The outer zone of subarea DII lacked a snow cover in the winter of 1998 and show a
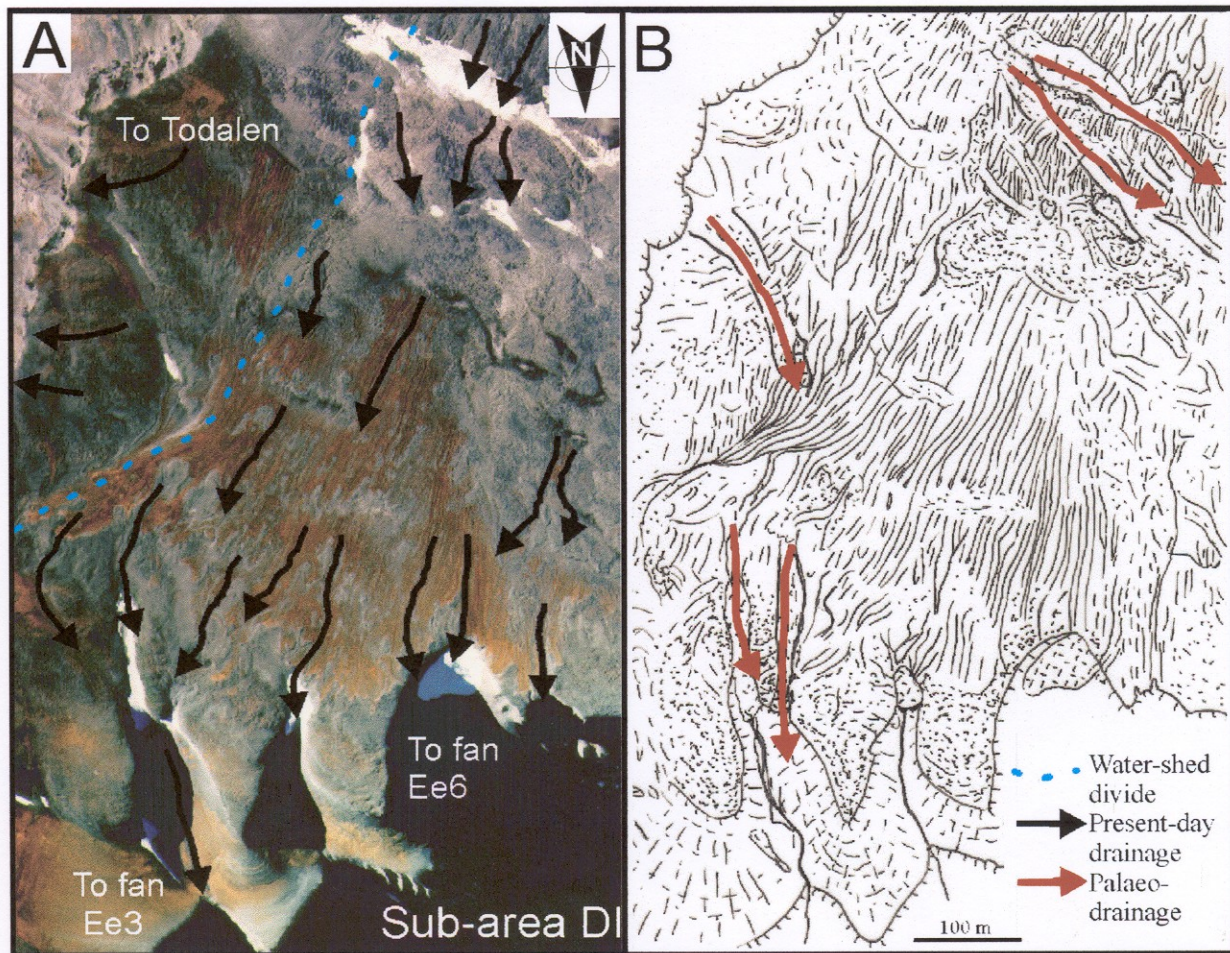
Figure 3.4: The drainage pattern is seen on the infrared aerial photograph A and this is further shown in B where the red arrows marks the interpreted palaeodrainage channels.

block field area in a sandy/gravelly matrix, but the central part hosted a thin snowpack covering the more *in situ* frost shattered silt- and sandstones. The central part of subarea DII is vegetated and the modern drainage pattern is readily recognizable in infrared aerial photographs (Fig. 3.1B- 3.4A). The meltwater from this area is mainly drained towards Endalen through three large ravines cut in the Basilika Fm., Firkanten Fm. and the uppermost Carolinefjellet Fm. leading to colluvial fan Ee3, Ee5 and Ee6. The altitudinal distance from the plateau edge to the ravine-fed fan apices is about 300 m. In the eastern part of subarea DII possible palaeochannels of a NW-SE orientation are interpreted from aerial photographs linked to the colluvial fan Ee3 (Fig. 3.4B). The channels are difficult to recognize and are not traced continuously over the plateau in field.

The northwestern part of subarea DII is covered with sandy/gravelly deposits with some cobbles and small boulders and is sparsely vegetated (Fig. 3.5). Most of the runoff percolates through the gravel, but some N-trending linear scours are recognizable in the aerial photographs. During the snowmelt period in 1998, three waterfalls were active at the plateau
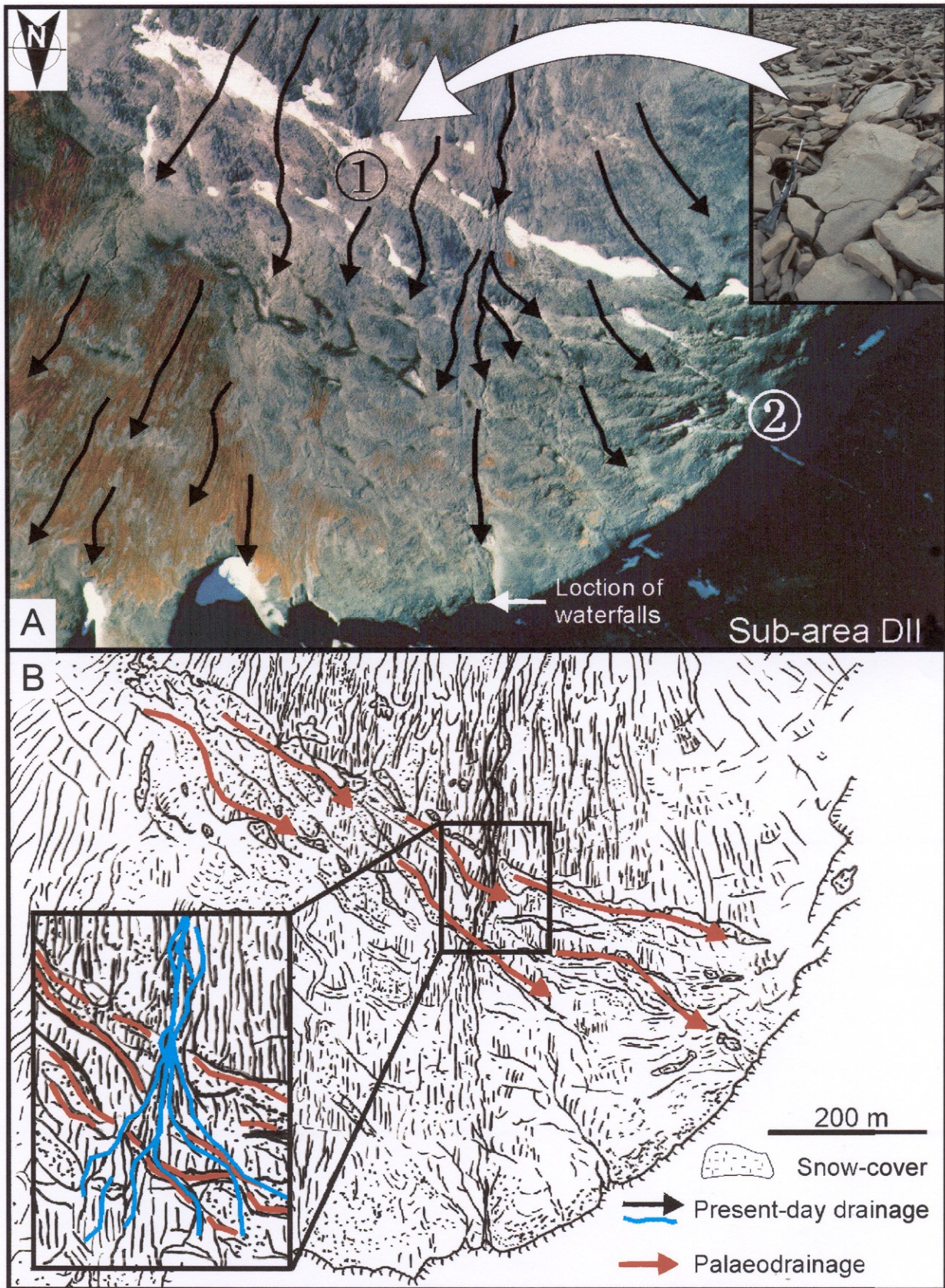
Fig. 3.5: **(A)** Norsk Polarinstitutt aerial photograph S-90, 5409. The middle part of subarea DII showing a flat, partly vegetated area with NE- to NW-trending channel and scours and a polished exposed bedrock surface (see Fig 3.6), to a more compact non-vegetated blockfield of cobbles and boulders (insert photo).(Numbers 1 and 2 refer to detailed pictures in Fig.3.6). **(B)** Photogrametric interpretation of subarea DII. The drainage pattern is interpreted from aerial photographs and field obsevations. Present day drainage from the inner plateau (subarea DIII) clearly crosses the deeper wider palaeodrainage channels.

edge near the entrance to Coal Mine 5 in Endalen (Fig 3.5). Deep ravines are cut beneath the waterfalls. Water also drains into Endalen to area C, and at least 18 small subsurficial conduits have been identified by recognizing the sound of flowing water. One of these channels was locally visible at the surface on the adjoining mountain slope. The observations pertain to the snow-melting season, and subsurficial conduits are interpreted to be the drainage pathway(s) of meltwater from subarea DIII through subarea DII.

The one channel with visible drainage is linked to several palaeochannels that here can be traced across the entire plateau (Fig. 3.4B & Fig. 3.6). The aerial photographs indicate that clearly an older, inactive meltwater channel is cross-cut by the modern drainage pattern extending from subarea DIII. In the central part of subarea DII, the northward direction of the modern water drainage locally shifts and follows the transverse pattern of palaeochannels leading to area C in Endalen (Fig.3.5). The palaeochannels are linear bedrock scours formed in a frost-shattered sandstone of the Grumantbyen Fm. Exposed bedrock with small kettlehole-like features are present within the palaeochannels in the central part of the plateau, while on the edge of the plateau over Mine 5, the channels end near the plateau edge with a deposit of large boulders (Fig. 3.6). The clean surface in the channels indicate a high water flow regime, while the deposits near the plateau edge to Endalen might have been caused by a decrease in the water-flow regime for instance indicating a small glacier dammed lake. On each side of the channel a 1-2 m thick cobble rich sediment dominates, with solifluction lobes overlying the clean surface of the channel bottom. Another possible interpretation for the deposits near the plateau edge is that the boulders are relicts from a lateral moraine from an early stage of the deglaciation and that all lower grainsizes have been removed with meltwater from the palaeochannels. Some of the palaeochannels were still filled with snow in the late July during the melting season in 1998, but not much meltwater was visible on the surface.

3.2.3. Subarea DIII

The highest parts of the plateau in the southern part (Fig. 3.2) consist of the Frysjaodden Fm., comprised of shales with sandstone and siltstone interbeds. Unlike the western plateau, where a row of erratic boulders are seen stretching towards the Trollsteinen mountain (outside the Endalen drainage basin) (see Fig. 3.1B & Fig 3.7A), the gravelly deposits on the plateau surface in subarea DIII seems to be of local derivation, and few erratic clasts have been found here.

Fig. 3.6: *Above*: Detail photograph from one of the channels crossing the plateau in a north-west direction (number 1 for location on Fig. 3.5(A)) . The bedrock (siltstone from the Grumantbyen Fm.) is wiped clean of sediments and frost shattering has broken up the surface (see rifle for scale).

Bellow: Surface photograph from the edge of the plateau where the same channel as above enter Endalen. The boulders are of the same formation as the bedrock around, but might still be transported some distance. The view is towards the center of the plateau and further up, the channel is still filled with snow in the middle of July (Field diary for scale, 20 cm).
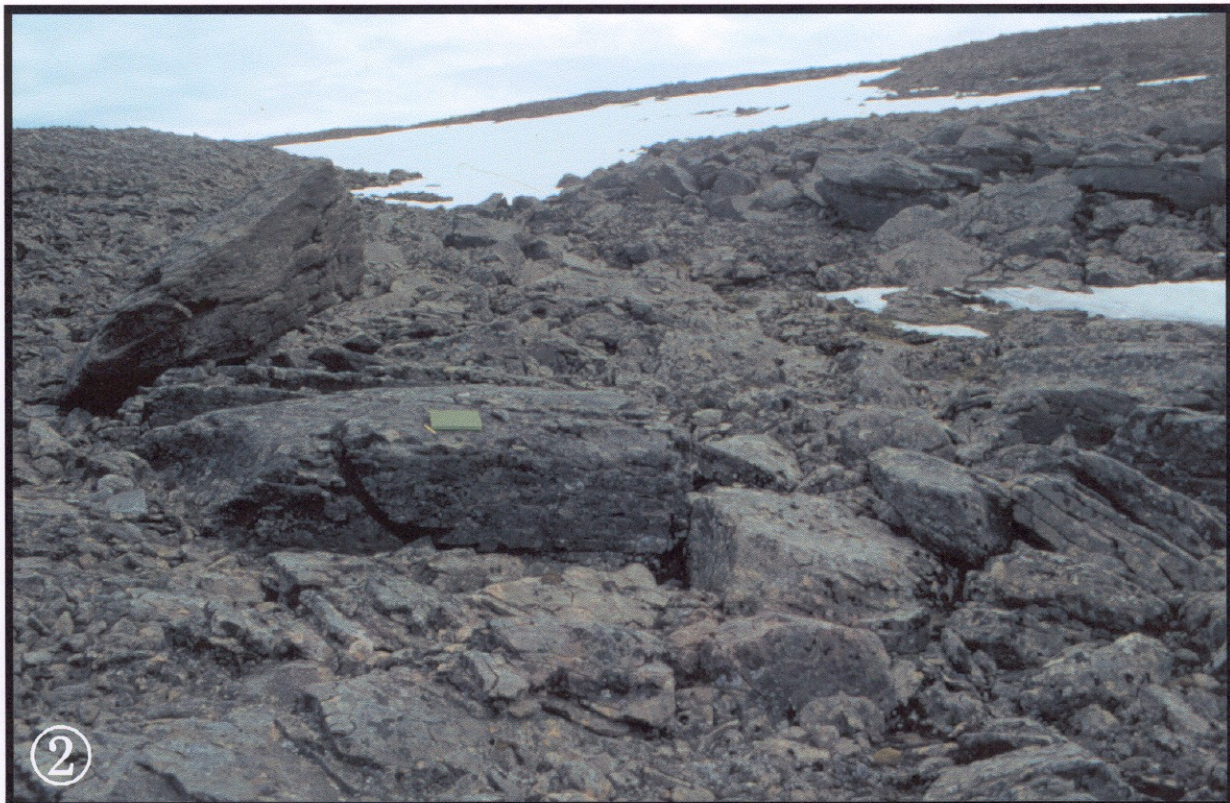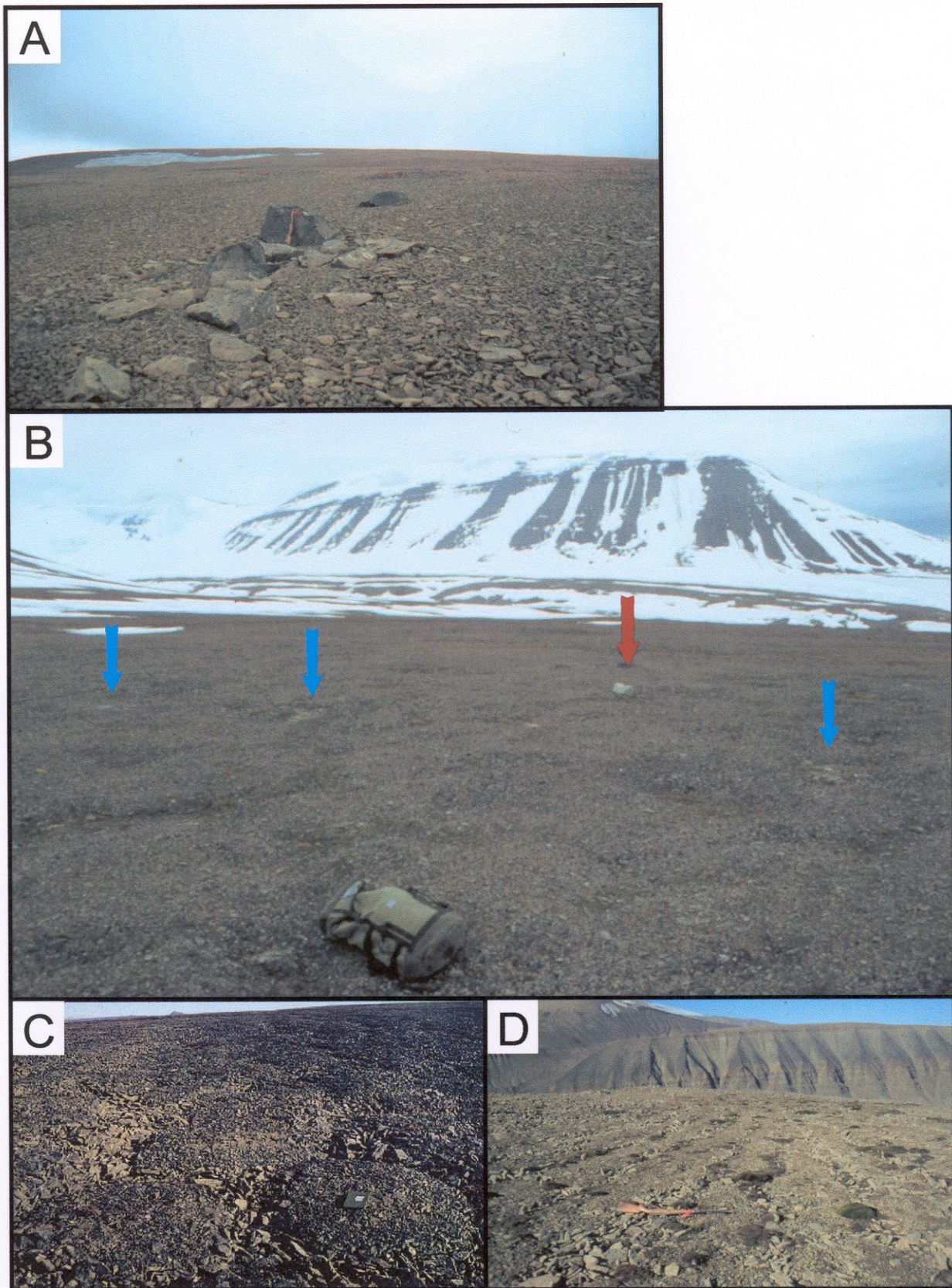
Fig. 3.7: **(A)** Frost shattered boulder erratics on the western plateau, marked with dark green in Fig.3.1B, interpreted to be lateral or medial moraine deposits from Trollsteinen. **(B)** In are DIII stone rings are probably smoothened by running water from melting of the glacier ice beneath the Karl Bayfjellet. Note the small boulder in the central part of the picture (red aroow). Is this the look of an ablation moraine? Several similar small boulders or cobbles are seen totally frost shattered in the same area (blue arrows). **(C)** Permafrost stone rings on the surface of the eastern plateau in the central part of subarea DIII (the notebook is 20 cm long). **(D)** Towards the edge of the plateau the stone rings reshapes to stone stripes.

However, some small rounded boulders are seen in the inner area DIII, frost shattered and spread out on the otherwise smoothened surface of shales (Fig 3.7B). In the central part of subarea DIII, well-developed permafrost stone rings and stripes are recognizable and some less-distinct stone rings occur in the southwestern part, between the Karl Bayfjellet glacier and the Bogerbreen (Fig. 3.7C & D). Some older, NW-trending meltwater channels are recognizable in front of the Karl Bayfjellet glacier moraine on the plateau, in the inner parts of subarea DIII. These channels are thought to have been formed in connection with the maximum extent of the local Karl Bayfjellet glacier during the Little Ice Age and are further discussed in section 3.4.2 and shown in Fig. 3.12. This local glacier cross the plateau and end in a large ravine in the inner part of area C in Endalen.

3.3. The valley-side gravel fans

The NW-facing, steep valley-side slope hosts an array of gravelly fans (Fig. 3.1A & B), which are fairly short and steep, have been formed by slope-wasting processes and are classified as *colluvial* (see Blikra, 1994; Blikra & Nemec, 1998). The plan-view lengths of these fans are in the range of 250 to 500 m, and their surface inclination varies from 15-36º at the apex to 2-6º near the toe. The morphometry, surficial features and textural characteristics of the fans show some variation along the valley-side slope, and are therefore reviewed separately for areas A, B and C (Figs. 2.2 & 3.2). The variation seems to be related to the size and geometry of the fan catchment, which is often a ravine, and also to the catchment's exposure to the sun. Some of the ravines are linked to abandoned channels on the plateau (Fig. 3.4), and the present-day morphology of the plateau's edge and the associated pattern of colluvial catchments are thought to have been determined to a high degree by the meltwater runoff from the plateau during the last deglaciation.

3.3.1. Area A

Three major colluvial fans occur in this area (Fig. 3.8). The fans are coalescing with one another and can be regarded as a colluvial apron. The southernmost fan A1 has the highest apex, in the lower part of Endalen Mb. (Firkantan Fm.) at an altitude of 220 m, whereas fan A2 and A3 have their apices at an altitude of ca. 160 m, directly below a package of fine-
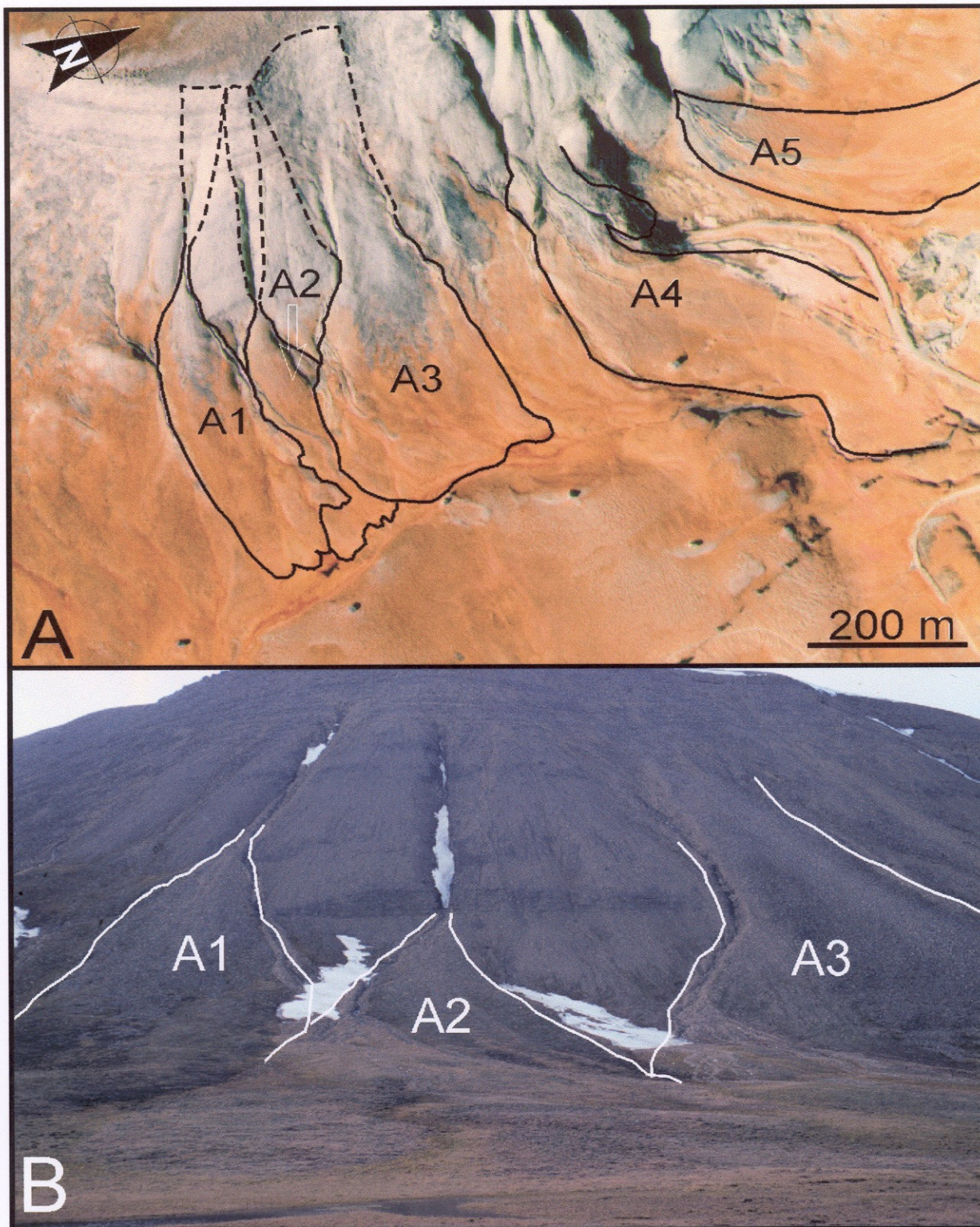
Fig. 3.8: (A) General view of area A showing colluvial fans A1-A5 (Norsk Polarinstitutt aerial photograph S-90, 5241). **(B)** Photograph of the northeast-facing valley-side slope in area A. Note the smooth surface of the middle sectors of the fans and the fresh debrisflow deposits between fans A1 and A2 and fans A2 and A3. The left-hand sector of fan A3 is covered with a large accumulation of rockfall deposits.

grained sandstone beds in the uppermost Carolinefjellet Fm. Fans A1 and A2 are similar. The fans have plan-view lengths up to 500 m and the profiles are concave upwards with only 2º inclination near the toe and up to 36º near apex. Their surfaces are fairly smooth, with small channel–like gullies extending from the upper to the middle fan segment in the axial sector, and with vegetated debrisflow lobes dominating the lower fan segment. The fresher debrisflow deposits are linked to a channel-like track in the right-hand fan sector. The right-hand sectors of fans A1 and A2 show fresh debrisflow deposits in the form of gully-and-tongue features, or strongly elongate lobes passing upslope into channel-like scours. Some of these gravel lobes extend into the lower segment of the fan's central sector. A large accumulation of lichen-coated rockfall debris occurs in the upper to middle part of the left-hand sector of fan A3. This lobate accumulation of bouldery gravel overlies the fan's debrisflow deposits and may represent one large late-Holocene rockfall or several consecutive rockfall events. The surface of the middle and lower segment of fan A3 shows a great resemblance to the surfaces of fans A1 and A2. Two other colluvial fans, A4 and A5, occur further to the north (Fig. 3.8A). These fans are slightly larger and associated with deeper ravines, but their surfaces have been strongly affected by the human activity related to Coal Mine 5 and the two fans are thus not included in the present study.

3.3.2. Area B

This area includes six major colluvial fans, Ee1 to Ee6, whose surfaces show fairly fresh debrisflow lobes. The larger fans (except for Ee6) are almost totally covered with such tongue-shaped deposits (Fig. 3.9A), whereas some of the smaller fans have smoother surfaces, with vegetated debrisflow lobes in the lower segments. The northernmost fan Ee1 has its apex at an altitude of ca. 110 m, at the base of a deep ravine. The upper fan segment shows a prominent channel, ca. 3 m deep and up to 5 m wide, apparently scoured by the most recent debrisflows, whose fresh deposits extend downfan from the channel in the fan's right-hand sector. One of the debrisflows has crossed the fan's middle sector, depositing levees about 0.5 m high and up to 8 m apart without eroding the older deposits. Scattered small clasts are deposited on top of cobbles and small boulders in this area indicating a snow avalanche deposit (Fig. 3.9B). The surface inclination of the fan varies from 1.5º near the toe to 18º near apex and the fan is about 320 m from apex to where the valley-axis river, Endalselva have cut of the toe of the fan. The left-hand sector of the fan has a smooth and strongly vegetated

surface. Fan Ee2 has its apex at an altitude of about 171 m and is composite, formed by debrisflows and rockfalls derived from two adjacent ravines. Rockfall deposits predominate in the upper and middle segments of the fan's central sector, whereas vegetated debrisflow lobes predominate in the lower segment.
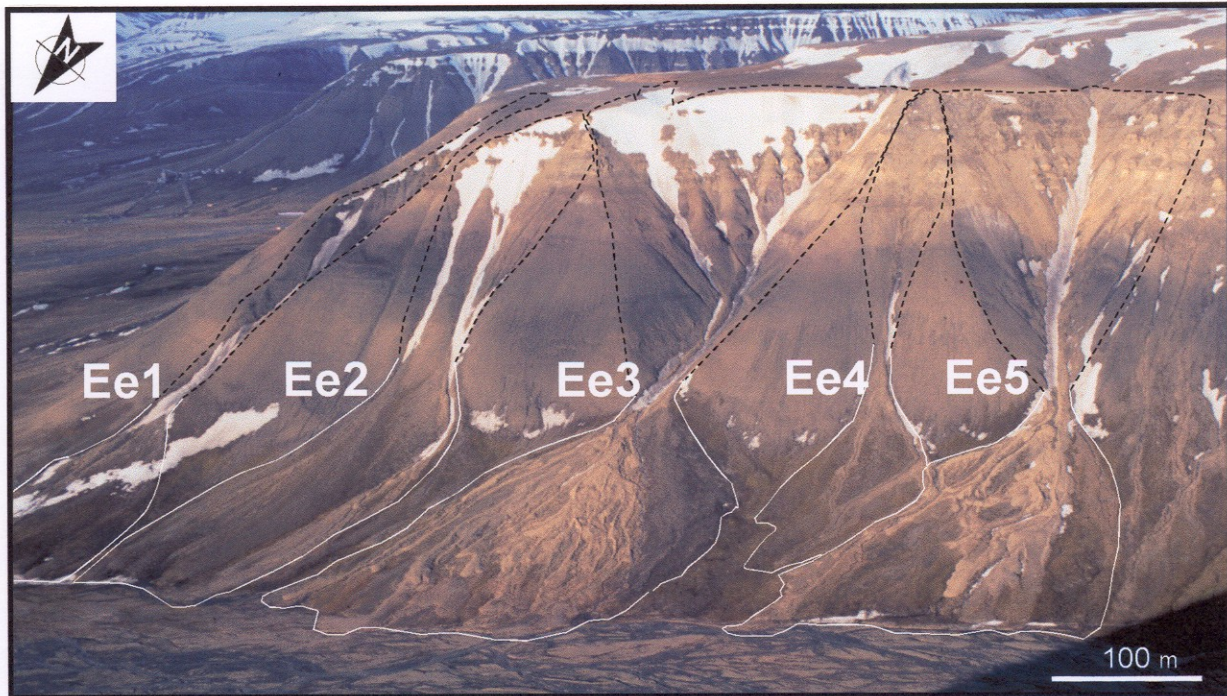
Fig. 3.9A: Colluvial fans Ee1- Ee5 outlined (white lines) and their catchment areas (stippled black); fan Ee6 is further to the right, outside this picture (see Fig. 3.9). Note the valley axis braided river Endalselva, at the bottom of the photograph.

The smaller and steeper fans Ee2 and Ee4 have small catchments, whereas the larger fans Ee3 and Ee5 are associated with deep, well-developed ravines that must have been scoured at the time of an abundant meltwater runoff from the plateau (Fig. 3.9A). The surfaces of the larger fans abound in relatively fresh debrisflow deposits, including bouldery levees and gully-and-lobe features, overlying the vegetated older fan surface. One or two of the fan gullies have been rescoured by several debrisflows and evolved into prominent channels up to 5 m deep, with levees up to 2 m high. Some of the associated tongue-shaped debrisflow lobes are more than 50 m long and up to 2 m thick in the frontal part. Some of the debrisflows have buried pieces of man-made installations (wires, cables, wooden planks and poles) and thus probably postdate the closure of Coal Mine 5 in 1973. The fans in area B range from 350-500 m in plan-view length and reach the active channel of Endalselva, which is presently eroding the fan toes.

Fig. 3.9B: Surface photographs of fan Ee1 showing possible snow avalanche deposits overlaying a wide debrisflow channel in the central sector of the fan. Smaller calsts are observed resting on top of cobbles and smaller boulders (note the shot gun for scale).
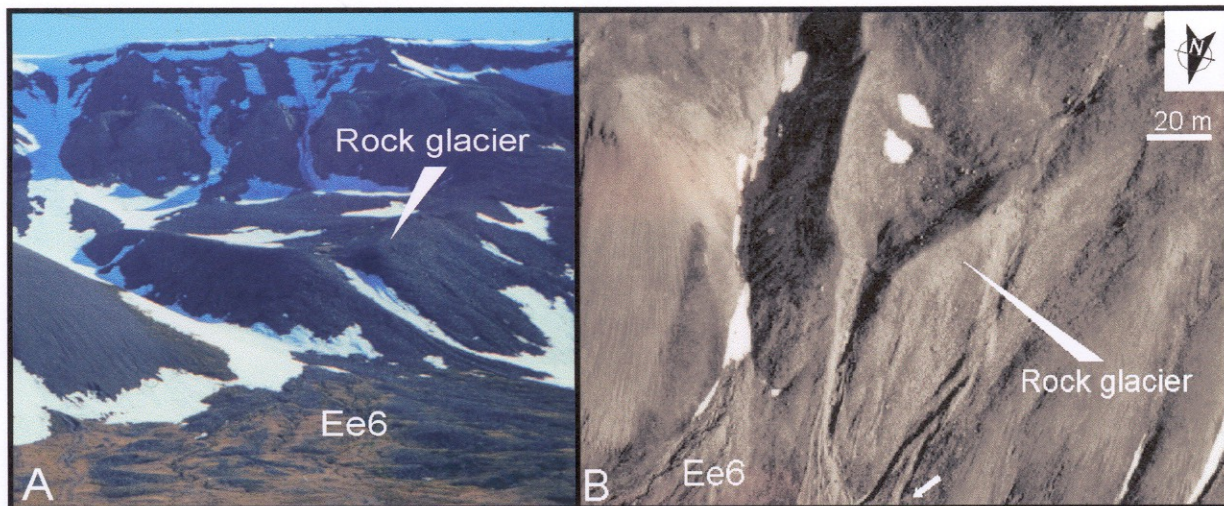
Fig. 3.10: (**A**) Photograph of the rock glacier taken from the valley floor. Note the rockfall dominated colluvial fans prograding onto the rock glacier. The plateau edge is about 200 m above the rock glacier. (**B**) Close-up from aerial photograph 1:7000 S-90 1032, showing boulders on top of, on the valley-side slope above and in front of the rock glacier (location of the erratic boulder found on this side of the Endalen valley is shown by the white arrow).

Fan Ee6 has not been studied in detail, because its surface was heavily disturbed by the human activity around Coal Mine 5. In the catchment of this fan, coarse-grained debrisflows extends from the collapsed steep front of a rock glacier (Fig. 3.10). The front of the rock glacier is ca. 20 m high in the central part. Above the flat vegetated area on top of the rock glacier, younger rockfall-dominated fans have onlapped the tongue-shaped body of the rock glacier. The two steep-wall topographic steps in the mountain slope directly above the rock glacier correspond to the Firkanten Fm. (the lower one) and the Grumantbyen Fm. (the higher one), and the steep cliffs generate rockfalls including boulder blocks several meters long. No measurements are available to determine whether the rock glacier is active or inactive.

In front of the rock glacier, at least one exotic small boulder of a diabase was found by the present author. A similar erratic boulder was found at approximately the same altitude of ca. 180 m on the other side of Endalen (Lægreid, 1999). Both clasts are well rounded, although not as smooth as the very well-rounded finer gravel (black chert debris) resting on the mountain plateaux. Notably, the sedimentary rocks in Endalen area are nearly devoid of gravel component (except for sporadic small quartz pebbles) and the nearest outcrops of diabases and other volcanic rocks are at the eastern coast of Spitsbergen (J. Nagy, pers. comm. 1998). If the exotic clasts have not been derived from the local Cretaceous-Tertiary bedrock, they must be erratics of glacial derivation, transported over a relatively long distance. Dalland (1977) reported on the occurrence of erratic clasts in the Basilika Fm. and the Grumantbyen Fm., described as well-rounded chert and quartz fragments of sand to

boulder size, but mainly granules to pebbles (> 95%). However, no clasts of diabase were recognized, and cobble- to boulder-sized clasts are generally rare (Dalland, 1977). On account of the glaciation, the diabase erratics are thought to indicate glacial derivation of some of the sediment in the valley.

3.3.3. Area C

The valley-side slope in the innermost part of Endalen is hosting three gravel-fan varieties: steep rockfall-dominated fans, slightly gentler debrisflow-dominated fans and fairly gentle glaciofluvial fan (Fig. 3.11 & 3.12).

The ravines at the outer edge of the plateau are numerous but small, and the direct meltwater runoff from the plateau here has apparently been sparse and poorly confined. This northern part of area C is dominated by small gravelly/cobbly cones formed by rockfalls and coalesced into a colluvial apron. The apices of these fans are located high on the slope, at altitudes around 350 m, where the Firkanten Fm. crops out, and plan-view lengths varies from 200-300 m. Some of the fans are supplied with debris from two or three small ravines. No waterfalls have been observed at the plateau edge, draining into area C, during the snow-melting season in 1998. The openwork, cobbly and bouldery debris has been derived from the Firkanten, Basilika and Grumantbyen fms. The longitudinal profiles of the fans are steep in the upper segments, and concave -upward to straight in the lower part. The surfaces of most of these fans show one or more relatively fresh channels scoured by debrisflows, and similar gullies occur also on the colluvial slope between some of the fans. Most of the associated debrisflow lobes are fresh, highly elongate gravel tongues, similar to those on the fan surfaces in areas A and B. However, most of the gravel appears to be covered with small lichen colonies, which indicates that the present-day activity on these fans is relatively low. Many debrisflows have spread in the middle fan segment, and some have reached the fan toe at the bank of Endalselva. The waterflow on the fan surfaces is insignificant, as the rain and snowmelt water readily percolates through the openwork gravel, and all the channels have clearly been scoured by debrisflows, possibly rich in wet snow or slush in some cases. All the fan channels have distinct bouldery levees, but not all have an associated gravel lobe. Boulders several meters long are not uncommon in the lower fan segments.

Directly further to the south, a large rockfall-dominated fan has formed outside a glacial palaeocirque (Fig. 3.11B). The fan apex is a wide zone of debris accumulation at the outer edge of the cirque depression, at an altitude of about 400 m on a very steep slope (with

Fig.3.11: (A) The valley slope in the outermost parts of Area C are dominated by amalgamated steep coarse grained rockfall dominated colluvial fans. (B) A large colluvial fan is also present in front of the cirque area. (C) The cirque glacier and associated fans in the inner Endalen. Note the Endalselva lower part of all three pictures.
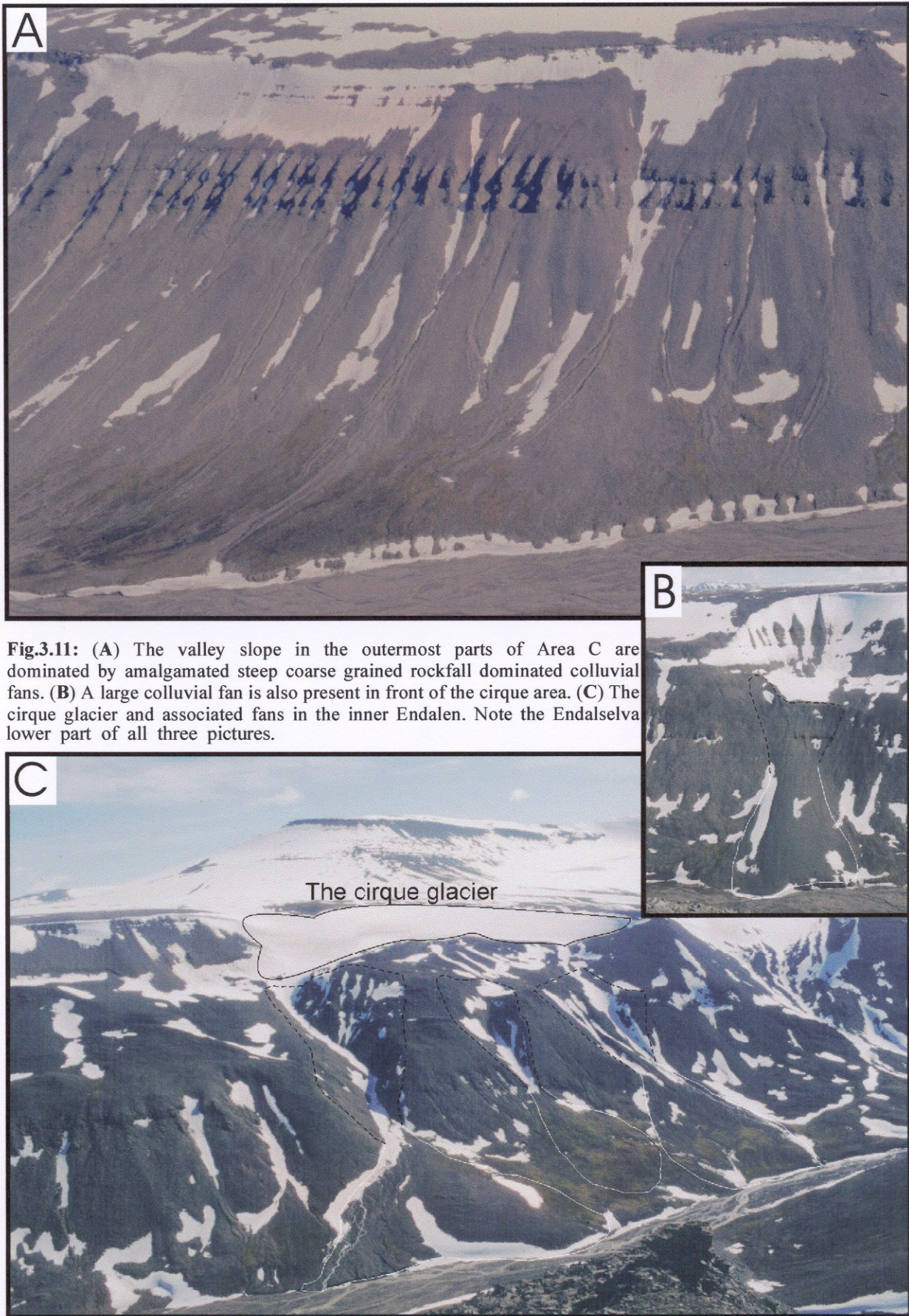
Figure 3.12: Portion of Norsk Polarinstitutt aerial photograph S-90 5470. Note the paleochannels west of the cirque glacier and north of the Karl Bayfjellet glacier's end moraine. The palaeodrainage indicated by the white arrow east of the canyon is interpreted to be of early Holocene age.

inclination possibly near 40º). Plan-view length is not more than 200 m. The fan consists of openwork cobble and boulder gravel, but has a fairly even surface, perhaps swept by sporadic snow avalanches. The gravel is coated with lichen colonies up to 10 cm in diameter, which indicates an inactive fan surface. The meltwater drained from the cirque area percolates through the gravel several meters below the fan surface. The fan's longitudinal profile is mainly concave upwards in the upper and middle segments, but slightly convex-upwards in the lower segment near the valley-axis river. Some small fresher accumulations of rockfall debris occur within the cirque depression, but no one of them has as yet reached the cirque's edge. However, these local piles of openwork cobble and boulder gravel render the cirque's floor rugged and highly vulnerable to possible sweeping by snow avalanches, if such events should occasionally occur here.

About 500 m further up-valley, three other colluvial fans, with different characteristics, have formed in front of the local cirque glacier (Fig. 3.12). The northernmost fan is the most active and has its apex at an altitude of ca. 260 m, at the base of a large ravine extending from the glacier. The fan is about 300 m long and its central (axial) sector has a convex-upward longitudinal profile, whereas the left-and right-hand sectors have slightly concave-upward to straight profiles. The fan's axial profile is estimated to have an average inclination of about 15º. The fan surface in the right-hand sector shows marked effects of the meltwater runoff from the glacier. The left-hand sector is largely abandoned and vegetated, whereas the central sector shows abundant openwork cobbly gravel of rockfall origin. Endalselva, the valley-axis braided river, has been eroding the fan's toe.

The middle of the three fans is apparently inactive. Its apex is at an altitude of ca. 250 m and the fan is shorter and has a slightly lower surface inclination than the previous one. The fan surface is covered with grass and moss, and the valley-axis river has eroded the fan's toe part. Inactive meltwater channels are recognizable above the ravine leading to the fan apex. The third, southernmost fan has an even lower gradient than previous and an apex located at ca. 240 m. Plan-view length is between the two previous fans mentioned. The fan does not stand out morphologically as a pronounced sediment accumulation, and also the ravine upslope is not particularly well developed. The fan has been strongly affected by the seasonal runoff from the cirque glacier, and the meltwater has scoured the ravine and formed streams that extend over the middle segment of the fan's left-hand sector. Most of the fan surface is vegetated and the low gradient indicates lack of rockfall deposits, but abandoned stream channels suggest that the fan has had a considerably greater meltwater supply in the near past. All the three fans have each an individual ravine catchment within the cirque glacier's

catchment area, but only the two largest fans receive meltwater from the small cirque glacier today. The water runoff is thought to have been much greater during the cirque glacier's retreat from its maximum extent in the Little Ice Age and the meltwater supply to the middle fan was probably cut off after the cirque glacier's retreat of some 40-50 m.

The innermost fan in Endalen is an active glaciofluvial outwash fan, supplied with meltwater from the unnamed glacier north of the Karl Bayfjellet mountain (Fig. 3.12). The apex of this fan is at the outlet of a large ravine, at an altitude of about 250 m. The mountain slope between this proglacial fan and the nearby Bogerbreen glacier is covered rockfall debris derived from the Grumantbyen Fm., and a few small rockfall cones have formed at the foot of the slope.

3.4. Glaciers and proglacial features

3.4.1. The modern glaciers

Three small valley glaciers occur in the head zone of Endalen: the Bogerbreen, the unnamed glacier at the foot of Karl Bayfjellet and the cirque glacier (Fig. 3.1A). The Bogerbreen is the largest, located at the head of the valley (Fig. 3.1A), ca. 2 km long and about 5.3 km^2 in surface area, spanning an altitudinal range from 990 to 250 m. This thin and narrow (ca. 400 m wide) glacier is probably cold-based. Most of the meltwater is drained into Endalen, but the western part of the glacier front supplies water to the adjacent Fardalen. Bogerbreen shows several transverse debris-bands on the frontal surface related to longitudinal shear zones and is fronted by a large, ice-cored moraine (Fig. 3.13). Based on the aerial photograph from 1936 (Fig. 2.2), this frontal ridge is interpreted to be the end moraine corresponding to the glacier's maximum advance during the Little Ice Age, which culminated in Spitsbergen at the beginning of the 20th century. In the middle part of the glacier's eastern margin, the mountain slope-wasting processes have led to the accumulation of rock debris in the form of an ice-cored lateral moraine. The unsorted, immature debris ranges from sand to boulders, and the fractured rock fragments have been heavily frost-shattered. The cobbles and boulders are often subrounded and represent mainly sandstone and siltstone, whereas the pebbles are made mainly of shale. The moraine abounds in finer-grained sediment, some of which has been washed out and deposited in small pits and other surficial lows sealed by permafrost.

The smaller glacier east of Bogerbreen, at the foot of Karl Bayfjellet, has a surface area of ca. 3 km^2 and extends altitudinally from about 800 to 400 m. Three amalgamated ice-cored moraines occur at its front and further to the east (Fig. 3.12). The glacier terminates on the edge of the plateau, but the adjoining ravine is filled with ice blocks and a large ice-cored moraine. Large quantities of shale debris have avalanched from the cirque recess in Karl
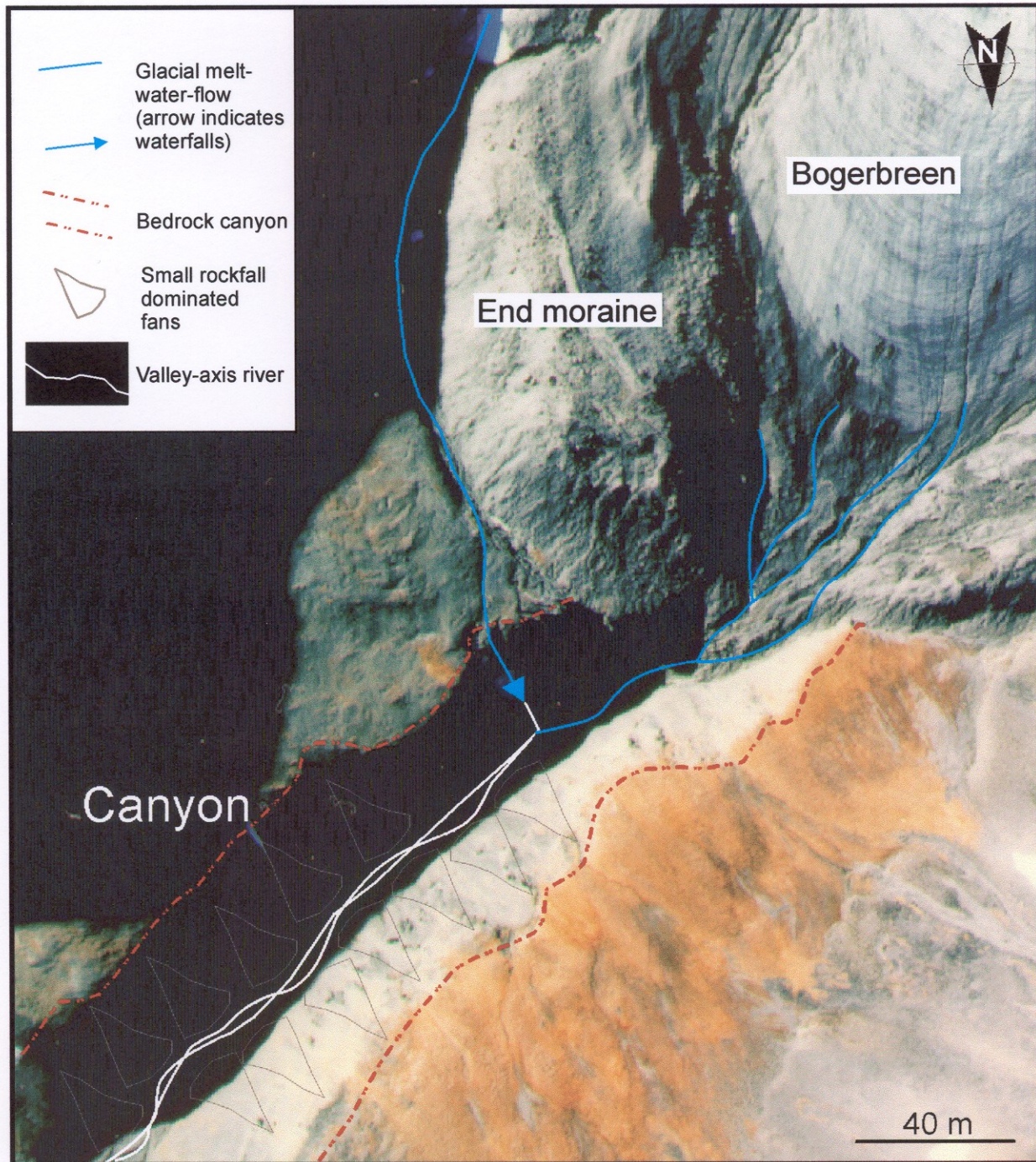
Fig. 3.13: The Bogerbreen end moraine has collapsed into the bedrock canyon. Some meltwater is entering the canyon via waterfalls of a channel in front of the end moraine (Norsk Polarinstitutt aerial photograph S-90 5470).

Bayfjellet onto the glacier surface. A long, narrow lateral moraine has formed along the glacier's eastern margin. The meltwater streams have scoured bedrock channels, 1-1.5 m deep and up to 3 m wide, outside the lateral moraine (see Fig. 3.12. These conduits are semi-abandoned today, but must have been very active during glacier retreat immediately after the Little Ice Age maximum.

The small cirque glacier in area C, referred to in the preceding section, is about 250 m wide and 50 m long, and is fronted by a third ice-cored end moraine recognizable in this part of Endalen (see Fig. 3.12). Despite its present modest size, the moraine was a large ice-cored ridge at the end of the Little Ice Age, as indicated by the 1936 aerial photograph (Fig. 2.2). The moraine surface material consists of openwork angular, cobbles- and boulder-sized sandstone and siltstone debris. The ridge is about 100 m long, 5-10 m high and 20-30 m wide. Between the glacier's front and the moraine ridge, three small ponds have formed, being drained through a breach in the northern part of the moraine.

3.4.2. Proglacial features

The Bogerbreen's end moraine seems to be melting progressively downwards. The central part of the moraine's front has collapsed, and the active slope-waste processes have considerably diminished the moraine. In front of the moraine, a bedrock canyon has been scoured by meltwater in the Basilika Fm. shales and the Firkanten Fm. sandstones. The canyon is ca. 200 m long, 10 m deep and 50 m wide, and is occupied by a braided river during the melting season. The canyon prevents the formation of a glaciofluvial outwash fan which thereby is absent. Small rockfall cones of frost-shattered pebble and cobble gravel have coalesced on each side of the river (Fig 3.14). Otherwise, the canyon is a non-depositional zone, with the glacial meltwater flowing directly into Endalselva, the braided axial river of Endalen. At a slightly higher altitude directly south-east of the canyon, the Endalen floor is covered with a rounded and well-sorted gravel, comprised mainly cobbles with a well-developed lichen coatings (see Fig. 3.12). The present-day water drainage through this area is entirely subsurficial. The mature and relatively old gravel is interpreted to be a glaciofluvial outwash deposited by a braided river during the last deglaciation, prior to the formation of the bedrock canyon. At present, the meltwater and rainwater percolate through the porous sediment and drains into the valley-axis river issuing from the glacier north of Karl Bayfjellet.

The large, ice-cored moraine fronting the glacier north of Karl Bayfjellet is also clearly melting. This moraine partly fills the large ravine and terminates in an outwash fan directly outside the ravine. This is the only outwash fan presently active in Endalen, with a high waterflow peak during the melting season (see Fig. 3.12). However, the ravine outwash pattern was far more extensive during the last deglaciation and also at the Little Ice Age decline at the beginning of the 20th century. As mentioned in a previous section, fluvial

Sediment description	Interpretation
Fine sand, vegetated top	Sheetwash
Un-sorted subangular to subrounded pebbles and cobbles floating in medium/ course sand matrix	Debrisflow(s)
Normal-graded silty fine sand with angular to subangular pebbles	High-density sheetflood
Clast-supported gravel with rounded to well-rounded pebbles and cobbles, and sand / granule matrix	Valley-axis alluvium

Fig. 3.14: Local log from fan Ee3, showing the colluvium onlapping the valley-axis alluvium. The outcrop is formed by the modern erosion of the fan toe by Endalselva.

Palaeochannels are readily recognizable in front of the lateral moraine on the mountain plateau in subarea DIII, with some of the modern snowmelt runoff still flowing through these channels and further into the adjoining ravine (see Fig. 3.12). Similar palaeochannels are recognizable in front of the cirque glacier's end moraine (see Fig.3.12). The colluvial fans developed at the ravine outlets have been dissected by the meltwater flow from the cirque glacier and might therefore have an underlying alluvial fan deposit, while the clearly dominance of debrisflow and rockfall processes now make them colluvial fans.

3.4.3. The valley-axis river

The meltwater from all three glaciers is drained by Endalselva, the 5-km long valley-axis river that drains the Endalen basin into the large Adventdalselva and effectively into the Adventfjord. The Endalen's axial river is active from approximately the end of May until the middle of September, and the same pertains generally to Adventdalselva. The uppermost reach of Endalselva is in the bedrock canyon in front of the Bogerbreen end moraine, where several meltwater streams merge. The glacier's main outlet of meltwater has shifted with time, and the outflow is presently entering the canyon through a 6 m high waterfall on the northern side (see Fig. 3.13). Outside the canyon, down the valley, the river has clearly shifted its course many times over from one valley side to the other, eroding both the bedrock and the valley-side colluvial fans. A sedimentological log from the frontal part of fan Ee3 (Fig. 3.14) shows that the colluvial fan has prograded over the early glaciofluvial deposits of the axial river. The river deposits consist of a mature gravel, comprised of mainly rounded pebbles, cobbles and small boulders of sandstone and siltstone, in addition to the coarse sandy to pebbly medial bars.

In the late 1950s, a road was build to the entrance to Coal Mine 5. The road crosses the river and has changed the river's course at the valley mouth. One of the results has been an increased erosion of the toes of the three northernmost valley-side fans. The outcrop log in Figure 3.14 is from such a section, exposed by the river erosion.

Most of the sediment load transported by Endalselva is deposited in the form of a broad and very gently inclined alluvial fan at the valley mouth. In spite of the strictly seasonal discharges, the fan has been actively prograding into the adjacent Adventdalen basin (Fig. 3.15).
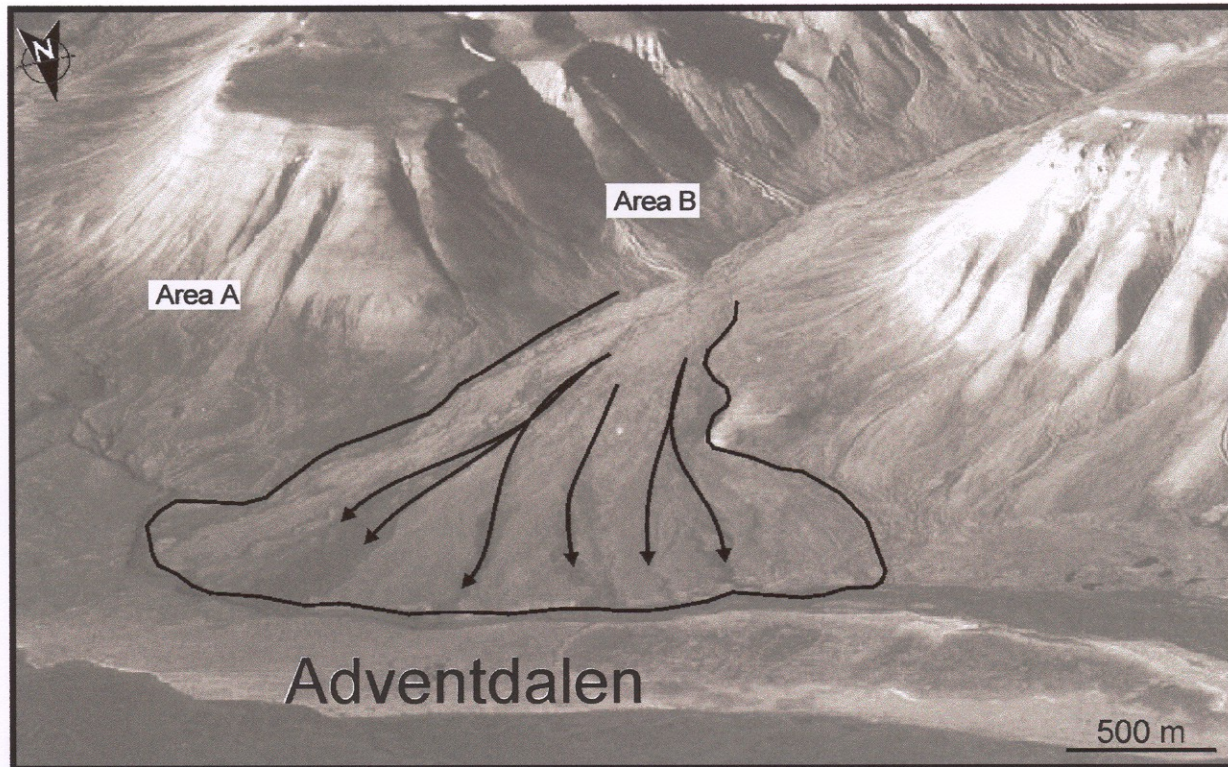
Fig. 3.15: The alluvial fan formed by Endalselva at the mouth of Endalen (Norsk Polarinstitutt's oblique aerial photograph S-36 2296).

3.5. The valley mouth

3.5.1. The lateral moraine

On the eastern side-slope of the Endalen mouth, spanning an altitude range from 45 to 115 m, the colluvial fan Ee1 has prograded erosively across a large, terrace-like vegetated mound of unconsolidated gravelly sediment (Fig. 3.16). A number of small-scale debrisflows and slumps have modified the mound's surface. In several places, the surficial soil layer, upper 50 cm thick, has slid downslope by 1-3 m as small debrisflows (Fig. 3.17A), exposing sandy, poorly sorted gravel containing rounded sandstone pebbles and cobbles. The slope's local meltwater runoff has adjusted to the mound's morphology, flowing around the debrisflow lobes and lateral terraces. On the surface in the same area rounded boulders up to 1 m in diameter are observed.

Sediment descriptiom	Interpretation
Slightly vegetated top.	
Fractured (frost shattered) subangular and subrounded siltstone pebbles and cobbles.	
Subrounded siltstone and sandstone cobbles and boulders	Lateral moraine deposit
[Sample SS-3]	
Pebbles, cobbles and some small boulders in muddy sandy matrix.	
In-situ fractured subrounded siltstone pebbles and cobbles.	

Fig. 3.16: (A) The inferred lateral moraine on the eastern side of the Endalen mouth; the insert photo shows sub-rounded boulders in an unsorted sediment.**(B)** Sedimentological log showing a diamicton of possible lateral moraine. The development of a compound lateral moraine involving resedimentation, is show schematically in Fig.3.13A-C.
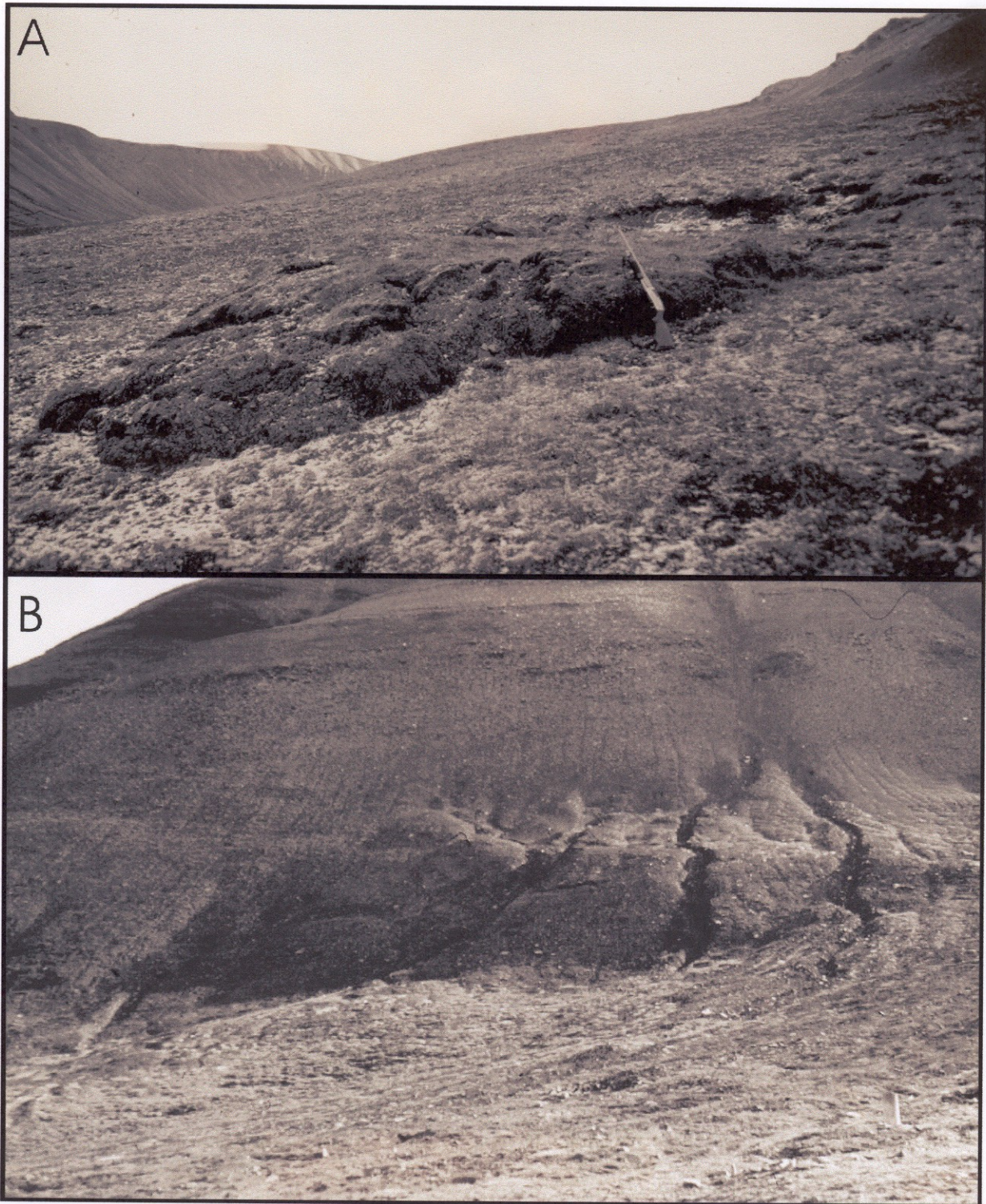
Fig. 3.17: (A) Debrisflow deposit formed by the resedimentation of the lateral moraine on the side-slope in outer Endalen. **(B)** Terrace-like feature 50 m west of the lateral moraine, interpreted as a possible continuation of the latter. The terrace is cut by debrisflows; it consists of unconsolidated sediment including large angular cobbles and boulders.

The gravely mound shows no evidence to have been deposited by slope-wasting processes. The clast fabric is disorderly, and there are no recognizable leveed channels or scour-and-lobe features of debrisflow origin, such as those typifying the adjacent colluvial fans. The mountain slope above the mound receives little or no meltwater from the plateau, and is too steep for an accumulation of slope-waste debris. The Firkanten Fm. is sparsely exposed along the plateau's edge, and some cobble-sized angular sandstone blocks have slid or rolled down to the base of the slope. However, there is no bedrock cliff to shed rockfalls, and the more mature gravel of the mound is clearly different from the immature debris of the adjacent colluvial fans. An analysis of the roundness of clasts in the mound's gravel (sample SS-3), based on the Krumbein (1941) visual scale, has indicated predominantly subangular clasts (Fig. 3.18) by a calculated mean roundness for the sample of 0,3 (siltstone and sandstone clasts where separated for distinguishing possibly differences due to the different hardness of the clasts). Consequently, the gravelly mound is thought to be a lateral moraine formed during a phase of the last deglaciation. The preservation of the moraine at this locality is apparently due to the favorable geomorphic setting and limited slope activity. Similar terraces are by Rapp (1960) interpreted as lateral ice-contact features, in a similar setting near Tempelfjellet (Fig. 2.1).

Other relics of terrace-like mounds are recognizable between the colluvial fans Ee1 and Ee2 (see Fig. 3.17B), at a similar altitude as the lateral moraine at the corner. Its surface is partly vegetated and covered with slope-derived shale detritus, but a few debrisflows have scoured the surface to a depth of 50 cm, exposing sandy gravel with angular boulders and large cobbles. This gravelly deposit may be a diamicton corresponding to the lateral moraine described above. However, it cannot be precluded, on the basis of the poor exposure, that this vague terrace is simply a sandstone or siltstone ledge of the Carolinefjellet Fm. outcrop, covered with slope-waste debris. Another very similar mound is seen between fans A2 and A3 (Fig. 3.19). Also here the surface material indicates a high rate of bypassing slope-waste material and also here it is possibly that a sandstone or siltstone ledge of the Carolinefjellet Fm. outcrop is present, even though it is not in the same altitude as the aforementioned terrace. The arguments for this being a lateral moraine is simply its morphology, its natural location and the fact that no mound of slope-waste material normally would build at a steep slope as this. A cartoon is shown in Fig. 3.20 on a possible development of a lateral ice-cored moraine.

Class value	Siltstone clasts	Number %	Roundness · %	Sandstone clasts	Number %	Roundness· %
0,1	-	-	-	1	2,9	0,3
0,2	10	15,2	3,0	9	26,5	5,3
0,3	18	27,3	8,2	12	35,3	10,6
0,4	27	41,0	16,4	9	26,5	10,6
0,5	9	13,6	6,8	3	8,8	4,4
0,6	2	3,0	1,8	-	-	-
Total number	66	100,1	36,2	34	100	31,2
	Roundness for siltstones: 0,36			**Roundness for sandstones: 0,31**		
	Mean roundness degree of the sample: 0,3					
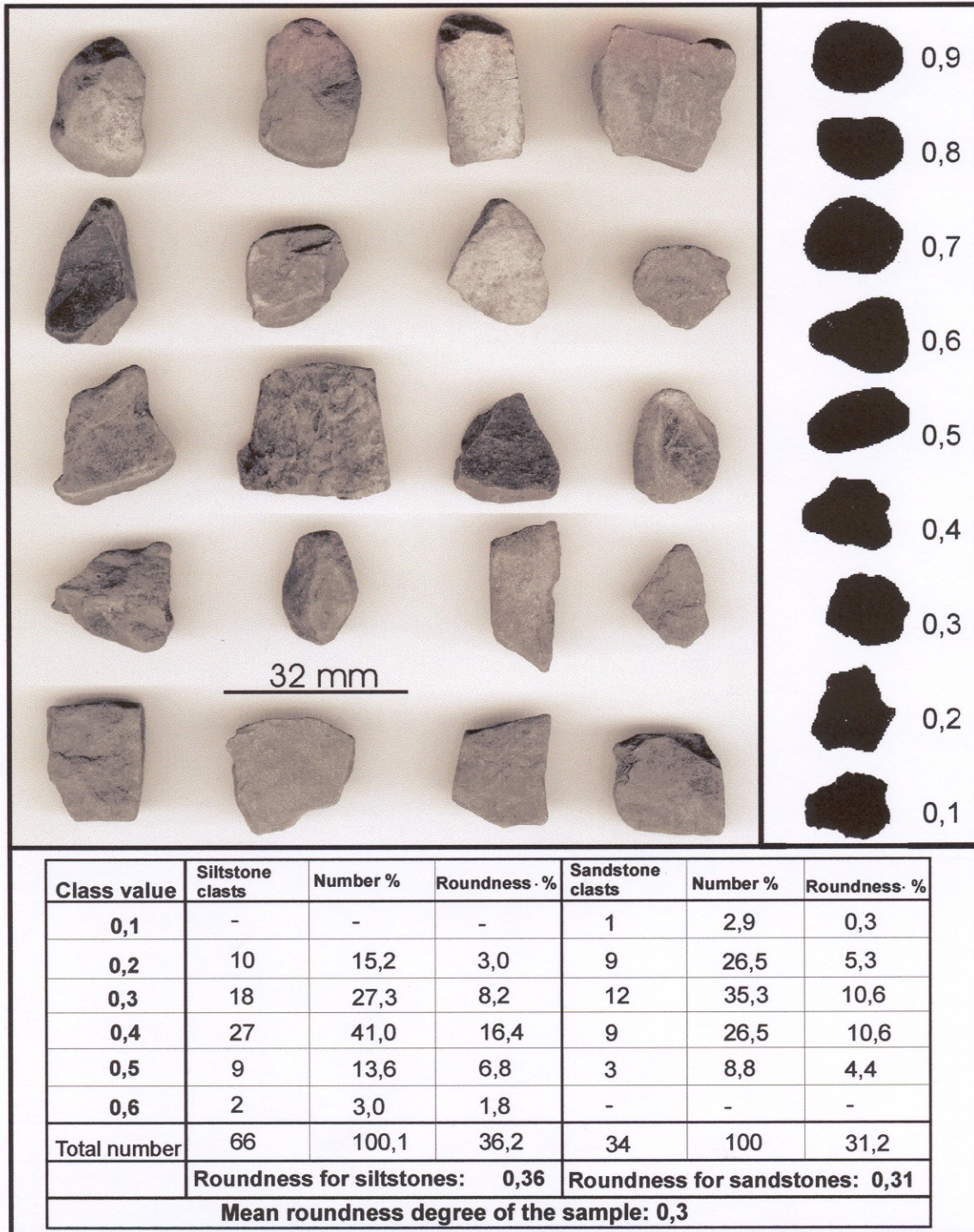
Fig. 3.18: A selection of clasts (from sample SS-3) showing the amount of fracturing on the subangular clasts from the inferred lateral moraine. The right part is examples from Krumbein (1941) and the table below are the results of the analysis of gravel from the same sediment (discussed in text).
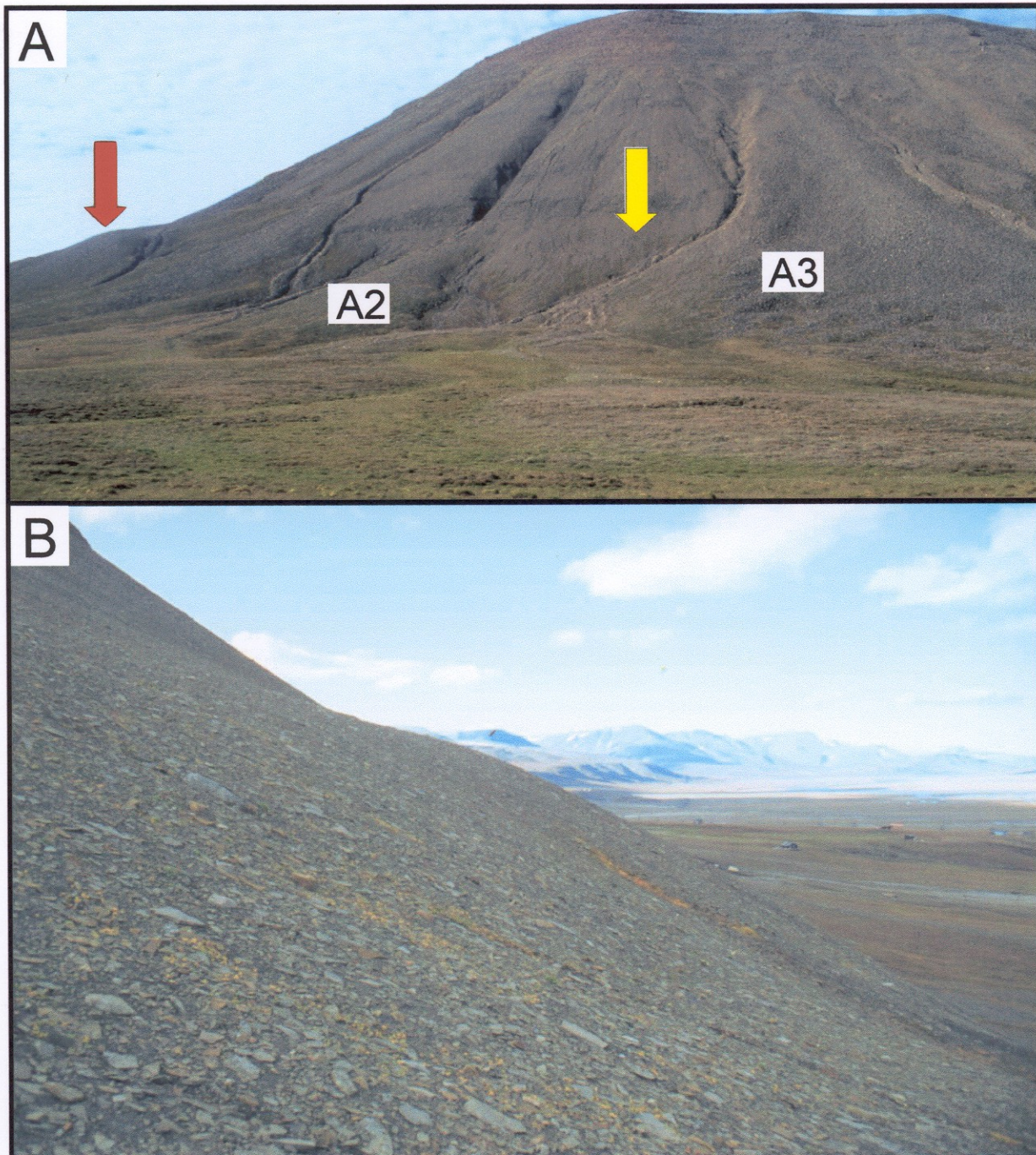
Fig. 3.19: (A) Two possible relicts from the last glaciation are visible in the southern part of area A. The red arrow points at a large mound on the northern corner of Todalen, showing a similar morphology with the interpreted lateral moraine at the southern corner of Endalen (see Fig. 3.17B), and could therefor also be a lateral moraine relict. The yellow arrow points at yet another mound, possibly formed as a lateral moraine, showing similarities in morphology with the lateral moraine inside Endalen, seen in Fig. 3.17B. **(B)** The surface material on this latter mound is clearly composed of slope-waste debris, but the location on the steep slope, however, supports the fact that the mound rather should be interpreted as a lateral moraine covered by postglacial slope-waste debris (Fig. 3.20).
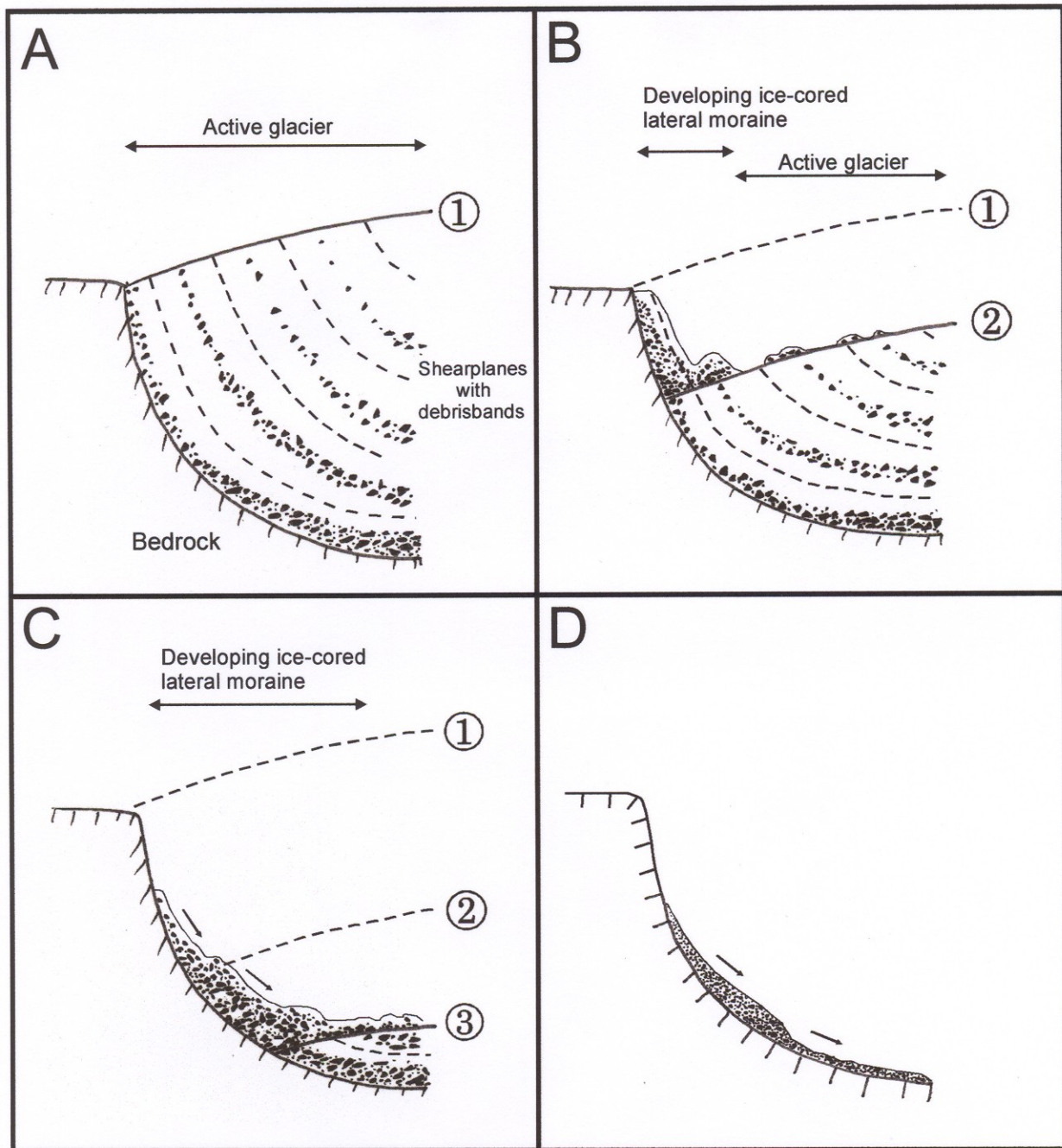
Fig. 3.20: The development of a lateral moraine in a schematic sketch of valley-margin cross-section. **(A)** The valley is filled by a glacier, stage ①, containing debris bands along shear planes. **(B)** The glacier has melted down to stage ②, developing an ice-cored lateral moraine; dirt cones are common on the surfaces of melting glaciers. **(C)** At stage ③, the ice-cored lateral moraine is still present, but subject to modification by slope-wasting processes (black arrows). **(D)** The glacier and the ice-cored lateral moraine have melted out, and the slope-wasting processes lead to erosion and resedimentation, leaving a smooth surface with few signs of the preceding history.

3.5.2. Raised beach terraces

Three parallel erosional terraces of the altitudes of 50, 57 and 63 m are recognizable in the lateral moraine mound in area A directly outside the Endalen mouth (Fig. 3.21). Another subtle erosional step in the slope topography is recognizable at an altitude of 36 m in the same area (Fig. 3.21). These terraces can be traced from the eastern corner of the Endalen mouth, where fan Ee1 has erosively prograded across the three higher features and post-dated them, to area A below fan A3 (Fig. 3.21). Samples of the terrace gravel have been taken for clast-roundness analysis from an outcrop scoured by the debrisflows of fan Ee1. The terrace deposit shows distinct subhorizontal bedding, marked by the alternation pebble gravel, very coarse sand and granule gravel (Fig. 3.22A). The planar fabric of coarse clasts, some signs of clast-shape segregation and the relatively thick layers of granule gravel point to a beach palaeo environment (see Bluck, 1967; Nemec & Steel, 1984; Postma & Nemec, 1990). No fauna shells or other datable organic material have been found, but the gravel shows good sorting and the clasts have apparently been well-rounded prior to being *in situ* shattered by frost (Fig. 3.22B). The gravel consists mainly of pebble-sized fragments of mudshale and siltstone, derived most probably from the Carolinefjellet Fm.
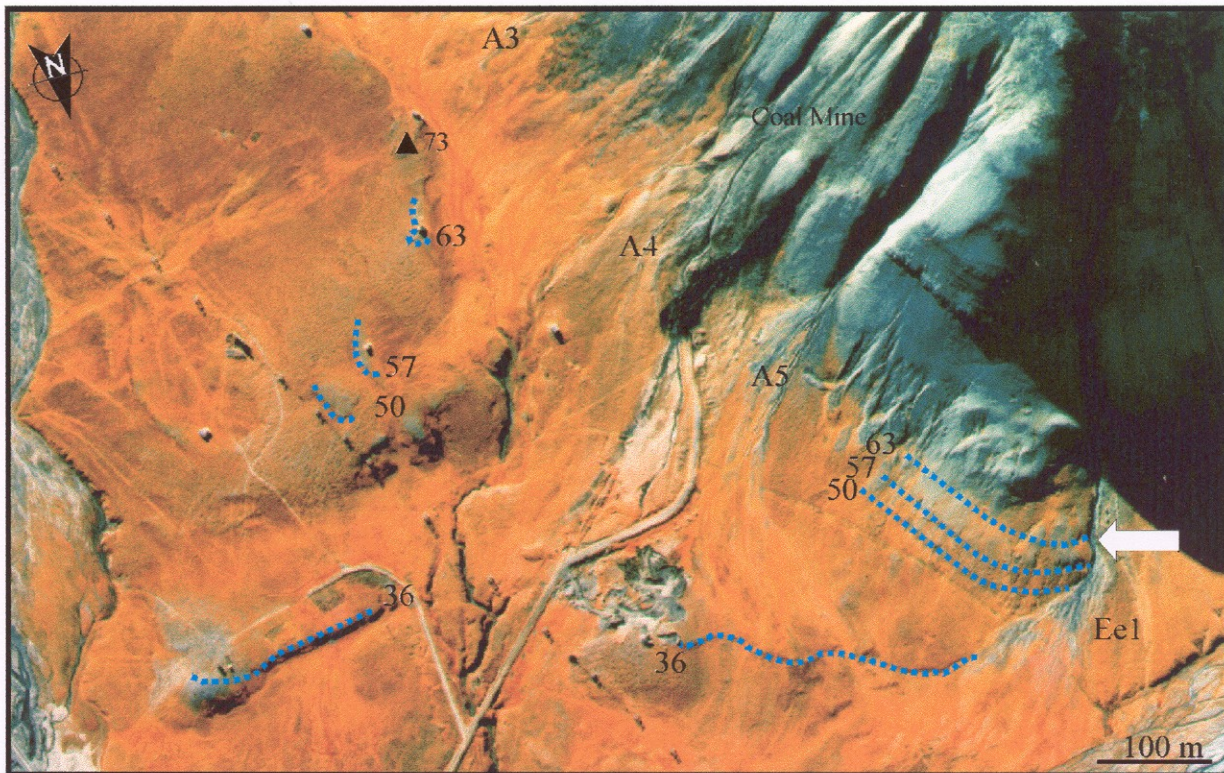
Fig. 3.21: Raised beach terraces at altitudes of 36 m, 50 m, 57 m and 63 m (stippled blue lines). Some of the lineaments visible in this photograph (Norsk Polarinstitutt S-90 5409) were formed by buldozers during the activity of Coal Mine 5. Note also the peak at 73 m altitude, unaffected of wave action.

These terraces of highly mature gravel are interpreted to be raised beaches. However, it should be emphasized that the lowest palaeobeach terrace, recognized below fan A3, is hypothetical, inferred on the basis of surface morphology and consistent altitude alone. The altitude of the marine limit is also uncertain. No marine levels higher than the altitude of 63 m are recognizable in the study area. The gravel scattered on the surface of a slight topographic high at an altitude of 73 m near the colluvial fan A3 shows no evidence of wave action. The marine limit must thus be lower than 73 m, provided that the area was not covered by glacier during the highest sea-level stand and that no debrisflows have reached up to this little topographic high.
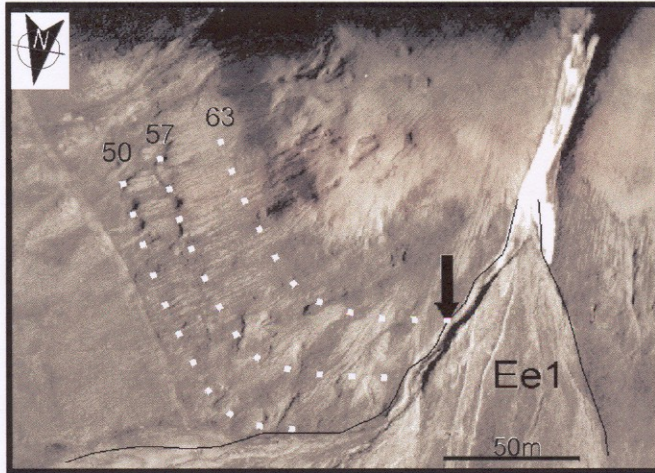
Fig. 3.22A: Norsk Polarinstitutt aerial photograph S-90 1030, showing the three beach terraces at altitudes of 50 m, 57 m and 63 m, formed in the lateral moraine; note the colluvial fan Ee1 cut through the beach terraces and post-dating them. The sedimentological log bellow shows the local facies succession with the sediment description and interpretations to the right. Locality of log is indicated by the black arrow in the aerial photograph.
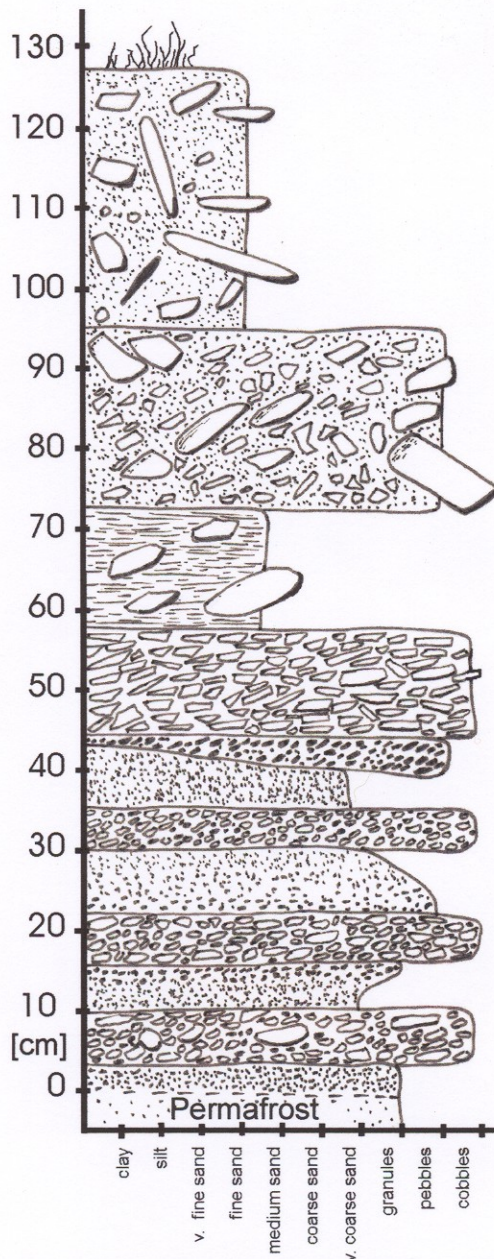
Sediment description	Interpretation
The top is vegetated with moss and flowers.	
Muddy fine sand with scattered pebbles and cobbles. D_{max} = 24 cm	Solifluction lobe
Matrix-supported pebble gravel with cobbles D_{max} = 20 cm	Debrisflow
Silty mud with scattered flat-laying cobbles. D_{max} = 20 cm	Mudflow
Coarse pebble gravel D_{max} = 7 cm. [sample SS-1]	Beach deposits
Fine pebble gravel D_{max} = 3 cm Very course sand-granule pinch-out Course pebble gravel D_{max} = 4 cm	
Granule gravel to vc sand Course pebble gravel	
Very course sand to granule gravel	
Course pebble gravel D_{max} = 7 cm granule gravel. [sample SS-2]	
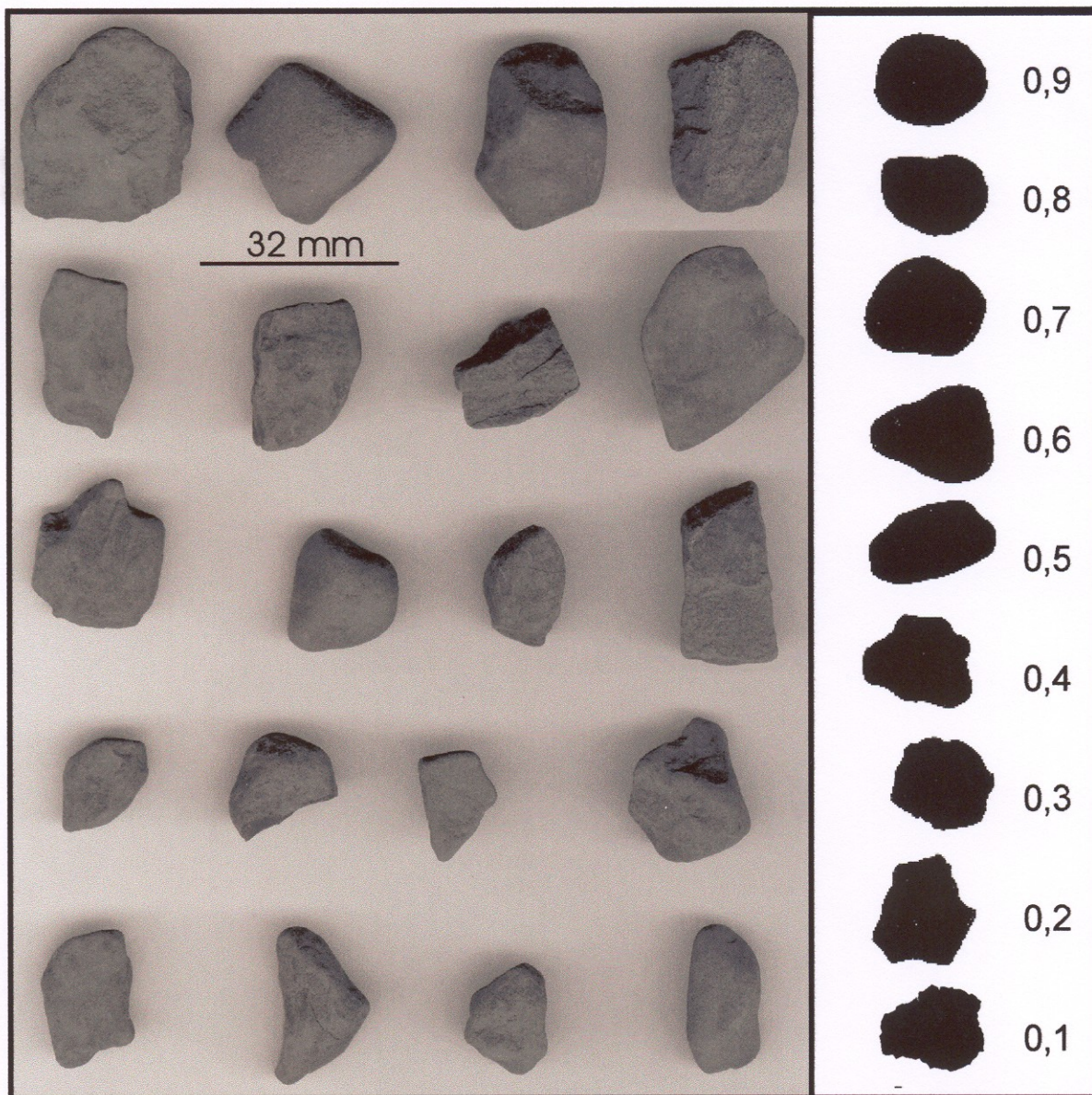
Class value	Siltstone clasts	Number %	Roundness · %	Sandstone clasts	Number %	Roundness · %
0,1	-	-	-	-	-	-
0,2	1	2,3	0,5	3	5,4	1,1
0,3	10	22,7	6,7	18	32,3	9,7
0,4	14	31,8	12,7	11	19,0	7,8
0,5	19	43,2	21,7	20	36,3	17,9
0,6	-	-	-	4	7,1	4,3
Total number	44	100	41,6	56	100	40,8
	Roundness for siltstones: 0,42			Roundness for sandstones: 0,41		
	Mean roundness degree of the sample: 0,4					

Fig. 3.22B: A selection of clasts showing the variable degree of fracturing of subrounded clasts, compared with examples from Krumbein (1941) to the right. Results of the analysis of gravel sample SS-2, from the beach terrace at 63 m altitude, is shown in the table above.

4. MODERN SNOW CONDITIONS IN ENDALEN

4.1. The seasonal snow cover

In order to assess the snow-cover conditions in the study area, the distribution of snow in Endalen has been studied systematically, on weekly basis, during one entire melting season (March-September 1998). The data were meant to shed light on the role of snow cover in the mobility and seasonal transport of sediment in this typical high-arctic valley. The semi-arid conditions render summer precipitation nearly insignificant, apart from sporadic rainstorms, whereas the long winter and rapid melting of local accumulations of snowdrift make the role of snow cover potentially very important. For example, it is widely recognized that the bulk of the summer runoff in Spitsbergen is due to the production of abundant meltwater.

The NE-trending Endalen is affected by both transverse and longitudinal winds. The cold easterly winds from the Barents Sea generally predominate during the winter and cause snowfall (Førland *et al*., 1997; Winther *et al*., 1998; also wind direction and force on weather maps in Appendix B), but the westerly winds from the North Atlantic are frequent and often bring some precipitation, too. The development of snow cornices at the plateau edges on the eastern and the western side of Endalen points to the importance of these cross-winds, paralleling the large adjacent Adventdalen and sweeping the mountain plateaux. However, the formation of snow dunes on the Endalen's floor and the accumulation of snow in the side-slope ravines testify to the important role of secondary topographically controlled up- and down-valley winds. The snow-cover thickness in Endalen varies generally from 24 cm in the valley-mouth zone to about 100 cm in the inner part of the valley-floor, and this spatial trend remains more-or-less stable during the whole winter. The only recognizable changes, discernible by field measurements, occur after a windless period of some days accompanied by snowfall, when up to 5 cm of fresh powder snow can be added to the existing snowpack. Interestingly, these valley-scale changes, revealed by the measurements in Endalen, are not recognizable from the conventional record of the nearby meteorological station at the Longyearbyen airport (see Appendix A). The low precipitation and windy conditions render measurements of the exact amount of snowfall very difficult. A meteorological station's data may thus not be reliable, and their extension to topographically different areas, even adjacent ones, requires much caution. In Endalen, an accumulation of snowdrift reaching 50 cm in

thickness have been recorded in the upper part of the valley after a period of strong northerly wind.

In March 1998, prior to the melting season, both side-slopes of the valley had a snow cover of a fully comparable, but highly varied, thickness. The snow was accumulated mainly in the slope ravines, fan channels and the topographic depressions between the colluvial fans. A snow-cover thickness of 138-149 cm has been measured between the apices of fans Ee3 and Ee4 as fix-point measurements (Fig. 4.1), and fairly similar snow thicknesses have been observed between many other of the fans at this higher level (Table. 4.1). The snow thickness between the debrisflow lobes in the lower fan segments, in the outer pa of the valley, was commonly 22-26 cm, slightly lower than the actual topographic relief of these gravel lobes.
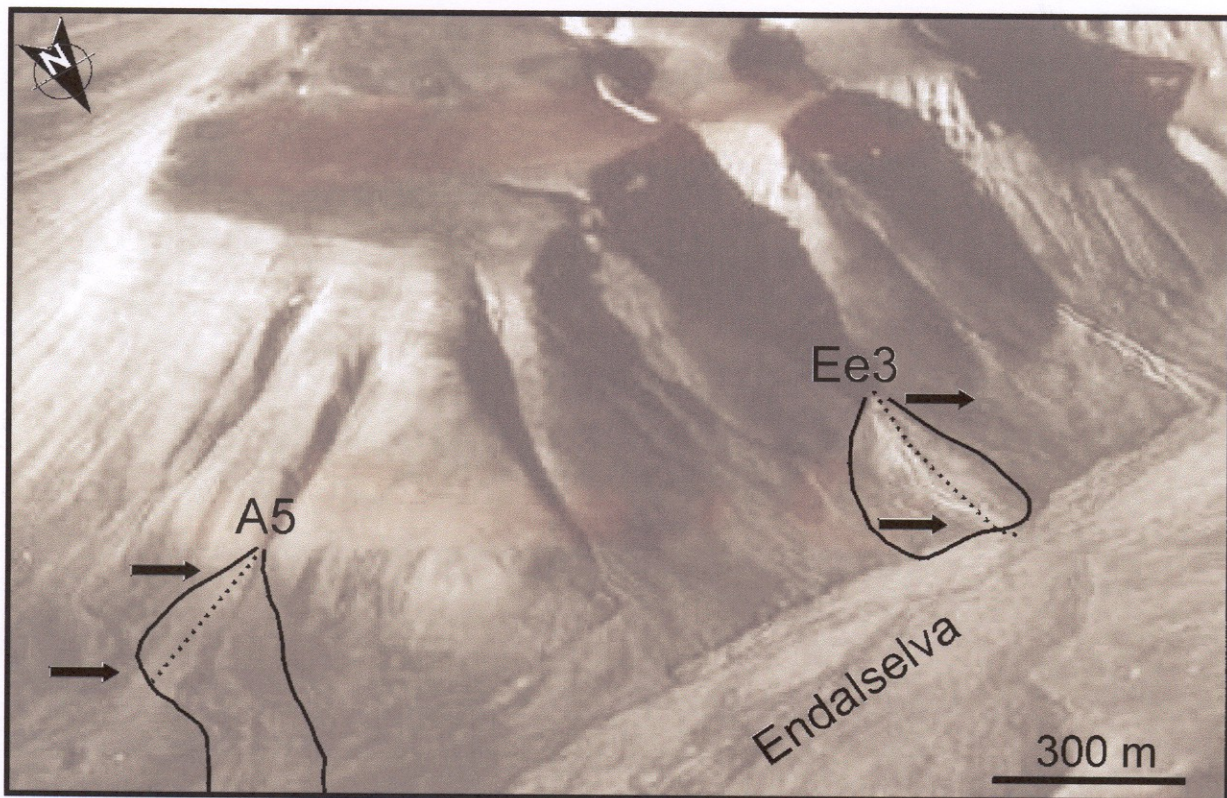
Fig. 4.1: The two valley-side fans selected for the systematic measurements of snow-cover thicknes. The measurement period was from March 10th till April 8th, 1998 (Norsk Polarinstitutt oblique aerial photograph S-36 2296). The arrows indicate the fix-point measurements presented in table 4.1 and the black (dottted) lines inside fans A5 and Ee3 are the profiled described in a later section.

Table 4.1: Fixed-point measurements of snow thickness (cm) in two parts of two different fans, with the maximum air temperature of the preceding week. The location of the fans is shown in Fig. 4.1. The measurements are from relatively smooth fan surface, outside channels. The date notation is dd.mm.yr. The upper parts of the fans were inaccessible for direct measurement on the last two dates, due to snowmelt. The temperature is a weekly mean of the two maximum air temperature readings from each day (data in Appendix A).

Date	21.04.98	28.04.98	05.05.98	13.05.98	20.05.98	27.05.98	03.06.98	10.06.98
Fan A5, upper part	51	47	44	45	51	49	-	-
Fan A5, front part	49	46	50	43	44	42	33	0
Fan Ee3, upper part	138	145	144	149	147	147	-	-
Fan Ee3, front part	26	24	24	24	24	22	15	0
Air temperat. (ºC)	-8.8	-6.0	-5.7	-4.7	-4.3	-4.6	-0.7	+1.9

A considerably thicker snowpack occurred in the colluvial channels, where the snowdrift has filled depressions up to 5 m deep. Several meters of snow have commonly accumulated in the mountain-slope ravines above the fan apices. Prominent snow cornices occurred at the plateau edges, at the margins of river terraces and the bedrock canyon on the valley floor, as well as at the edges of the bedrock slope ravines. Most of the lower-altitude cornices indicated an important role of the up- and down-valley winds, and a similar pattern of valley winds was indicated by the forms of snow accumulation in Longyeardalen, the sister valley to the west. The cornices on the alluvial terraces of Endalselva were locally up to 5 m thick and occasionally seen collapsing into the river channel.

In the inner, flatter parts of the adjacent mountain plateaux, the snowpack thickness was around 100 cm and decreasing towards the plateau edges. The snow cornices at the plateau edges were clearly due to the sweeping cross-winds, responsible also for most of the precipitation. The better-developed cornices on the eastern side of valley corresponded rather well with the predominance of easterly winds accompanied by snowfall (Appendix B). On the western plateau "drop-shaped" ridges were formed of snow deposited by local winds blowing vertically up from the valley floor. The head part of the snow ridge is formed at the plateau edge, whereas the body and thin tail extend far into the plateau area westwards. The ridges formed in connection with these strong easterly winds can be up to 10 m wide, 5 m high and 100 m long (Fig. 4.2).

The cross-sectional topographic profile of Endalen is slightly asymmetrical, with the western valley-side slope somewhat steeper than the eastern one, but the hanging cornices are more common and more prominent on the eastern cliff edge above the valley. These conditions may have important implications for possible occurrence of snow avalanches, although the process has not been observed in Endalen in 1998 and reports on snowflows in Spitsbergen are few. However, it should be emphasized that: (a) some cornices were observed
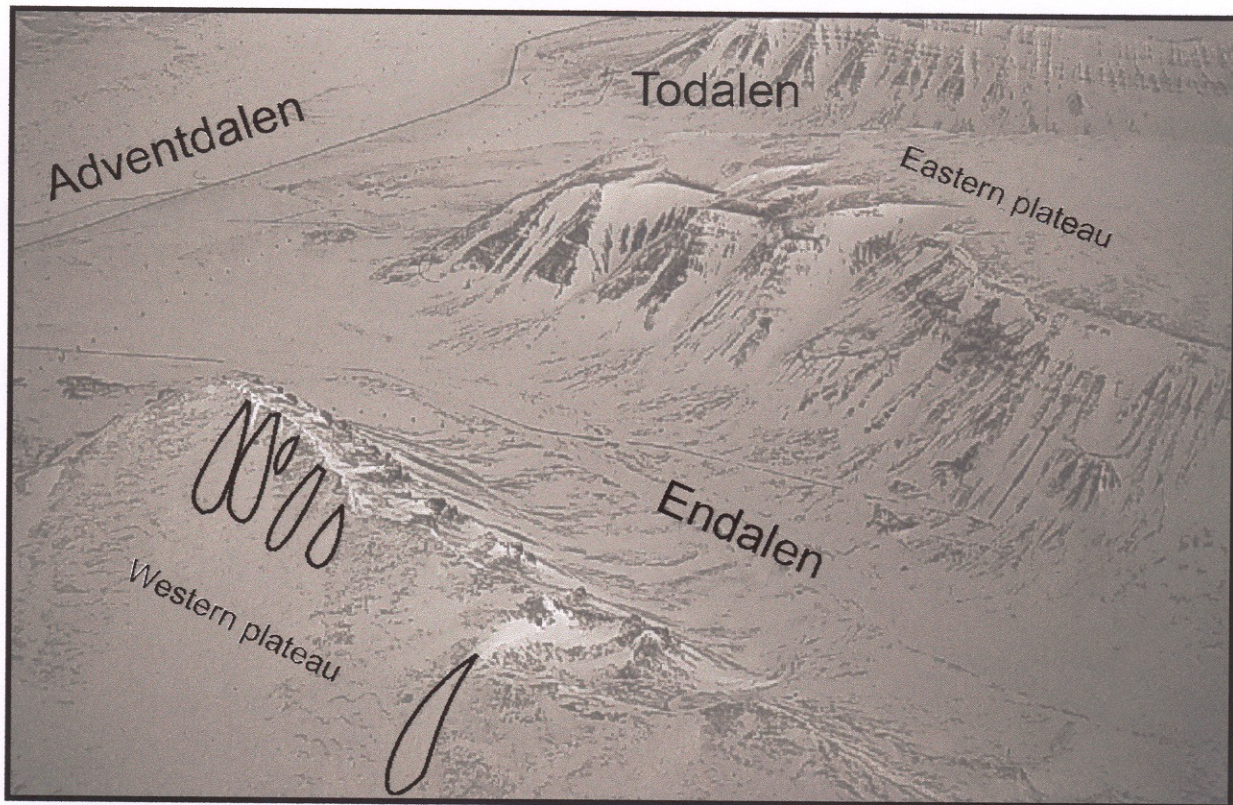
Fig. 4.2: Oblique aerial photograph showing the mouth of Endalen and adjacent plateux on March 3rd, 1998. Note the inverse cornices on the western plateau (marked as black lobes) and the absence of snow on the edge of the eastern plateau. Photograph courtesy of I. Lønne.

to form and grow on weakly basis; (b) a snow avalanche in the local conditions would have a duration of little more than 10 seconds and be readily obliterated by snowdrift; and (c) the sparse population and the winter perennial darkness render the recognition of possible avalanches very difficult, limited to chance. As discussed in a subsequent chapter, there are sedimentological reasons to believe that snow-rich debrisflows, and possibly occasional snowflows, have been involved in the colluvial sedimentation in the valley (see Fig. 3.9B, see also Lægreid, 1999).

The frost-shattered bedrock cliffs are exposed throughout the winter and shedding considerable amounts of debris, by rockfall processes, onto the colluvial fans and the thick snowpack in the ravines. Trail marks of bouncing pebbles and cobbles have commonly been observed, and the snowpack was in many places covered with a carpet of shale debris. The sweeping effect of valley-parallel winds on the colluvial-fan surfaces render the elevated debrisflow levees and lobes virtually snow-free through most of the winter time, although considerable amounts of snow are entrapped by the openwork, cobbly to bouldery surficial gravel. The sandbrush effect of wind carrying ice particles causes abrasion of the exposed debris and bedrock, generating significant quantities of fine sediment. Fine-grained shale and

coal detritus mixed with snow particles, commonly drapes the lee sides of snow dunes and the snowpack surface in the wind-shadow areas behind topographic obstacles.

The river terraces at the valley floor tend also to be snow-free, due to the strong wind sweep, and the exposure of vegetation renders these areas an attractive grazing ground for reindeer. Likewise, large parts of the mountain plateaux are snow-free. In Bayfjellnosa area, at the plateau corner between Endalen and Adventdalen, the frost-shattered bedrock surface remains snow-free practically throughout the winter (see Fig. 4.2).

4.2. Snow-cover thickness and meteorological conditions

Snow depth profiles of the snow cover in Endalen has been measured systematically, once a week from March 10th till April 8th (1998), at a number of fixed points along the longitudinal line on the surface of the colluvial fan Ee3 (see location in Fig. 4.1). An attempt has been made to collect similar data from the surface of fan A5 on the adjoining side-slope of Adventdalen, but the snow cover there appeared to be thin and discontinuous. This indicates high wind erosion and little deposition of snow and the measurements are thus disregarded.

The thickness of the snow cover on the surface of fan Ee3 was highly varied (Fig. 4.3), depending upon the local topographic relief of the debrisflow channels, levees and lobes. The snow was considerably thicker in the channels (see profile segments around 150, 240 and 320 m in Fig. 4.3) and due to the transient development of snow dunes (see fluctuations in the profile's inter-channel segments, Fig. 4.3). The snow cover was markedly thicker within the uppermost 80 m segment of the profile (Fig. 4.3), due to the deeper channels and the wind-shadow effect of the higher levees, the appearance of a distinct snow mound on the 1st of April has been attributed to a transverse movement of a snow dune. It is difficult to assess as to how much of the snow-cover thickening in the profile was due to snowfall and how much due to the snowdrift alone. The corresponding data on precipitation during those 5 weeks indicated a total snowfall of merely 7.8 mm in the Longyearbyen airport area. However, the windy weather (Table 4.2) rendered the measurements unreliable.
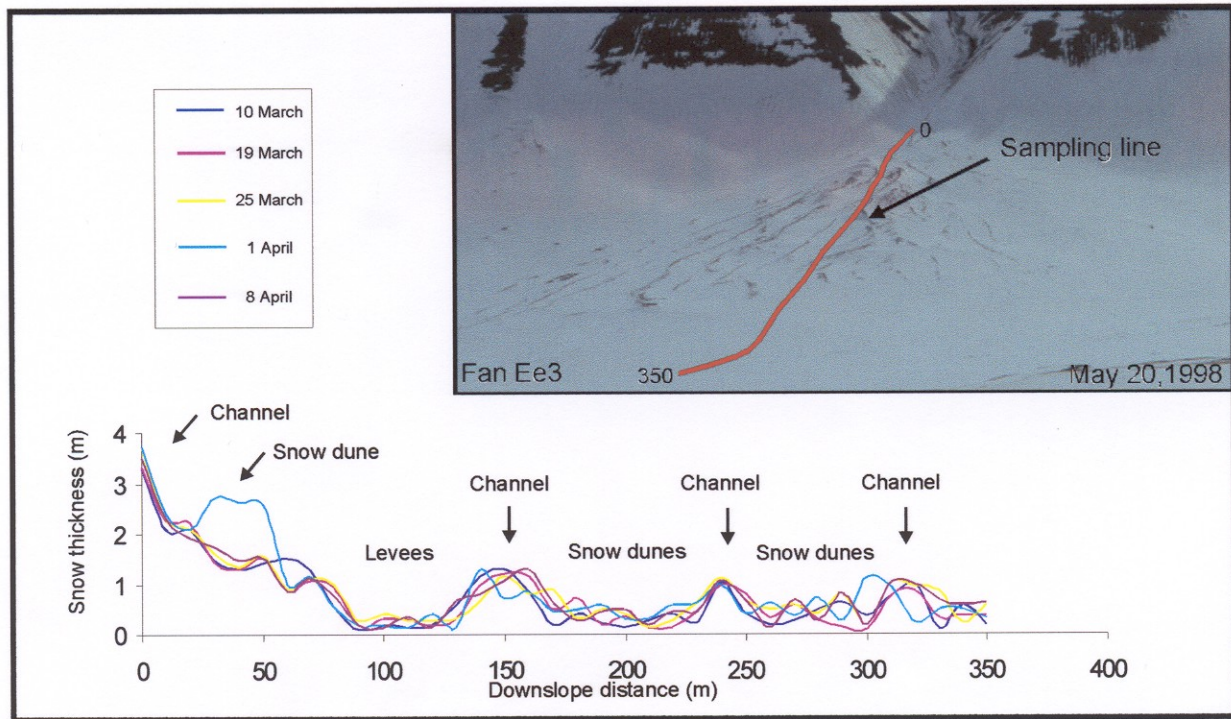
Fig. 4.3: Snow-cover thickness profiles from the surface of fan Ee3 marked with red in the picture (see location in Fig. 4.2).

Table 4.2. Average weekly wind speed calculated from 28 measurements taken each week 10 m above the ground at the Longyearbyen Airport (Appendix 1).

Calendar week's (mid-March to mid-April)	11	12	13	14	15
Windspeed (knot)	11,3	12,7	19,9	8,2	4,4

4.3. Photographic documentation of snow cover

During the March to June season of 1998, the areal changes in the snow cover on two of the valley-side fans (fans A5 & Ee3 in Fig. 3.8; Fig. 3.9A) have been documented by taking photographs taken from a fixed point once a week (Fig. 4.4; Fig. 4.5). Fan Ee3 is facing the northwest whereas fan A5 is on the side-slope of Adventdalen and facing the northeast. Their exposure to both wind and sun were thus not the same. The photographic documentation was meant to show changes in the snow distribution and the extent of snow-free areas from week to week.

The snow cover persisted throughout the winter and began to disappear very slowly, without any signs of meltwater flow. The changes in the areal distribution of snow were

minor and limited to areas with the thinnest snowpack. The snow gradually became granular and compact near the end of the winter, and several surficial patches of ice crust developed in the snowpack above fan Ee3, indicating temperature fluctuations around the melting point. However, the nearest meteorological station (airport) seldom recorded any temperature rises above 0°C (see meteorological data in Appendix A), and neither was any meltwater runoff noted in Endalen, except on the 16th of May, when water was seen dripping from a horizontal siltstone bed in the ravine above fan Ee3. At the end of the winter, the sun apparently began to warm up the snow cover and particularly the snow-free darker areas, which then quickly expanded. The sunlight heat from the midnight sun must have accumulated and caused brief local melting, following by refreezing and the formation of surficial ice crust.
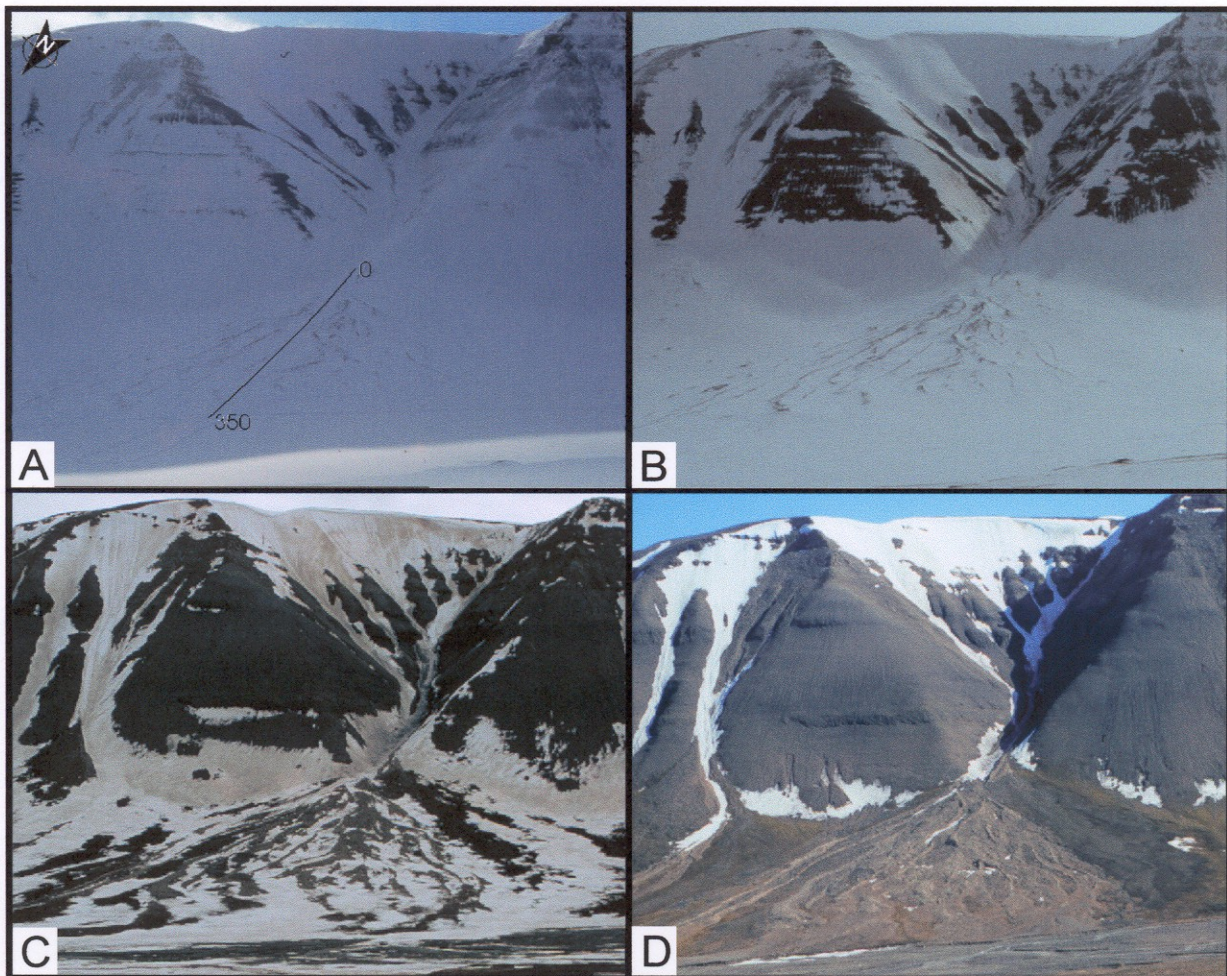
Fig.4.4: Areal changes in the snow cower on fan Ee3: (**A**) 21. April 1998, note the location of the 350-m snow depth profile shown in Fig. 4.4; (**B**) 20. May 1998. (**C**) 10. June 1998; (**D**) 24. June 1998.
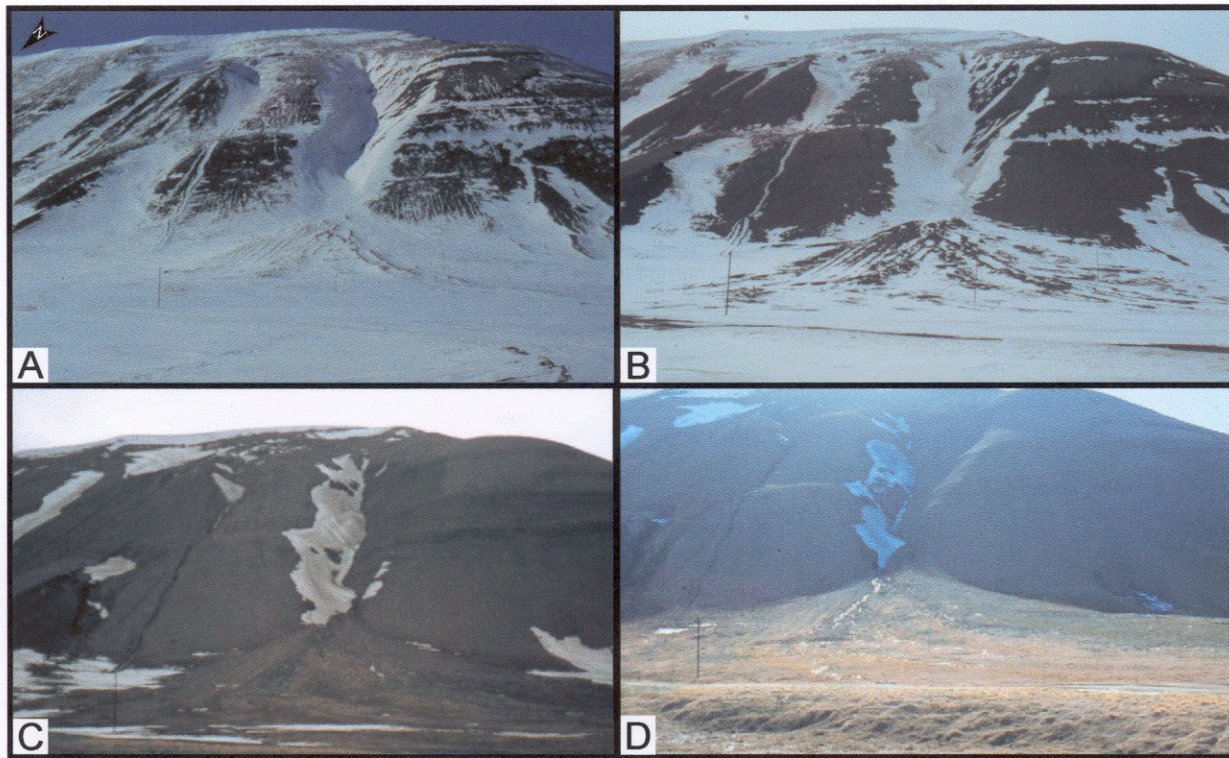
Fig. 4.5: Areal changes in the snow cover on fan A5: (**A**) 21. April 1998; (**B**) 20. May 1998; (**C**) 10. June 1998; (**D**) 24. June 1998.

During the calendar week 22, the air temperature continuously fluctuated around 0°C and a full-scale melting began. On the 27th of May, ponds of meltwater appeared on the flat floor of Adventdalen, but no running water was yet observed in Endalen, although the corresponding photographic documentation showed marked shrinking of the snow cover. The following week 23 was even warmer, and the meltwater formed a maze of channels beneath the snowpack and was seen flowing in the pre-existing channels in fan-apex areas. At this time three waterfalls were observed at the plateau edge above the entrance of abandoned Coal Mine 5. During the following two weeks, nearly all snowpack in Endalen had melted, and the surficial runoff of meltwater from snow persisted in the valley and on the valley-side slopes until the early July. Later, the main part of the surficial waterflow – increasingly limited to the valley axis – was derived from the melting of the active layer and glacial ice. The slope soil cover remained saturated with seeping water so long as the air temperatures stayed above the freezing point. Permafrost prevents water from draining down through the sedimentary cover, whereby all the drainage is shallow and results in the complete soil saturation. The least stable parts of the slope's sedimentary cover often fail in these conditions (e.g., see Fig. 3.17).

Due to their different locations, the fans studied are characterized by different exposure to sun and wind. For example, fans on the western side of the valley (Ew1 & Ew2 described in Lægreid, 1999) receives more sunlight than Ee3 and A5, whereas fan A5 is more exposed to wind and consequently the west side fans have a higher rate of melting while on A5 the snow gets little chance of accumulating in the first place. However, in the ravine above fan A5, an extensive and thick snowpack had accumulated due to lee-side accumulation during the winter, and its melting then resulted in waterflow that scoured a new small channel on the fan surface. Small-scale debrisflows were generated by the local collapses of slope derived debris deposited in depocenters near the fan apex (Fig. 4.6).

Fig. 4.6: Small debrisflow on the surface of fan A5. The levees consists of pebbly gravel derived from the Carolinefjellet Fm., and debrisflows like this are common during the peak of the melting season (May-June). The notebook (scale) is 20 cm long.

5. THE VALLEY-SIDE FANS AND SLOPE-WASTING PROCESSES

This chapter focuses on the development and detailed surficial characteristics of the coarse-gravelly colluvial fans on the eastern side-slope of Endalen. The discussion puts special emphasis on the depositional processes and their implications for the slope-sediment dynamics in this high-arctic semiarid valley.

5.1. Terrestrial fan categories

Colluvial fans are, as defined in Blikra & Nemec (1998)*,* generally much smaller and steeper than common alluvial fans (Fig. 5.1), and are situated in the foot zone and lower part of a mountain slope, with the apices located higher on the slope, often at the bases of slope ravines acting as the fan catchments (see Fig. 2.7). The depositional slope typically ranges from 15-20º near the fan toe to 35-45º near the apex, but may be significantly lower where long-runout snow avalanches predominate or other factors have come into play, causing major downfan transfer of sediment (e.g., upper-fan erosion by snowflows, waterflow processes or stream incision). The plan-view radius of a colluvial fan seldom exceeds 0.5 km. The sediment is typically gravelly and very immature, derived locally by slope-wasting processes, and the debris found near the fan toe is often as coarse as that near the fan apex (Rapp, 1960; Åkermann, 1984; Blikra & Nemec, 1998). However, due to the gravity differences between clasts, rockfall dominated colluvial fans often show an upslope-fining of the gravel causing an increase in the slope roughness towards the fan toe (Blikra & Nemec, 1998; Nemec & Kazanci 1999). Most colluvial fans have a concave-upward longitudinal morphometric profile, but some may evolve into convex-concave or show nearly straight segments, depending on the predominant processes and the magnitude of sediment transfer from the fan apex to the toe. Colluvial fans dominated by rockfall processes are some of the steepest and shortest, although the steepness of a fan depends upon the avalanche size and runout distance (Blikra & Nemec, 1998). Colluvial fans dominated by cohesive, high-viscosity debrisflows are typically comprised of relatively broad gravel lobes and generally steeper than those dominated by the more mobile, lower-viscosity debrisflows (watery, or wet snow-bearing), where the fan surface typically shows elongate scour-and-lobe features comprised of a
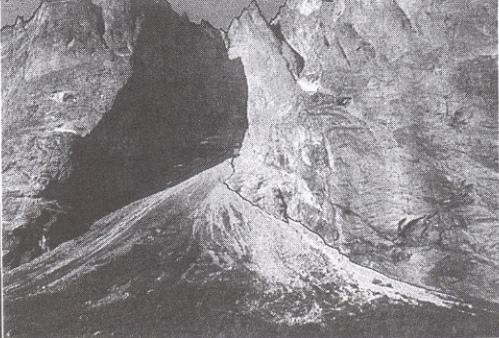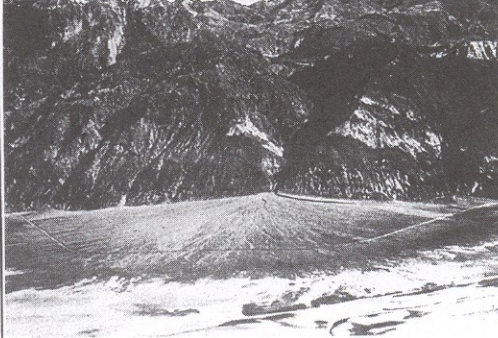
TYPICAL CHARACTERISTICS	colluvial fan	alluvial fan
Geomorphic setting:	mountain slope and its base (slope fan)	mountain footplain or broad valley floor (footplain fan)
Catchment:	mountain-slope ravine	intramontane valley or canyon
Apex location:	high on the mountain slope (at the base of ravine)	at the base of mountain slope (valley/canyon mouth)
Depositional slope:	35-45° near the apex, to 15-20° near the toe	seldom more than 10-15° near the apex, often less than 1-5° near the toe
Plan-view radius:	less than 0.5 km, rarely up to 1-1.5 km	commonly up to 10 km, occasionally more than 100 km
Sediment:	mainly gravel, typically very immature	gravel and/or sand, immature to mature
Grain-size trend:	coarsest debris in the lower/toe zone	coarsest debris in the upper/apical zone
Depositional processes:	avalanches, including rockfall, debrisflow and snowflow; minor waterflow, with streamflow chiefly in gullies	debrisflow and/or waterflow (braided streams)
EXAMPLES	The Brotfonna colluvial fan, Trollvegen near Romsdal, Norway; one of the world's largest colluvial fans, with a height of 830 m and a plan-view radius of 1.5 km.	The Badwater alluvial fan, eastern side of Death Valley, California; a modest fan, with a radius of c. 6 km.

Fig. 5.1: A comparison of the distinctive features of colluvial fans and alluvial fans (from Blikra & Nemec, 1998).

tongue-shaped bouldery lobe passing upslope into a boulder-leveed channel (Rapp & Nyberg, 1981; Blikra *et al.*, 1989; Blikra & Nemec, 1998).

Alluvial fans, in contrast, are typically larger and much less steep, formed at the mouths of mountain valleys, where a stream emerges from the valley, or canyon, and expands to deposit sediment on the floor of an adjoining larger valley or a piedmont/coastal plain (Hooke, 1967; Bull, 1972, 1977; Wasson, 1974; Harvey, 1984, 1989, 1992; Hooke & Rohrer, 1977, 1979; Rachocki, 1981; Hubert & Filipov, 1989; McArthur, 1987; Lecce, 1991; Whipple & Dunne, 1992). In short, alluvial fans are commonly formed as intersection-point deposits, unlike the majority of colluvial fans. Some very small alluvial fans may be only a few tens of meters in radius, but the majority of alluvial fans in mountainous terrains are larger, ranging from a few kilometers to more than 100 km in size. The depositional slope of an alluvial fan is seldom more than 10-15° near the apex and often less than 1-5° near the toe (Fig. 5.1). The sediment may be immature, but generally tends to be mature due to the longer transport distance and the greater ability of flowing water to segregate gravel and sand. The coarsest sediment tends to be deposited in the fan-apex area, where the main loss of stream competence occurs. Most alluvial fans have a concave-upward longitudinal morphometric profile, although it may consist of a series of nearly straight segments, rather than be a smooth curve. Both alluvial and colluvial fans may coalesce into broader aprons. Textbook reviews invariably contend

that the alluvial fans in semiarid climatic settings are generally dominated by sheetfloods and sediment-gravity flows, whereas those in humid climatic conditions are dominated by streamflow processes. However, this notion does not hold for the semiarid arctic conditions, where the alluvial fans are dominated by meltwater flow, even where debrisflows and/or snowflows are involved, and are commonly developed as proglacial outwash features. The large alluvial fan formed by Endalselva at mouth of Endalen (Fig. 3.16) is a typical example of such a system.

Both an alluvial and a colluvial fan can be subject to incision in the upper part and develop an intrafan intersection point, below which deposition and aggradation prevail. The location of the intersection point along the fan's profile depends on the fan steepness and the frequency and amount of discharge passing over the fan surface. A decrease in discharge tends to move the intersection point downfan (Bowman, 1978). Lægreid (1999) has recognized this kind of development to characterize the colluvial fans on the side-slope of Adventdalen directly west of Endalen's outlet. Similar characteristics are also typical for some of the colluvial fans in area B.

In semiarid settings, debrisflows are typically generated by infrequent torrential rainstorms, with the runoff flushing debris that has accumulated in the fan catchment area (Blissenbach 1954; Caine, 1980; Larsson, 1982). Debrisflows are equally common in humid climates, where heavy rainfall is a recurring feature and where there is an abundance of fine-grained sediments available in the source area. The behavior of a debrisflow depends upon the sediment grain-size composition, especially the contents of cohesive clay; the amount of water or possibly snow admixed; and the slope gradient and surface roughness (Johnson & Rodine, 1984; Blikra & Nemec, 1998). Rheologically, a debrisflow is a simple- to pure-shear plasticoviscous flow, which means that the granular material shears and tends to spread, behaving like a single-phase fluid. The pore-fluid pressure, nearly sufficient to cause liquefaction, may persist in debrisflow interior till the grain contact friction and bed friction, particulary at the flow margins, reach a finite shear strength leading to the flow braking (Major & Iverson, 1999). When the shear stress declines to the shear-strength level, the flowing mass "freezes" *en masse*, typically forming a well-defined, steep-fronted lobe, often with a very pronounced fabric pattern. Debrisflows may be cohesive or cohesionless (frictional), depending upon the nature of the shear strength (Nemec & Steel, 1984), and either category may range from high to low viscosity, depending chiefly on the content of water or wet snow/slush (Blikra & Nemec, 1998) (Fig. 5.2).

SEDIMENTARY FEATURES	DEPOSITIONAL PROCESSES					
	rockfall/debrisfall		debrisflow (AVALANCHES)		snowflow	waterflow
TYPE/GEOMETRY OF DEPOSITS — three-dimensional view	Fresh rock debris; Resedimented gravel; Upslope fining; Varied runout; Scattered clasts. Lobate or "patchy" accumulations of debris; scattered large "outrunners".		Relatively broad lobes; Highly elongate, tongue-shaped lobes (upslope fining); Levées; Spill-over lobes. High-viscosity debrisflow / Low-viscosity/watery debrisflow.		Toolmark grooves; "Debris horn"; Longitudinal grooves, debris ridges & clast-thick levées; One clast-thick levées; Small "digitated" lobe with frontal wash-out sand; "Debris shadow"; "Patchy" lobes; Scattered clasts. Drier snowflows / Slushflow.	Levées of bypassing debrisflows; Overbank sand; Narrow, gully-type channels; or shallow channels with braid-bars.
vertical cross-section	Upward fining; Openwork; Infilled by "tail"; Upward fining; Openwork.		Tabular beds. Large "floating" clasts.	"Imbricate" beds. Lenticular beds with "imbricate" or more complex stacking.	Indistinct boundaries; Melt-out clasts in precarious positions; Lens with sandy downslope "tail"; Stratified waterlain infill of larger interstices; Redeposited humic soil; Waterlain infill.	Remnant debrisflow deposits; Tractional infill. Isolated channel-fills (up to 1.5 m thick).
TEXTURE AND STRUCTURE	Highly immature debris; mainly angular clasts	Mature debris; subrounded to rounded clasts	Matrix-rich to clast-supported. Sandy/muddy matrix. Common "coarse-tail" inverse grading and outsized cobbles or boulders.	Clast-supported, bouldery to cobbly "heads" and clast- to matrix-supported, pebbly upslope "tails". Common normal grading.	Unsorted, scattered clasts and gravel "patches" infilled with waterlain sand or pebbly sand. The sand in large interstices shows stratification, but is massive, very fine/silty and possibly shell-bearing in submarine deposits.	Clast-supported, pebbly to cobbly gravel interlayered with poorly sorted/stratified sand. Matrix-supported gravel occurs as debrisflow remnants.
	Boulder to sand size grade. Clast-supported and commonly openwork, with pebbly to sandy infill at the top. Deposits often infilled with waterlain sand and/or redeposited soil material.					
CLAST FABRIC	Boulders and large cobbles often show "rolling" fabric, $a(t)$ or $a(t)b(i)$, when emplaced frontally in isolation. Many large clasts upslope show "sliding" fabric $a(p)$, but a disorderly "adjustment" fabric predominates; "shear" fabric $a(p)$ often typifies the avalanche's overriding tail, when evolved into a grainflow.		Large clasts mainly aligned downflow, $a(p)$ or $a(p)a(i)$, but showing $a(t)$ orientation along the lobe front.	Common "rolling" fabric $a(t)$ in the frontal and top part of the debrisflow head; common "shear" fabric $a(p)$ or $a(p)a(i)$ in the flow's tail.	Mainly disorderly (chaotic "melt-out" fabric). Boulders and cobbles deposited from turbulent snowflows may have "rolling" fabric $a(t)$, but the scattered debris is vulnerable to rotation by subsequent avalanches. Dense snowflows and slushflows may create "shear" fabric $a(p)$, but this loses order during the melt-out.	Common tractional fabric; poorly developed in gullies due to clast pivoting and adjustment to banks. Many large clasts are rotated in situ to $a(p)$ position by less competent waterflow.
DEBRIS SOURCE	Weathered bedrock.	Glacial till and valley-side kame terraces.	Glacial till, kame terraces and upper-slope colluvium.		Glacial till and upper-slope colluvium, including fresh bedrock. Common slope-soil erosion.	Upper slope colluvium and glacial till.

Fig. 5.2: Summary of the main depositional processes and facies of colluvial fans/aprons, with special reference to the postglacial colluvium in western Norway (from Blikra & Nemec, 1998).

The high-viscosity debrisflows are less mobile and their deposits are relatively broad, non-erosive lobes containing large "floating" clasts in almost any segment. When deposited on the steep slope of a colluvial fan, the lobe may be elongate and slightly erosive in the upslope part, but characteristically steep-sided and fairly uniform throughout. The lobes of high-viscosity debrisflows may range from clast-supported to matrix-rich, with the large clasts mainly aligned downflow, showing $a(p)$ or $a(p)a(i)$ fabric, but often $a(t)$ orientation in the lobe's frontal part. The fabric of the large discoidal and blade-shaped clasts may tend also to planar. The low-viscosity debrisflows are more mobile, possibly somewhat turbulent, and their deposits are highly elongate tongues passing upslope into leveed, channel-like erosive furrows, possibly with some smaller, spillover lateral tongues (see Fig.5.2). These tongue-shaped lobes commonly show a pronounced upslope thinning and fining, whereas their downslope/frontal parts are relatively thick and rich in large cobbles/boulders. The frontal part often shows a "rolling" clast fabric $a(t)$, paralleling the lobe margin, whereas fabric $a(p)$ or $a(p)a(i)$ may be more common in the upslope part (Blikra & Nemec, 1998). The same kind of fabric, including marked $a(t)b(i)$ clast orientation in some cases, has been reported in

Spitsbergen (Larsson, 1982) and are also demonstrated by the recent experimental studies of pebble-gravel debrisflows (Major, 1998).

Rockfall is a gravitational movement of fragmented bedrock, liberated abruptly from a steep headwall, with the components tumbling freely downslope by rolling, bouncing and sliding. Large blocks often disintegrate upon impact, "splitting" into smaller debris. The rock debris is characteristically angular and immature. In a rockfall, the clasts typically move through a series of impacts on the colluvial slope, which may retard the clast, accelerate it, or stop it instantly (Blikra & Nemec, 1998). Factors controlling the runout of a falling clast include the clast size and shape and the gradient and the roughness of the slope surface (Parsons & Abrahams, 1987). Clasts roll down easier on relatively smooth, low-roughness slopes. The amount of debris involved in a rockfall often determines the mobility of such an avalanche. In a rockfall, the larger clasts are often outpacing the smaller ones, whereby the resulting gravel tongue shows a downslope coarsening. The downslope part is typically openwork, composed of boulders and large cobbles, whereas the finer-grained upslope part is smoother, often infiltrated with granule-rich sand. Small rockfalls may accumulate in ravines or other slope recesses, and tumble further down as a loose mass once the threshold of frictional yield has been exceeded. Likewise, rockfall deposits that have accumulated in the apical part of a colluvial cone may become unstable and move further downslope as a secondary rockfall or a debrisflow (Blikra & Nemec, 1998). The later might bee a grainflow or a cohesive debrisflow if the fan-head gravel has been illuviated with mud (Nemec & Kanzanci, 1999). The fabric of rockfall boulders and cobbles on a low-roughness slope may be of a "rolling" type, a(t) or a(t)b(i), but is most often random on high-roughness slopes (Blikra & Nemec, 1998).

The slope-waste processes in Spitsbergen include both debrisflows and rockfalls. Åkerman (1984) has recognized in Adventdalen area that the debrisflows are more common on the east- and north-facing slopes, where the slopes lie in the shadow. The degree of insolation affects also other parameters important for the slope-wasting processes forming the gravel fans, such as the high air temperature fluctuations during winter cause on a local scale, favorable conditions for frost weathering. During summer the midnight sun, by the same reason, cause a greater activity of rockfall processes than observed at lower subarctic latitudes (Åkerman, 1984). The steep margins of the mountain plateaux are shedding solitary bedrock clasts and small rockfalls on daily basis, with some of the debris falling directly onto the colluvial slope, but the main part accumulating in the slope ravines. The impact of direct solar radiation, maximized by the sparse vegetation and the absence of snow cover, renders the

thawing of the active layer deeper, with a high chance of debrisflow occurrence due to almost every rainstorm (Larsson, 1982). Such catastrophic slope-waste events have a recurrence period of 50 to 400 years in the Arctic mountains of northern Sweden (Rapp & Nyberg, 1981), but may be more frequent in the Svalbard region, as indicated by the historical observations from the adjacent Longyeardalen (see also review by Lægreid, 1999).

5.2. Description of the valley-side fans

The valley-side gravelly fans, considered to be colluvial, have been introduced and briefly described in chapter 3, and their morphology and depositional processes will now be discussed in more detail on some of the fans in area A and B. All these fans are related to the mountain plateau on the eastern side of Endalen. The fans located in area B are in Endalen itself, whereas those located in area A are on the side-slope of the Adventdalen (see Fig. 2.2)

5.2.1. Colluvial fans in area A

Compared to most of the fans in areas B and C, the fans in area A have very small catchments (see Fig. 3.3A) and abut on a mountain slope exposed to the strong winter winds from the northeast, which prevents the accumulation of a thick snowpack. The ravines above the fans are relatively small and poorly developed. The uppermost part of the bedrock slope consists of the Firkanten Fm., but lacks the steep rock wall and ravines which is present in area B. The underlying Carolinefjellet Fm. consists of shales interbedded with sandstones, where ravines up to 2-4 m deep have developed (Fig. 5.3A). Rainfall and the meltwater from permafrost thaw are practically the sources of surficial water runoff on these fans. Some meltwater is produced by the snowpacks accumulated in the ravines, especially at fan A2

   Colluvial fan A1 – The apex of this fan is poorly defined, at an altitude of ca. 220 m, and the deposits are clearly products of slope-waste processes. The fan-feeding ravine is shallow and wide, with diffuse outer margins (Fig. 5.3B). The ravine has apparently been formed mainly by rockfall processes, as indicated an extensive accumulation of angular boulder-block scree in the upper to middle segment of the fan's central sector derived from the Firkanten Fm. This scree deposit overlay a smoothened vegetated fan surface. The apex is poorly defined and it is possible that some of the sediment in this fan has been derived from a mountain-side lateral moraine. This is a speculative suggestion because no moraine has
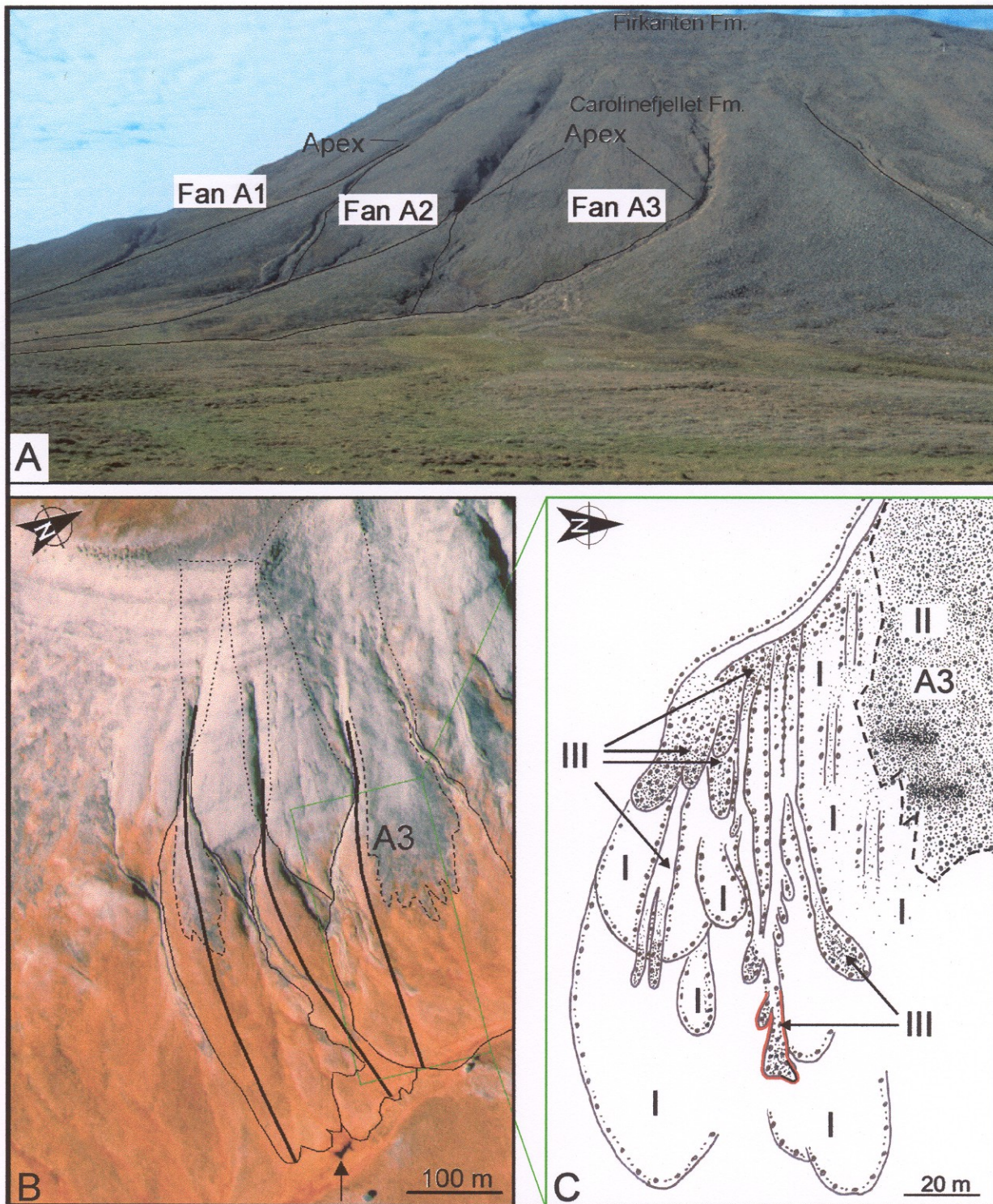
Fig. 5.3: (**A**) Photograph of fans A1, A2 and A3. Note their apex positions and the vegetated surface of their lower segments. (**B**) Aerial photograph showing the fan catchment areas and adjacent colluvial deposits. The morphometric profiles of the fans are measured along the blue lines (see Fig. 5.3D). Note the large accumulation of rockfall scree in the upper part of fan A3. (**C**) Field sketch indicating probable age relationships between debrisflow lobes, (l is the oldest). Clast fabric measurements are done on the red-marked lobe (see Fig. 5.4). (**D**) Next page: Longitudinal morphometric profiles of fan A1, A2 and A3, with cross-profiles over the debrisflow channels extending from the apex; α = the slope gradient measured over 20-m slope segments.

definitely been recognized at this locality, except for the mountain slope morphology, which resembles that of moraine-covered slopes elsewhere in the valley. Some small lateral terraces parallel to Adventdalen are present on the mountain slope, but one cannot preclude that these terrace might be sandstone benches of the Carolinefjellet Fm. (see Fig. 3.20). A prominent debrisflow channel extends along the left-hand flank of the fan, with pronounced levees of sandstone cobbles and boulders in the mid-fan segment and several small gravel lobes in the lower segment also containing an abundant amount of fine grained sediments (Fig. 5.3C). The morphometric longitudinal profile of the fan is shown on Figure 5.3D (top). The concave-upward profile is fairly smooth, with little evidence of channels and lobes, and its inclination decreases from 33° below the apex to 4° at the toe. In the middle segment and the lower part of the upper segment, the fan's central sector includes an older depositional surface with vegetated low-relief levees indicating debrisflow channels. The debris is coated with mosses and lichen, and the fan surface seems to have been smoothed by the action of frost, wind and possibly snow avalanches. The lower segment of the fan is densely vegetated, showing little more than vague morphological characteristics of debrisflow lobes not seen in the profile (see Fig. 5.3B). Scattered cobbles and boulders of possible rockfall or snowflow derivation are locally protruding above the fan surface, but the majority of the debrisflow lobes here are broad, low-relief features with fairly smooth surfaces and probably a matrix-rich texture. The runout distance of the debrisflows on this fan ranges from about 360 to 531 m, with some of the flows having reached the lower fan slope of merely 2° inclination. The heavily vegetated surface and lack of good exposures precluded detailed observation on the texture and clast fabric of these debrisflow lobes.

This fan clearly show a three stage development with the oldest vegetated fan surface and long runout debrisflow lobes as the first deposit, a rockfall deposit in the upper and middle segment as second and the fresh debrisflows crosscutting both aforementioned deposits as the third stage deposit.

Colluvial fan A2 – This is the middle fan of the three studied in area A (Fig. 5.3A). The fan is slightly smaller (max. runout: 370 m) and less steep than fan A1, and has the apex at an altitude of 160 m (Fig. 5.3D), where the sandstone beds in the Caroline Fm. render the bedrock slope outside the ravine almost vertical. The ravine is well defined, cut in the shales, but the catchment area of fan A2 is also relatively small. Boulders and cobbles are not particularly abundant on the fan surface even though the Firkanten Fm. sandstone is exposed at the top of the mountain slope. Most the sandy sediment and matrix-rich gravel in fan A2

Channel cross-profiles   Longitudinal morphometric profiles

Fan A1

Fan A2

Fan A3
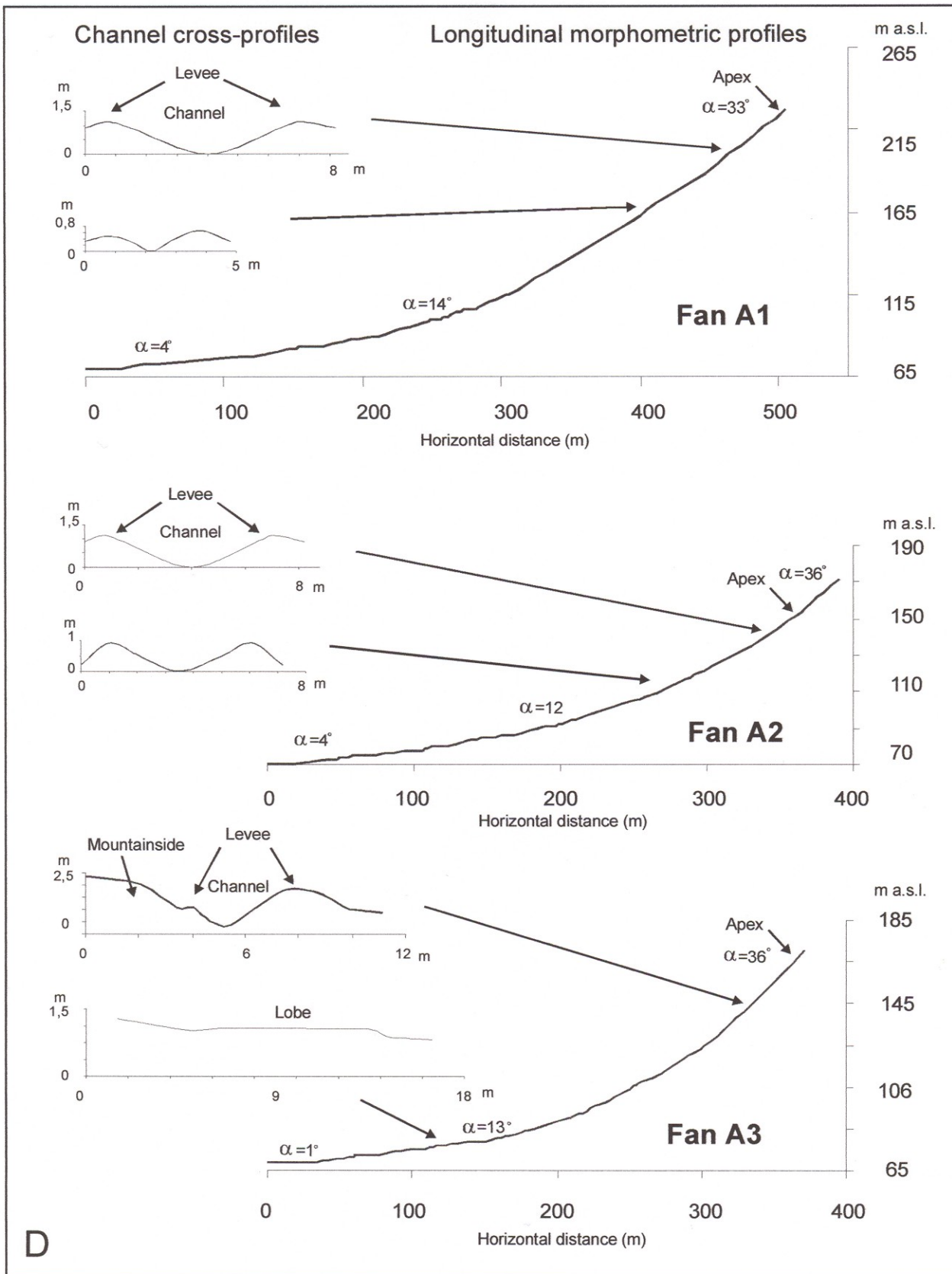
are derived from the lower-lying Carolinefjellet Fm. The upper and middle segments of the fan show an older, vegetated depositional surface with poorly recognizable debrisflow levees, indicating shallow channels. A small amount of scattered cobbles and boulders occur on the surface of the fan's upper segment, probably due to sporadic small rockfalls, and a steep debrisflow channel extends from the ravine into the fan's right-hand sector. Below the apex, the channel turns towards the right-hand sector of the fan, and the left-hand overbank area shows spillover gravel with some cobbles and small boulders spread out over the fan surface. Fan A2 has coalesced with the two adjacent fans, A1 and A3. Some of the lobes in the lower segment are highly elongate vegetated tongues with steep fronts, 50-70 cm in relief. The lower part of the slope in area A is covered with moss, grass and mires, with a small pond formed in a local depression due to the permafrost-hindered drainage (Fig. 5.3B). The lack of a good sedimentological description is in this area caused by problems related to the freeze and thaw cycles permafrost and the highly vegetated surface. The lower segment is therefore only morphologically described.

The slope profile of fan A2 is also very smoothened and show a clear concave-upward trend in the profile from a 4º inclination near the toe to 36º just above apex. Fan A2 only show a two stage story where deposits of relative age I and III are present as the smoothened surface and the fresh debrisflows respectively, while the rockfall deposit of stage II is absent. The ravine intersection point stays at the apex position (Fig. 5.3D).

Colluvial fan A3 – The apex of this fan is at an altitude of about 160 m at a sandstone-shale boundary, and shows a channel much like the apex of the previous fan, although the ravine here is less well developed. However, the catchment area of fan A3 is larger and steeper, and a greater part of the sediment is derived from the Firkanten Fm. The mountain slope above the fan is covered with cobbles and boulders of frost-shattered sandstone, with slope-waste processes transferring this sediment episodically onto the fan surface. The fan slope profile is very similar to that of fan A2 (Fig. 5.3D) due to the location of the profile not crossing the rockfall deposit (see Fig. 5.3B). The fan's central sector show the same characteristics, of an old smoothened surface (stage I) with some vaguely visible debrisflow channels and levees, as the central sectors of fans A1 and A2. All three fans in area A are overrun by fresh debrisflows (stage III) and a relative age relationship between deposits on the fans is established only by interpreting differences in vegetation cover and lichens on rocks and noting onlapping and crosscutting relationships. The stage I deposits have the longest measured debrisflow runout . The old smoothened surfaces on the three fans in area A are interpreted to be of the same relative age referred to as stage I in figure 5.3C. The fan

surface has a low roughness slope, but shows low-relief cobbly levees and old, vegetated channels formed by debrisflows (Fig. 5.3C).

A rockfall deposit has covered the entire left-hand sector of the fan (see Fig. 5.3). Most of the rockfall deposit has a cover of lichens and therefore a dark gray color, while the central part of the rockfall deposit show a fresher light gray color indicating resent rockfall activity in the area (Fig. 5.3A). The fabric of cobbles and boulders in these deposits is locally of a "rolling" type a(t) or a(t)b(i) on the lower slope, but are mainly random. The a(t)b(i) fabric may partly be due to the angular flat sandstone debris derived from the Firkanten Fm. This deposit, overlying the stage I smoothened surface, is cut by fresh debrisflows and therefore interpreted as a stage II deposit.
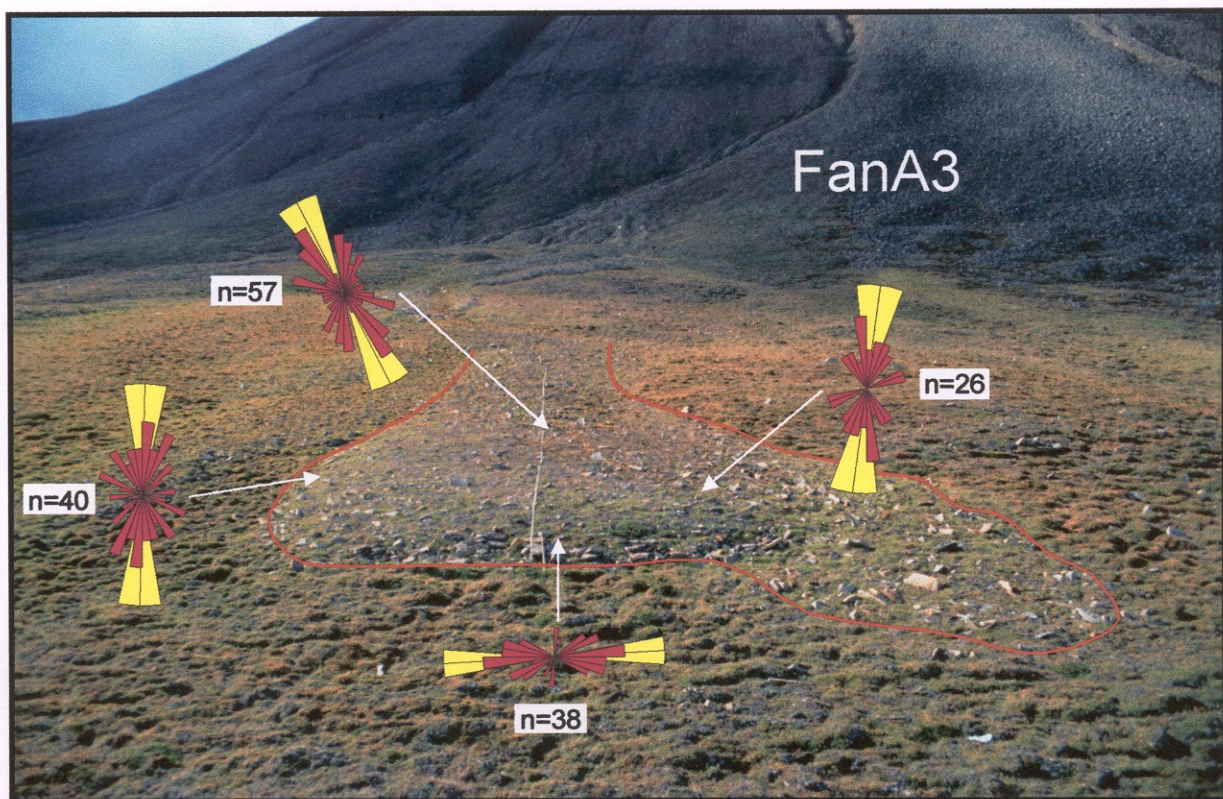
Fig. 5.4: Clast fabric of a relative fresh debrisflow lobe on the surface of fan A3. The rose diagrams summarize data from different parts of the lobe; n = number of measurements. For location, see the red-outlined lobe on Fig. 5.3C. The debrisflow lobe is about 11 m wide at the front and stretches over a downfan distance of about 50 m.

In the upper segment of the fan, sheets of cobbles and boulders are spread out on the surface as spillover deposits from the fresh debrisflows bypassing apex. The debrisflows bypassing have been directed to the fan's right-hand sector, scouring the older stage I depositional surface. The right-hand sector is dominated by these relatively fresh debrisflow

channels with cobbly to bouldery levees developed in the upper and partly middle fan segments and coarse-grained tongue-shaped gravel lobes in the middle segment and muddy/sandy sheet-like lobes in the lower segment. The coarser mid-fan lobes show a predominantly flow-transverse, "rolling" fabric a(t)a(i) in the frontal part and an a(p) fabric in the finer-grained upslope part (Fig. 5.4). These deposits overlay and crosscut previous described deposits and are interpreted to be stage III deposits.

5.2.2. Colluvial fans in area B

The colluvial fans in area B abut on the eastern side-slope of Endalen (Fig. 3.9A). The slope has a northwesterly exposure and consists of the sandstone-rich Firkanten Fm., overlain by the Basilika and Grumantbyen fms. directly above the plateau edge (Fig. 3.2). Fans Ee3, Ee5 and Ee6 receive meltwater from the adjoining larger portions of the plateau's area D. These fans are associated with relatively large and deep bedrock ravines, whose steep walls seem to be shedding abundant debris by rockfall processes, although the fan surfaces abound in leveed debrisflow channels and elongate chute-and-lobe features, without much evidence of rockfall scree. The neighboring fans Ee1, Ee2 and Ee4 are smaller and have smaller catchments.

Colluvial fan Ee1 – This fan is small, but morphologically distinct and readily recognizable, with the apex at an altitude of about 110 m, at the base of a well-developed ravine (Fig. 5.5A). The sandstone bedrock is exposed in many places at the ravine bottom, which indicates fairly recent erosion. In its lower part, the ravine is V-shaped and about 8 m deep, cut into the soft lateral moraine described in chapter 3. The fan's longitudinal morphometric profile is concave upwards, with the inclination decreasing from 33º near the apex to merely 1.5º at the toe (Fig. 5.5C). The gentle middle segment (ca. 12º) and nearly flat toe zone render this fan similar to some of the fans in area A (see previous section). The low apex position render a short debrisflow runout, but it should be emphasized that the fan toe has been eroded and that the oldest debrisflows possibly where at least 10-20 m longer.

The surface of fan Ee1 is mainly smooth, lacking distinct channels or lobe mounds in the old surface showed as stage I deposit in figure 5.5B. The lower and middle fan segments are covered with vegetation, whereas the upper segment has a lot of fresh looking boulders and cobbles scattered on the surface, probably derived by rockfalls or snowavalanches and emplaced on a snow-covered surface during the winter. At least one large, highly mobile debrisflow has left a relatively fresh trace along the fan's central sector. The debrisflow

Fig. 5.5: (A) Aerial photograph of fan Ee1 (Norsk Polarinstitutt S-90 1030). (B) Sketch showing the outwash lobe in the lower right-hand sector and the overbank deposits spilled from the debris-flow channel at it's right-hand bend. The Roman numbers I, II and III indicate the relative age sequence of the deposits on the fan surface. (C) The fan's longitudinal morphometric profile and two cross-profiles measured in the central fan sector (see line in A). The cross profiles are located near the apex at 95 m a.s.l. and across the large debrisflow channel in the central sector of the fan at an altitude of 43 m.

entered the fan slope directly from the ravine and ran straight to the valley-axis river (Fig. 5.5A) and due is to the fresh look interpreted as a stage III deposit. The debrisflow was probably watery, slushy or snow-bearing, and the fan surface at that time was likely snow-covered or frozen, because the flow has scoured the older surface very slightly, while depositing a pair of cobbly levees, 20-50 cm high, and a forming an apparent channel 5-8 m wide. The fan's left-hand (southern) sector has been smoothed by the development soil cover, but includes a small channel that seasonally conveys the meltwater that drains from the ravine and percolates through the fan apex. The right-hand sector hosts a larger, more active meltwater channel that extends directly through the apex and has formed a fresh gravelly little outwash lobe in the lower fan segment (Fig. 5.5B). The channel levees are rich in angular sandstone cobbles, apparently derived from the Firkanten Fm. This channel is up to 2 m deep and 5 m wide, incised in the fan's older depositional surface and cutting also through the lateral moraine and palaeobeach deposits (described earlier in section 3.5.2). Small spillover debrisflow lobes have been emplaced in the left-hand overbank zone at the rightward bend of the channel in the lower fan segment, below the moraine terrace (Fig.5.5B). The channel has apparently conveyed, perhaps alternatingly, both low-viscosity debrisflows and the meltwater flow. The channel levees in places show clast imbrication with the sandstone cobbles slightly oblique to the channel axis and dipping steeply towards the latter, but a disorderly fabric predominates.

Colluvial fan Ee2 – This fan has its apex at an altitude of about 170 m and has a relatively large mountain wall above apex, involving little or no meltwater drainage over the plateau edge (Fig. 3.2; 5.6A). The fan's concave-upward longitudinal morphometric profile 1 is quite steep, decreasing from 35º at the apex to ca. 20º in the middle segment to 4º at the toe (Fig. 5.6C). Profile 2 is a mountain-side profile steeping to 40º and more above apex and the intersection point. A freshly formed debrisflow channel, ca. 2 m deep, extends through the fan's left-hand sector (Fig. 5.6A), and this part of the fan is virtually dominated by these stage III deposits related to the channel (Fig.5.6B). Large amounts of debris are transported through this channel to the lower fan segment, apparently by low-viscosity debrisflows, whereas some higher-viscosity flows have nearly plugged the narrow channel in its upslope reaches (Fig. 5.6C). These high viscosity lobes show a well-developed "rolling" fabric a(t)a(i) in the frontal parts and a clear upslope fining. The fan surface in the central and right-hand sectors is relatively smooth, showing few signs of recent debrisflow processes, although an older, vegetated and smoothened debrisflow channel with vague levees is recognizable the former
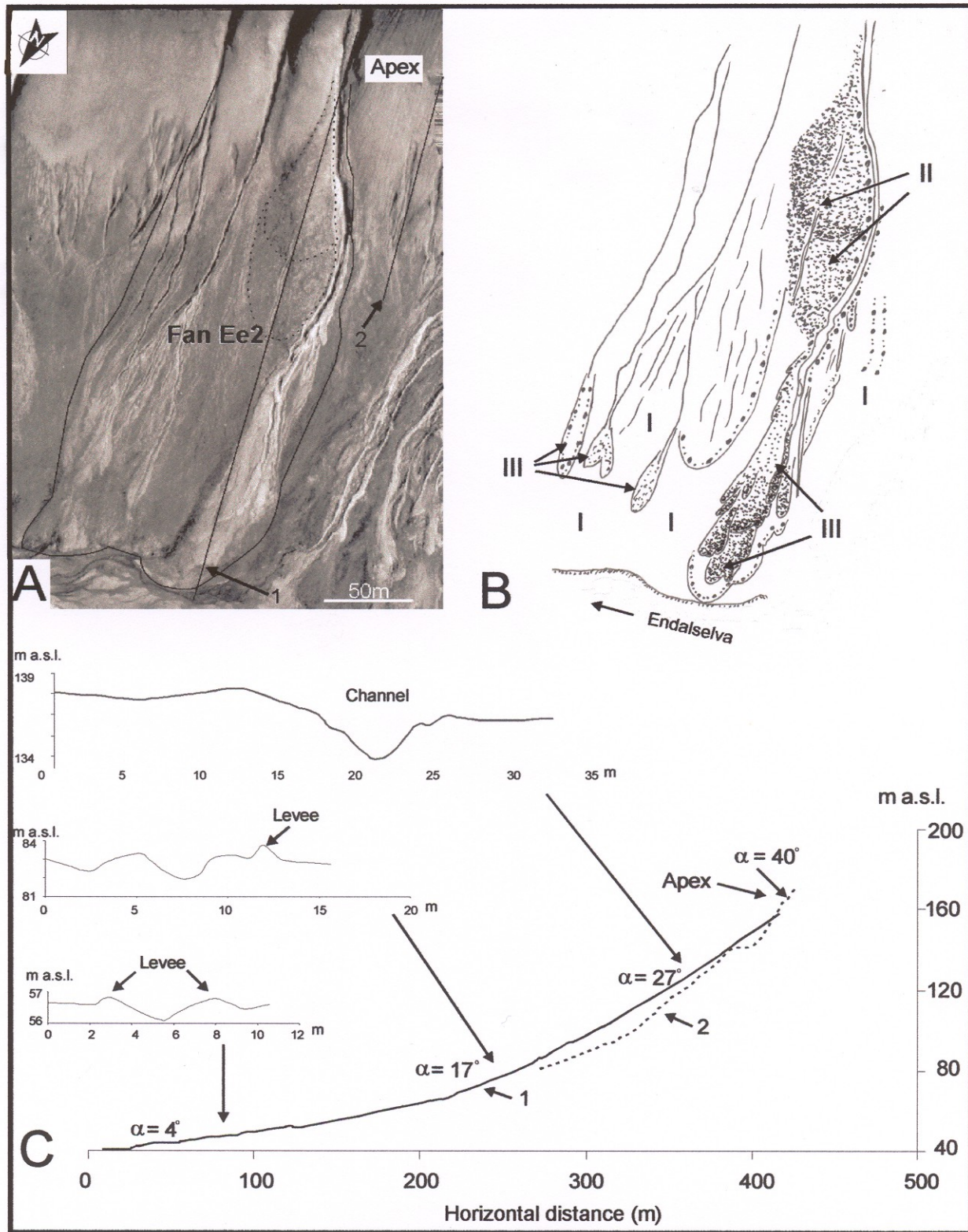
Fig. 5.6 : (**A**) Aerial photograph of fan Ee2 (Norsk Polarinstitutt S-90, 1030) showing the location of the slope profiles. Note the rockfall deposits in the upper part of fan Ee2 (stippled lines). (**B**) Sketch of the surface deposits indicating the relative age sequence (Roman numbers). (**C**) Slope profile 1 is of fan Ee2 and profile 2 is of the adjacent mountain-slope between fans Ee2 and Ee3. The cross-profiles have been measured in the leveed debrisflow channel in the most active left-hand sector of the fan.

sector (Fig. 5.6B). Also on this fan it is the oldest debrisflows which has the longest runout reaching out in the Endalselva. The surface of the two sectors shows evidence of rockfalls and possibly some spillover debrisflow sheets spread laterally from the fan's left-hand sector. A rockfall accumulation of gravel (bouldery scree), interpreted as a stage II deposit, has covered the older depositional surface of the fan's upper to middle segment, particularly in the central sector (Fig. 5.6A & B).

The mountain slope between the apices of fans Ee1 and Ee2 shows traces of numerous gravitational failures. The resulting debrisflows originated in the shale-rich middle part of the slope and came to rest in the lower part, a few tens of meters above the slope foot (Fig. 3.18), which indicates cohesive, high-viscosity flows. The debrisflows originating in ravines are much more mobile, forming leveed channels and commonly flowing to the valley-axis river plain (Fig. 5.6B). The channels are around 1 m deep and 2 m wide, scoured in the older depositional colluvial or glacial derived (see section 3.5.1) surface, and the associated levees are ca. 0.5 m in relief.

Fan Ee2 is steep and has a relatively small catchment area. The fan is thought to have commenced its development, after the deglaciation, chiefly by rockfall processes, but debrisflows have come play a major role after the Little Ice Age, modifying the fan-surface morphology (Fig.5.6A). The abundant evidence of low-viscosity debrisflows points to snow- or slush-bearing flow varieties and possibly some sporadic snow avalanches.

Colluvial fan Ee3 – This is the largest and probably most active colluvial fan in the study area (Fig. 5.7A & B). The fan apex is at an altitude of about 130 m, at the mouth of a large ravine, and the fan's catchment includes also a considerable portion of the outer plateau (see Fig. 3.9A). The slope part of the catchment includes steep bedrock walls, which shed abundant debris to the ravine. The altitude difference between the fan apex and the top of the ravine is more than 200 m. A large boulder block, ca. 6 m long, has blocked the ravine ca. 50 m above the apex, causing accumulation of a large volume of rockfall debris in the middle part of the ravine. The thick accumulation is still preserved, as a terrace, on the right-hand side of the ravine, behind the obstacle, but has been removed from the unobstructed axial and left-hand part, where the bedrock is now exposed. Coarse debris with at least one similarly large boulder, 4 m long, is resting on the surface of the upper right-hand sector of the fan, possibly derived recently from the ravine.

The fan is 344 m long in plan view and extends down to the valley-axis river. The fan's longitudinal morphometric profile is in the lower and middle segment gently concave-upwards and not particularly steep, with the surface inclination decreasing from 13° in the
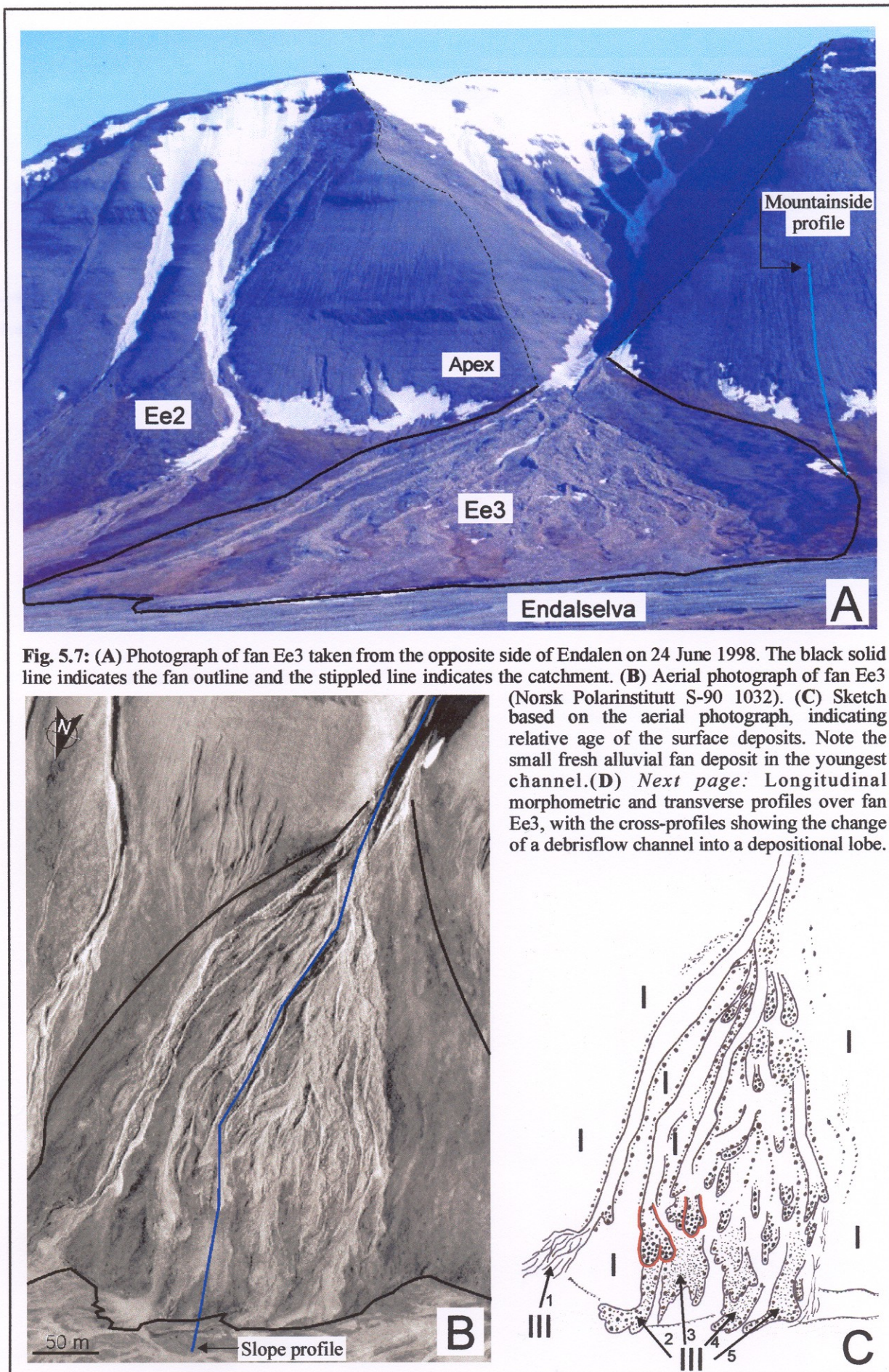
Fig. 5.7: (A) Photograph of fan Ee3 taken from the opposite side of Endalen on 24 June 1998. The black solid line indicates the fan outline and the stippled line indicates the catchment. (B) Aerial photograph of fan Ee3 (Norsk Polarinstitutt S-90 1032). (C) Sketch based on the aerial photograph, indicating relative age of the surface deposits. Note the small fresh alluvial fan deposit in the youngest channel.(D) *Next page:* Longitudinal morphometric and transverse profiles over fan Ee3, with the cross-profiles showing the change of a debrisflow channel into a depositional lobe.

middle segment to 6° at the toe (Fig. 5.7D). The upper segment of the fan show a nearly straight to slightly convex profile, with an inclination of 15° near the apex, indicating more pronounced deposition in the upper segment, due to the limited runout of the debrisflows. The youngest, fresh-looking channel runs through the right-hand sector of the fan and nearly reaches the fan toe (Fig. 5.7B & C). This debrisflow-scoured channel is up to 5 m deep and 8
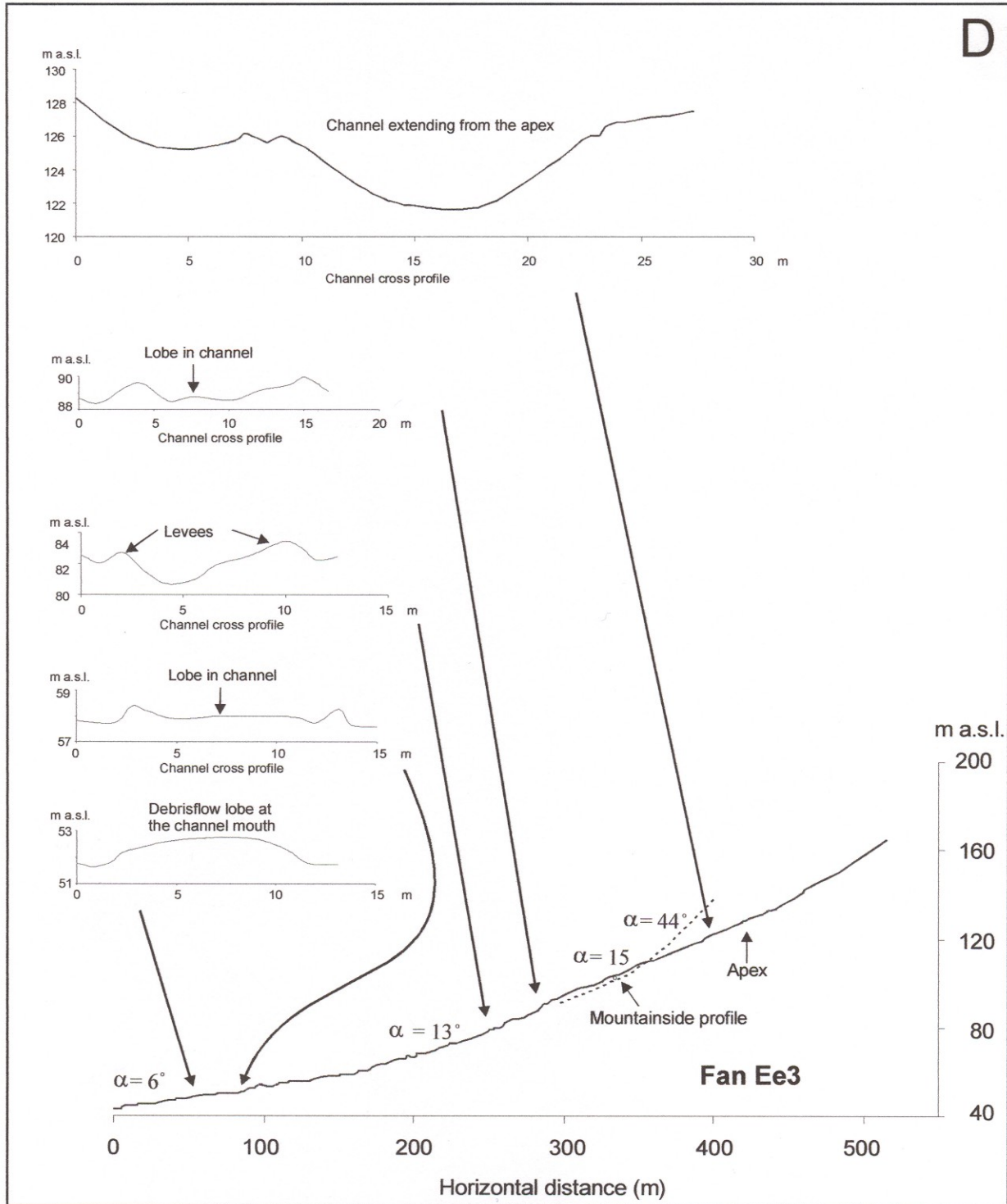
m wide near apex, and has prominent bouldery levees, averaging 1 m in relief. Several other distinct channels are recognizable in the lower part of the fan's upper segment, particularly in the central sector, where some of them are up 4 m deep and 10 m wide, with prominent levees of openwork, angular cobble gravel. In the fan's left-hand sector and along the right-hand margin, channels are poorly recognizable in the surficial layer of relatively old, coalesced debrisflow lobes coated with lichen and extensively covered with modern soil and vegetation (Fig. 5.7B & C). Little more than a few "imbricate" debrisflow lobes (*sensu* Blikra & Nemec, 1998) and coupled levee ridges are recognizable on this old depositional surface, although more readily from an aerial photograph than directly in the field (Fig. 5.7C). Broken electric-power cables and poles, from the time of the activity of Coal Mine 5, are as mentioned found on the vegetated surface, commonly overlain by the younger and often quite fresh debrisflow lobes. The mining activity in Endalen ended in 1973. The older debrisflow lobes consist of (sub-angular) cobbly to bouldery gravel and seem to have mainly an openwork texture, but are insufficiently exposed for the clast fabric to be measured.

The fan slope in the central sector changes abruptly from 12º to 6º at an altitude of around 60 m (Fig. 5.7D). This morphometric change marks the transition from the fan's middle segment, dominated by leveed channels, to the lower segment – dominated by debrisflow lobes. Most of the gravel in the central sector is relatively fresh, non-vegetated and showing little or no lichen coating. The debrisflow lobes, much like the levees upslope, consist of angular large cobbles and boulders derived chiefly from the Firkanten Fm. sandstones. The gravel has a clast-supported and predominantly openwork texture, and the lobes generally show an orderly clast fabric, characterized by steep imbrication. The debrisflow lobes are elongate, often tongue-shaped and fining upslope, typically with a flow-transverse clast fabric a(t)b(i) in the frontal part and a flow-aligned fabric a(p) in the upslope tail (Fig. 5.8). The same type of spatially variable fabric is shown by a spillover debrisflow lobe associated with the lower segment of the longest, far-right channel in the fan's right-hand sector (Fig. 5.9A). This fabric type is a common characteristic of the tongue-shaped lobes of low-viscosity debrisflows in the lower part of the fan's middle segment.

The debrisflow lobes in the middle to lower segment of the fan's central and left-hand sectors are broader, low relief, sheet-like, with a matrix-supported gravel texture (Fig. 5.9B). The matrix is rich in muddy sand and the gravel includes small floating boulders. The frontal parts of these lobes contain outsized boulders floating in a pebbly sand matrix, oriented mainly transverse to the local flow direction, with a(t) fabric. In the upslope part of a debrisflow lobe, the large clasts tend to be aligned parallel to the flow direction, with a(p)
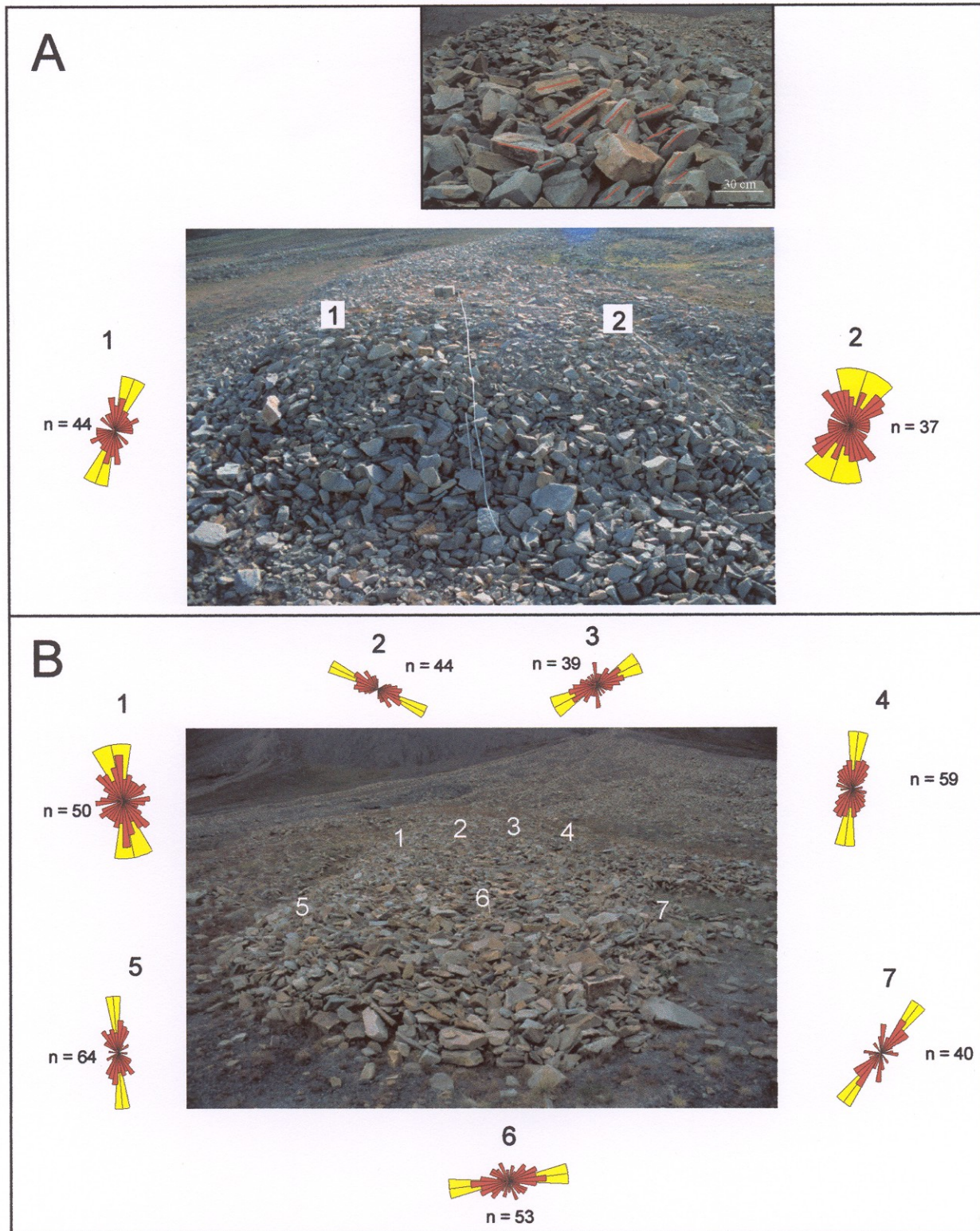
Fig. 5.8: **(A)**Clast fabric in the eastern of the two red-marked lobes in Fig. 5.7C. The lobe (lower picture) shows a flow parallel shear fabric, a(p), better developed in the right-hand part of the lobe. Note the more chaotic fabric of the lobe front. This debrisflow lobe is about 7 m wide and 2.5 m high. This is the second debrisflow derived from the same channel; An earlier, more sheet like debrisflow deposit occurs further downslope (see Fig. 5.7B & C). This debrisflow "froze" after having reached the lower fan segment at the break in the slope profile (see Fig. 5.7D). The close up picture on top shows examples of imbricated clasts in a younger lobe front further upslope the two aforementioned debrisflow lobes and above the slope break.

(B) Clast fabric in the western of the two red-marked lobes on Fig. 5.7C. The data from the two cross-profiles show a flow-parallel fabric, a(p) a(i), along the margins and flow transverse fabric, a(t) b(i), in the frontal part. This lobe is coarser grained than the other longer-runout debrisflows from the same channel and has been deposited directly below the slope break.
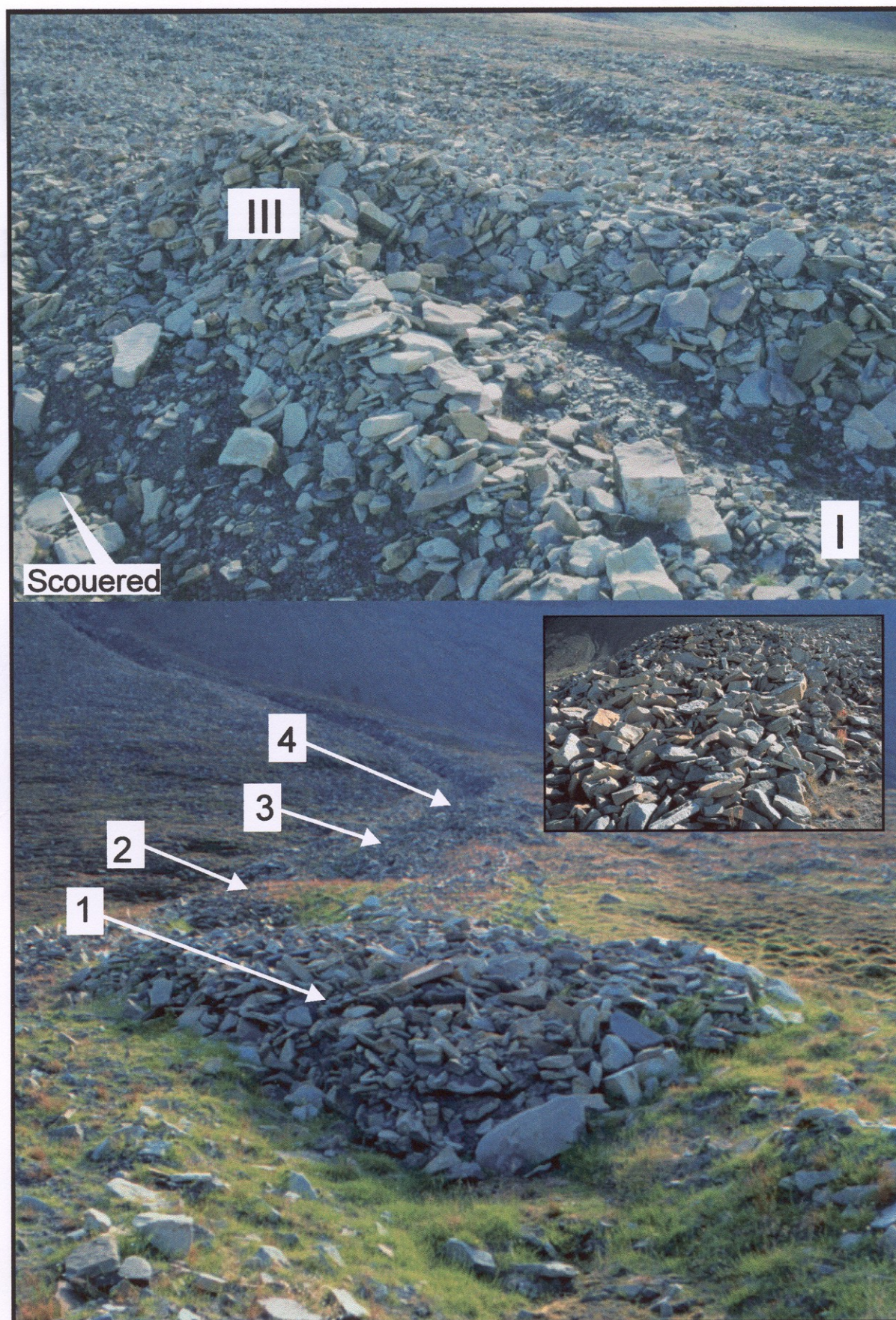
Fig. 5.9A: *Top:* Clast-supported levee deposits on the surface of fan Ee3 in the middle segment of its central sector, The levees here are ca. 1 m high. The Roman numbers refer to relative age sequences showed in Fig 5.7C. *Bottom:* Four successive debrisflow lobes issued from one channel. The closest (no. 1) is the oldest. *Insert photo:* Close up of steep imbricated cobbles in a openwork debrisflow lobe.
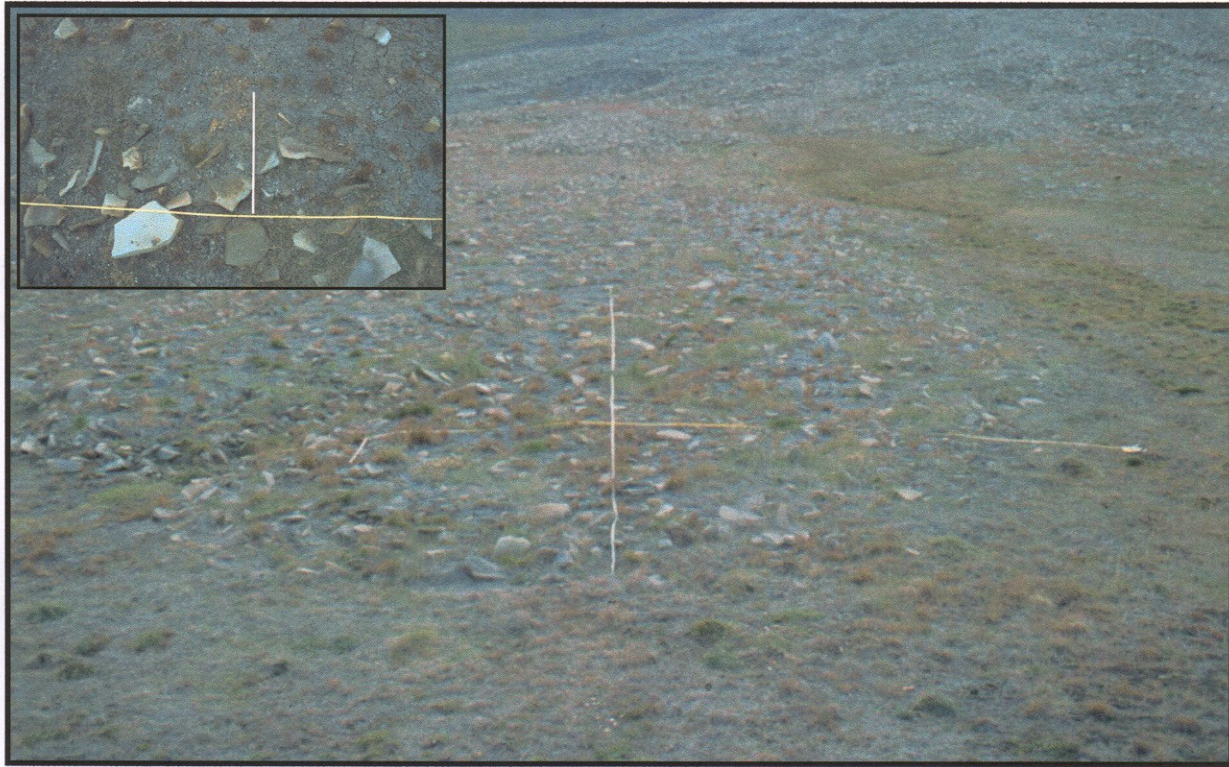
Fig. 5.9B: A 7 m wide sheet-like low relief cohesive debrisflow lobe in the lower segment, central sector of fan Ee3. The insert photo show the surface sediment cover with large cobbles floating in the muddy/sandy matrix.

fabric. Most of these older debrisflows were probably cohesive, characterized by a high viscosity. Their deposits in the lower part of the fan's middle segment are commonly overlain by the tongue-shaped lobes of low-viscosity debrisflows. These early, cohesive debrisflows were apparently quite voluminous, since the fan's older depositional surface extends to Endalselva. The younger, low-viscosity debrisflows have been less voluminous, but more mobile, hence often reaching the valley-floor river, too, particularly in the fan's right-hand sector.

The northernmost channel, on the far right-hand flank of fan Ee1, is presently draining meltwater from the fan catchment area. The runoff occurs in the summer only, but the large gravelly outwash lobe at the channel terminus testifies to a relative abundance of meltwater. To the south, the relatively old left-hand flank of fan Ee2 has slightly coalesced with the older part of fan Ee3. The valley-axis river, Endalselva, has eroded the inactive toes of both fans, and many of the youngest debrisflows have clearly reached the river and been eroded (see Fig. 3.15). This means that both stage I and stage III generated debrisflows with runout more than 353 m.

Colluvial fan Ee4 – This fan is fairly similar to fans Ee2 and A1 described above. There is almost no surficial meltwater over the plateau edge at this locality, and the fan catchment area is steep and subject to active rockfall processes. The fan apex is rather difficult to identify, but is approximately at the altitude of 215 m, with some leveed gullies in the ravine extending all the way up to an altitude of 235 m. A distinct ravine extends another 100 m upslope (Fig. 5.10A & B).

The fan is steep and relatively long consider it's small ravine catchment, with a nearly 400 m long true runout (Fig. 5.10C). The slope inclination in the central sector decreases from 34º near the apex to 21º in mid-fan segment to 6º at the toe. Much of the fan surface is covered with soil and vegetation, but contains small scattered boulder and large cobbles of rockfall and/or possibly snow-avalanche derivation. Three debrisflow-scoured channels with levees are well recognizable and the most recent one along the left-hand margin of the fan (Fig. 5.10B). The debrisflow deposits in the right-hand sector are covered with soil/plants and their primary depositional topography has largely been obliterated, while the other debrisflow deposits are fresher and only slightly coated with lichen. Most of the stage III debrisflows have had a plan view length of about 150 m. None of the fresh debrisflows has reached the bank of Endalselva at the valley floor below. The fresh levee and spillover debrisflow lobes at the left-hand margin make the fan coalesce with the adjacent fan Ee5 to the southwest. likewise, the morphology of the latter fan has affected the development of the former. For example, the main debrisflow channel at the fan's left-hand flank has clearly been deflected to the right, with the deposition of highly elongate, but thin and sheet-like, lobes in the lower part of the fan's central sector (Fig. 5.10A & B). The channel is locally up to 2 m deep and its bouldery levees are discontinuous in the upper to middle segment, but fairly continuous, though smaller, in the lower segment. The channel bend, in turn, has caused the deposition of a large outer levee and spillover gravel lobes at the left-hand margin of the fan's middle segment. These debrisflow deposits are clast-supported and openwork, but their depositional form and orderly clast fabric indicate low-viscosity debrisflows. No systematic measurements of clast fabric have been done on the surface of this fan, but the orientation of the coarse debris is visually consistent with that documented on the three previous fans.

Colluvial fan Ee5 – The apex of this fan is at an altitude of around 160 m, with a wide 4 m deep channel extending from the adjoining ravine onto the fan. The fan has a plan-view length of 331 m and gently concave-upward morphometric profile that decreases from ca. 12º near the apex to 4º at the toe (Fig. 5.10D). The catchment area of fan Ee5 is of about the same size as that of fan Ee3, with a large portion of the plateau subarea DII drained by the ravine.
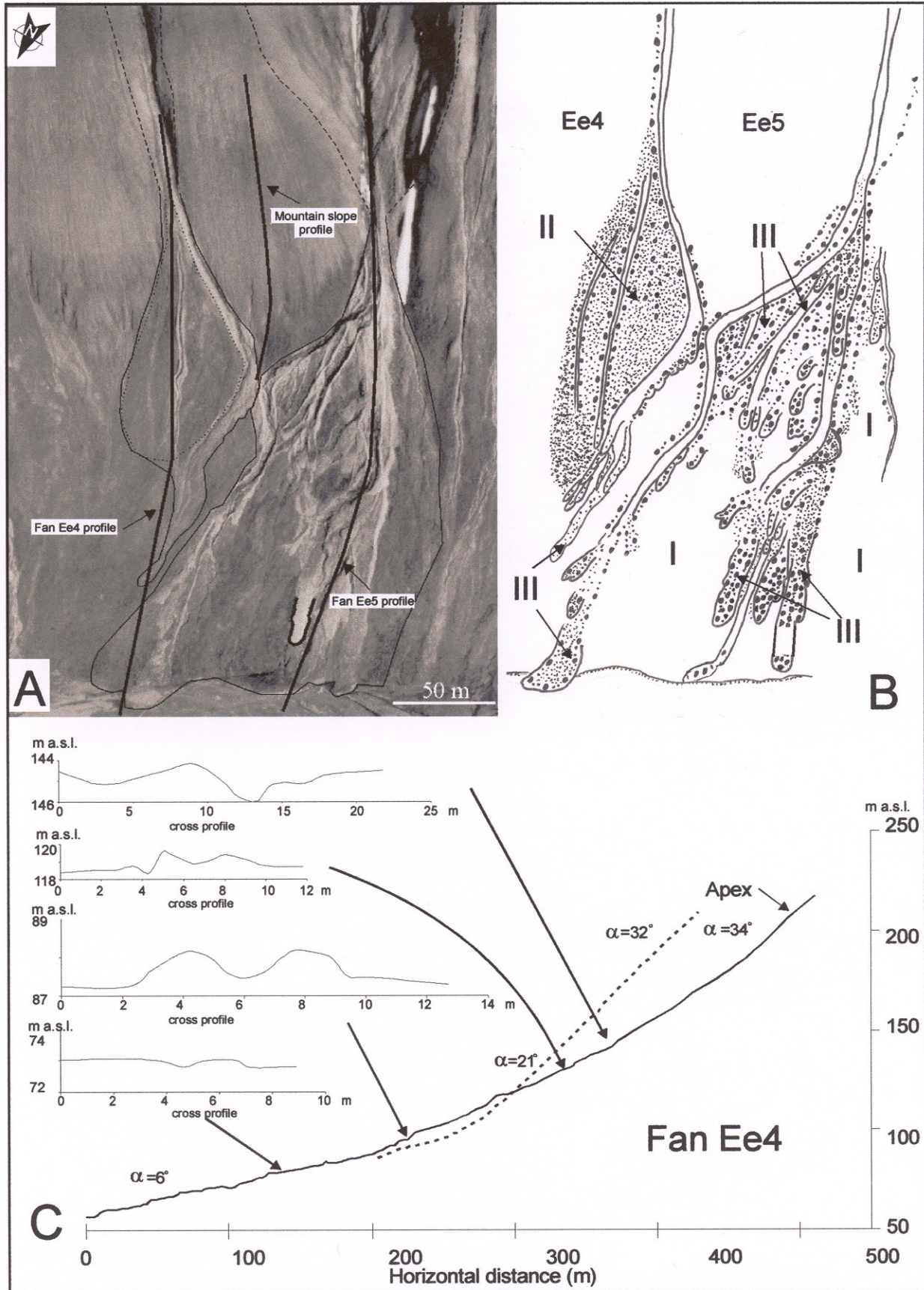
Fig. 5.10: (A) Aerial photograph (Norsk Polarinstitutt S-90 1032) showing coalesced fans Ee4 and Ee5 and the locations of slope profiles. **(B)** Interpretation of the fan deposits and their relative age (I, II and III are progressively younger). **(C)** The longitudinal slope profile of fan Ee4, showing several lobes in the channel. The cross-profiles have been measured through the largest channel in the left-hand sector of the fan. **(D)** *Next page:* Profiles of fan Ee5 and the adjacent mountain slope.
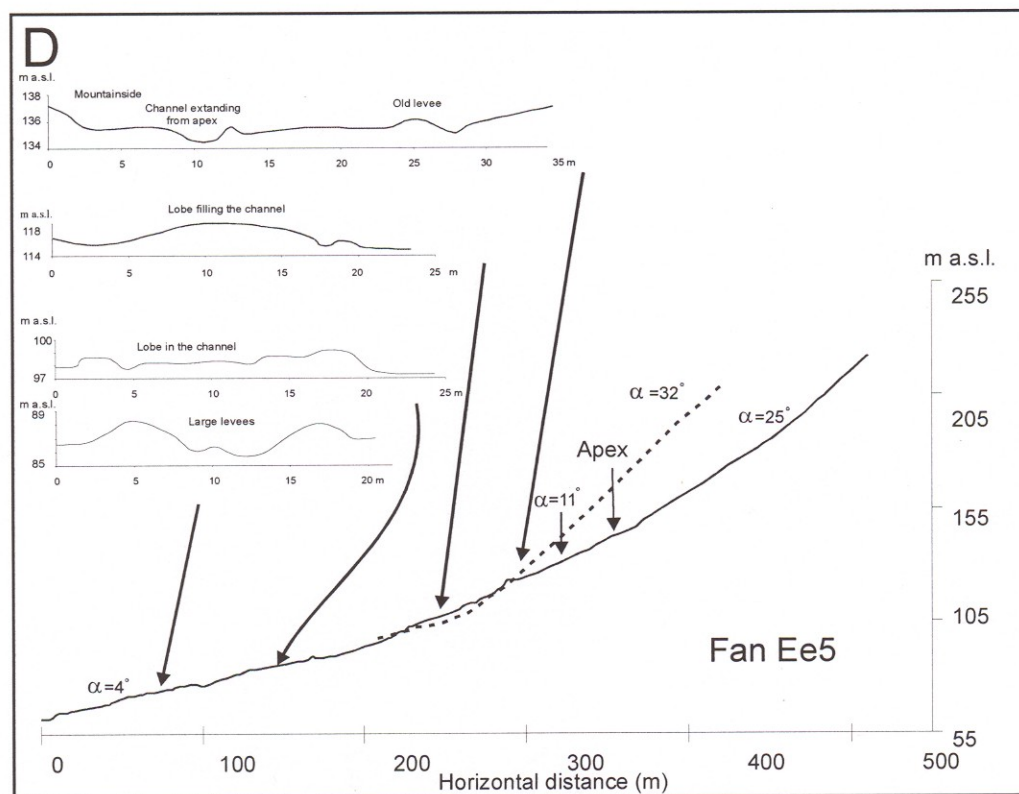
In fact, the fan itself is fairly similar to fan Ee3, although it is smaller and the debrisflow features not as numerous as on Ee3. Debrisflow runout range from 342 m, mostly for the stage I deposits, but is partly eroded in the lower segment. The slope ravine has steep bedrock walls with numerous gullies and an abundant accumulation of coarse debris along the bottom. The meltwater from the plateau percolates through this debris, below the surface. Some debris creep seems to have occurred within the ravine, as is indicated by lobate mounds of debris blocking the bottom channel. At least one large boulder block, 2 m long, is buried in the ravine-floor debris and another, slightly smaller one is visible in the apical part of the fan itself. The large blocks and abundance of openwork boulder debris indicate active rockfalls from the headwall scarp of the ravine, where the Firkanten Fm. sandstones are exposed. The channel extending from the ravine has been filled with the bouldery tongue-shaped lobes of low-viscosity debrisflow lobes, often stacked upon one another (Fig. 5.10A & B). The plugging of the channel made the descend path of the younger debrisflows switch to the fan's right-hand sector, where a newer channel has been established and most of the meltwater runoff occurs (Fig. 5.10B). The upper segment of the fan shows several shorter subrecent channels, with large cobble-rich levees, indicating the preceding episodes of the progressive shifting of debrisflow paths. Much of the deposition here seems to have occurred in the form of levees, as the channels terminate in sheet-like lobes of matrix-supported fine gravel, emplaced onto the fan's middle segment. It is possible that these sheets consist of sediment

washed out by meltwater runoff and have buried some debrisflow lobes. The most recent channel, at the fan's right-hand flank, has conveyed some of the mobile debrisflows all the way down to the bank of the valley-axis river (Fig. 5.10B), and the occurrence of several spillover lobes on both sides of the channel indicates episodic plugging by debrisflow deposits. In the lower fan segment, broad lobes of matrix-supported gravel predominate, overlaying the older depositional surface, now vegetated and covered with soil.

The fan's older depositional surface in the right-hand sector is covered with soil and vegetation, and a few small meltwater streams passes through the right-hand and central sectors in the middle and lower fan segments. Near the apex, the central sector has been completely remolded by, or covered with, fresh debrisflow deposits in the form of scour-and-tongue features. At the transition from the upper to the lower segment, the surface of the central sector has been smoothed by soil and vegetation cover. The fan's left-hand sector shows large tongue-shaped lobes of low-viscosity debrisflow deposits in all three segments. The plan-view runout distance of some of these mobile debrisflows reaches 331 m, although the few the youngest ones are shorter (Fig. 5.10B). Between the fresh debrisflow channels and their up to 2 m high levees, the fan's older stage I depositional surface is preserved and exposed. In the upper middle to upper fan segments, spillover debrisflow lobes have locally covered the vegetated surface without erosion. The change in the fan gradient in the middle segment marks the downslope change from levee deposits to lobe features. At least three generations of imbricate stage III debrisflow lobes can be distinguished in the middle and lower part of the left-hand to central fan sector, with the oldest deposits at the far left and the youngest at the far right. All of them are related to the large channel in the left-hand fan sector (Fig. 5.10B). The oldest debrisflow lobe is about 75 m long, 12 m wide and 0.5-0.8 m in thickness, and consists of clast- to matrix-supported with angular cobbles to boulders. The clasts show a pronounced downflow alignment, or a(p) to a(p)a(i) fabric, in the upslope tail of the lobe, but are aligned parallel to the lobe front, with a(t) fabric, in the downslope part (Fig. 5.11). The varied and well-developed fabric and the long runout of the lobe indicate a low-viscosity debrisflow, which means that the muddy sand matrix was probably very watery. The other debrisflow lobes are more clast-supported, showing a steeply imbricated flow-transverse fabric a(t)b(i) in the frontal parts and a flow-parallel shear fabric a(p)a(i) in the upslope tail parts, which are often slightly finer grained. The fine-grained matrix consists mostly of sand, excluding other origins of the material as for example aeolian material, which should have been mostly silt.   The far-right lobe has spread over the vegetated and flat old surface without erosion, whereas the middle lobe has been semi-confined by the uneven topography of the

pre-existing fan surface and is slightly erosive. Despite their openwork bouldery texture, all these lobes are deposits of relatively mobile, low-viscosity debrisflows. The valley-axis Endalselva has eroded the lowest part of fan Ee5 (Fig. 5.10A & B).
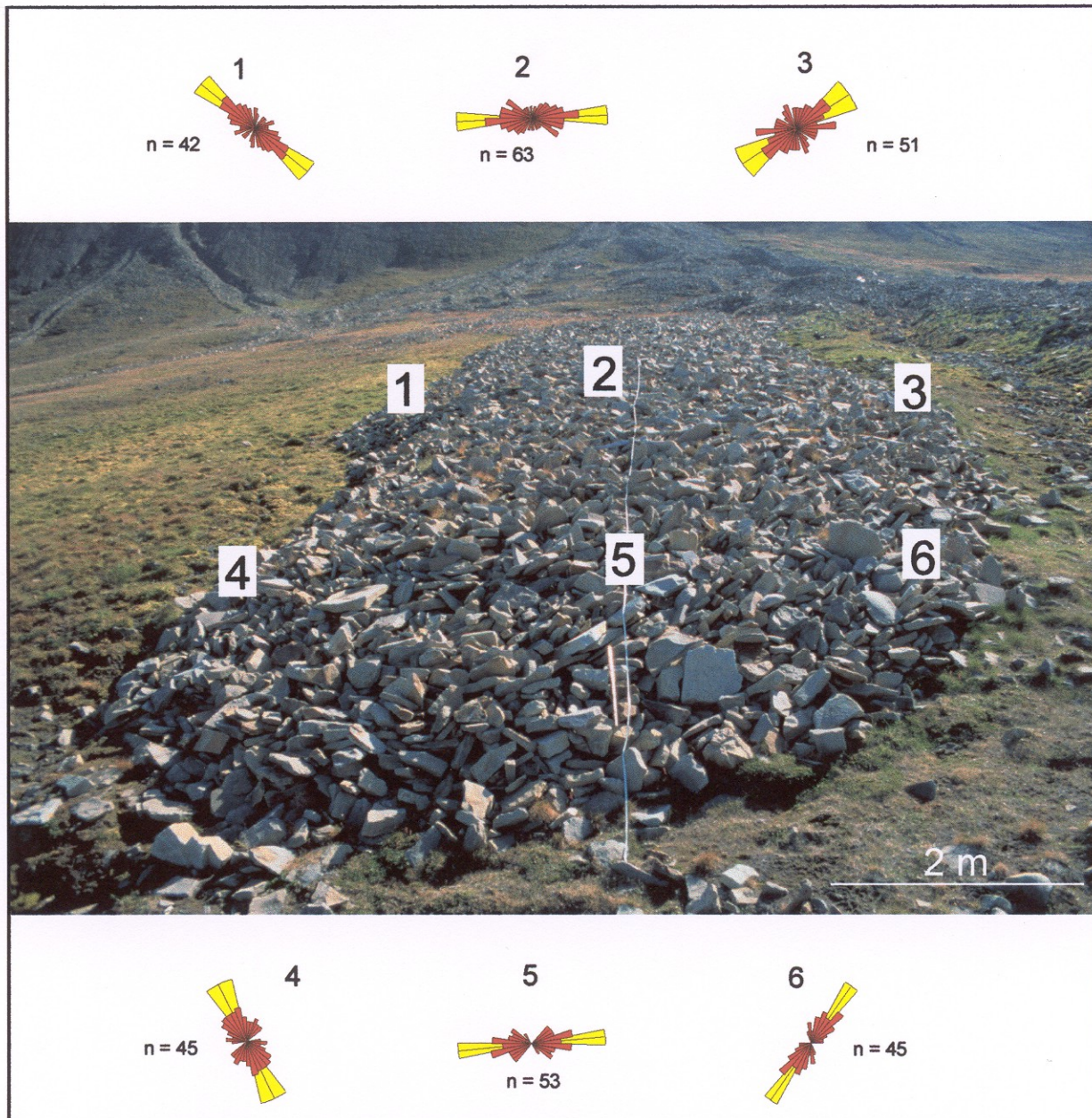
Fig. 5.11: Clast fabric on the black-marked debrisflow lobe in Fig. 5.10A. The measurements show a flow-transverse fabric, a(t) b(i), in the central part of the lobe, while most clasts seems to orient with a flow-parallel shear fabric a(p) a(i) and a(t) b(i) along the margins. This debrisflow lobe is about 70 m long, lying on top of the older vegetated surface (see Fig. 5,10B) with a maximum high of 1 m. The deposit is clast to matrix supported with cobbles at the surface and a sandy matrix below.

Colluvial fan Ee6 – This fan is relatively large and associated with a ravine much larger than the others are. The fan catchment includes also large parts of the plateau subareas DII and DIII. No measurements are done on this fan, but the fan apex is approximately at an altitude of 190 m and the fan has a plan-view length of about 350-400 m. At the top of the

ravine, above the outcrop of the sandstone-rich Firkanten Fm., a huge permanent cornice of snow and ice has developed. This cornice may probably be regarded as a small cirque glacier, because it apparently survive the summer melting season and is visible on aerial photographs since at least 1936. Piles of immature cobble-rich debris have accumulated in front of this glacier, but cannot be regarded as an end moraine, analogous to that developed in front of the larger cirque glacier described in chapter 3 (see Fig. 3.12). The right-hand headwall of the ravine is smooth and covered with scree, whereas the left-hand headwall includes several vertical bedrock cliffs exposing both Firkanten and Grumantbyen fms. At the base of this latter headwall, a large amount of rockfall debris has accumulated, onlapping a rock glacier adjacent to the apex of fan Ee6. The channel that extends from the base of the ravine down onto the fan has been filled with clast-supported, openwork cobbly/bouldery gravel, making the meltwater runoff totally subsurficial.

Colluvial fan Ee6 has not been studied in the same detail as the other fans, because its surfaces and ravine was considerably affected by the mining activity in this part of Endalen. Unlike fans Ee3 and Ee5, this fan shows no fresh debrisflow deposits derived from the ravine although it is larger than the former two. However, in the upper segment of the fan, some debrisflows have deposited cobbles and boulders in chaotic pattern in front of the rock glacier. No pronounced gravel lobes are recognizable. The meltwater from the plateau and the cirque glacier drains in the form of several small surficial streams in the fan's right-hand and partly central sector.

5.2.3. Implications of the debrisflow characteristics

Most of the colluvial fans in Endalen and the adjoining Adventdalen show a development trend involving an early stage I dominated by cohesive, high-viscosity debrisflows (broad matrix-supported lobes), a stage II recognized as rockfalls (bouldery scree deposits), and a later stage III dominated by the more mobile, lower-viscosity debrisflows (highly elongate channel-and-lobe features). Stage III has often caused strong incision in the fan apex and upper segment, with channels a few meters deep and the associated "telescoping-style" progradation and aggradation of the fan's lower segment (Bowman, 1978, see also Lægreid, 1999). Admittedly, the change in processes is not well recognizable in all the fans, hence it is postulated tentatively here, especially since its actual cause is uncertain. Can it be that the late

Holocene climatic conditions promote more watery debrisflows on the mountain slopes? Or can it be that the role of snowpack has increased?

In Endalen, the winter snowpack is obviously a crucial source of meltwater, active during the summer and contributing greatly to the runoff caused by episodic rainfall and the melting of the active layer and glacier ice. The permafrost prevent deep percolation and the ground tends to be saturated with water, and a rainstorm in this conditions commonly triggers debrisflows, as shown by the previously mentioned historical events in the adjacent Longyeardalen (see also review by Lægreid, 1999).

However, the snow cover may also be contributing more directly to the slope-waste debrisflows. Many of the steep mountain-slope ravines are capable of accumulating several meters of snowdrift during the winter, while being prone also to the accumulation of abundant rockfall debris. The melting snowpack has a great potential to destabilize the ravine's latent stock of debris, once accumulated and metastable, and thus result in a snow-laden debrisflow. There are reasons to believe that such "mixed" massflows may have been particularly common in the late Holocene, as is indicated by the abundance of the relatively fresh deposits of low-viscosity debrisflows.

The well developed a spatially varied clast fabric indicates a fully shearing debris mass, with a sufficiently low apparent viscosity to allow a remarkably good adjustment of the casts to the varied shear-strain pattern within the debrisflow. The low apparent viscosity and high mobility of a clast-supported bouldery gravel is difficult to explain, since the very coarse and angular debris has an enormous frictional strength and would normally not yield on a slope even as steep as 45-50°. Large (heavy) and blade-shaped clast, like those sandstone slabs in the present case, are the least mobile debris, nearly impossible to roll. The apparent "rolling" (flow-transverse) orientation and steep imbrication of the sandstone slabs are clearly due to an internal bulldozing effect in the frontal/marging and surficial part of the debrisflow, which supports the notation of a fully shearing mass of lubricated debris. The water runoff alone cannot serve as an explanation, because the cobbly to bouldery debris has little capacity to accumulate or retain any significant amount of water, whereas flash floods are very unlikely to have occurred in the mountain ravines in the postglacial times. The debrisflows must have obviously been lubricated by some interstitial medium, and there seem to be two possibilities, not necessarily mutually exclusive: (a) the debrisflows may have originally contained an abundant fine-grained watery matrix, which has subsequently been washed out from the deposits; or (b) the debrisflows may have contained an abundant admixture of wet snow or slush, which subsequently melted, leaving a largely openwork gravel. The amount of

interstitial medium must have been low enough to allow the clast fabric to be fully preserved, instead of causing its collapse when washed out or removed by melting, which is indicated also by the distinct clast supported texture of the deposit. Ice coatings on the clasts, due to frost, may have aided the lubrication, but this factor would most likely be associated with snow-bearing, rather than watery debris mass conditions. Unfortunately, the field evidence in the present case is not quite conclusive and the assessment can only be speculative.

The tongue-shaped, openwork gravel lobes (such as those shown in Figs. 5.8, 5.9B & 5.11) do often contain a muddy sand matrix in their lower parts, but it is by no means clear as to whether this fine-grained sediment is a relict of an original matrix, or rather a result of infiltration with fines carried by the percolating meltwater runoff. Notably, many of the fresh gravel lobes lack any evidence of matrix having been washed out in the form of a muddy sand sheet extending downslope from the lobe front. Furthermore, a geometrical comparison with the matrix-supported deposits of the earlier, cohesive higher-viscosity debrisflows suggests that even if the younger, more mobile debrisflows did contain an abundant matrix, the latter must have been highly watery or rich in slush. In short, it is likely that many of the highly mobile, low-viscosity debrisflows have been lubricated by slush or wet snow, whether alone or in combination with a fine-grained sedimentary matrix. Needless to add, an admixture of slush or wet snow would act as a perfect, low-friction lubricant for the rock debris (see review by Blikra & Nemec, 1998).

Similarly, it is likely that some of the ravines have occasionally spawned debris-bearing snowflows, or dense snow avalanches. For example, there is some good evidence of such massflows on the other side of Adventdalen (W. Nemec, personal comm. 1999), and the occurrence of sporadic snow avalanches has been observed in the similar setting neighbor valleys. The fact is that the elevated tops of many large cobbles and boulders scattered on the surfaces of the colluvial fans in the study area often host finer debris, which could only have been deposited by melting from a snowpack, most probably a snowflow body. When shed by rockfall from a mountain cliff onto a snowpack, fine debris is unlikely to roll more than a few meters away from the cliff foot, which obviously cannot account for the occurrences of precariously perched "pockets" of fine pebbles in the middle or lower part of a colluvial fan.

However, it should be emphasized that even if snow avalanches do sporadically occur on some of the fans in Spitsbergen, their role in the downslope transport and deposition of debris here is minimal, incomparably lower than, for example, on the sub-arctic mountain slopes in western Norway (Blikra & Nemec, 1998).

6. The deglaciation and morphological development in Endalen

6.1. A tentative model for the deglaciation of Adventdalen area

The deglaciation of the Barents Sea shelf commenced ca. 15 ka BP and was relatively rapid due to the ice-sheet calving in deep troughs. According to Landvik *et al.* (1998), most of the Barents Sea was free of ice by ca. 12 ka BP (Fig. 2.4). The deglaciation of the western margin of Spitsbergen was interrupted by a minor re-advance that culminated shortly after 12.4 ka BP. During the Younger Dryas time, valley outlet glaciers draining the ice-sheet remnants still occupied the inner fjords (Landvik *et al.,* 1998), but the fjords were then rapidly deglaciated around 10 ka BP (Svendsen et al., 1996).

Few moraine ridges or other glaciogenic features on land have survived postglacial erosion, and the knowledge of the spatial pattern of glacier retreat and the morphological development in Spitsbergen area during the deglaciation is very sparse. Analysis of infrared aerial photographs, as used in the present study, has proved to be useful in deciphering the areal pattern of meltwater drainage and other geomorphic features of the deglaciation process (I. Lønne, unpubl. data and pers. comm., 1998). The tentative model for the deglaciation history of the Adventdalen area suggested below is based on the aerial photographs and field data from the Endalen area and its close neighbourhood, and should thus be considered as a preliminary and partly hypothetical interpretation.

After the ice-sheet re-advance around 12.4 ka BP, the glacier had rapidly retreated from Isfjorden, the local 1st-order ice-drainage basin, while its former tributary ice-flows persisted as calving glaciers in the adjoining, smaller 2nd-order basins, among them Adventdalen (Landvik *et al.*, 1998). The glacier in Adventdalen was probably in a still-stand phase, grounded and calving at the valley mouth (Fig. 6.1A). This still-stand phase might give reason to believe that ice cored lateral moraines where present along the glacier, but a rapid retreat of the ice front from here render a smaller chance of lateral deposition. The solar radiation and atmospheric temperature increased slightly due to a maximum of the Earth axis tilt around 11 ka BP (Berger *et al.,* 1984), and this factor, combined with the generally unfavourable conditions for snow accumulation in flat and wind-swept areas, caused glacier melting and rendered the plateaux around Adventdalen ice-free. During the still-stand phase, the lateral drainage of meltwater from the Adventdalen glacier is thought to have resulted in surficial waterflow across the bedrock plateaux on both sides of the
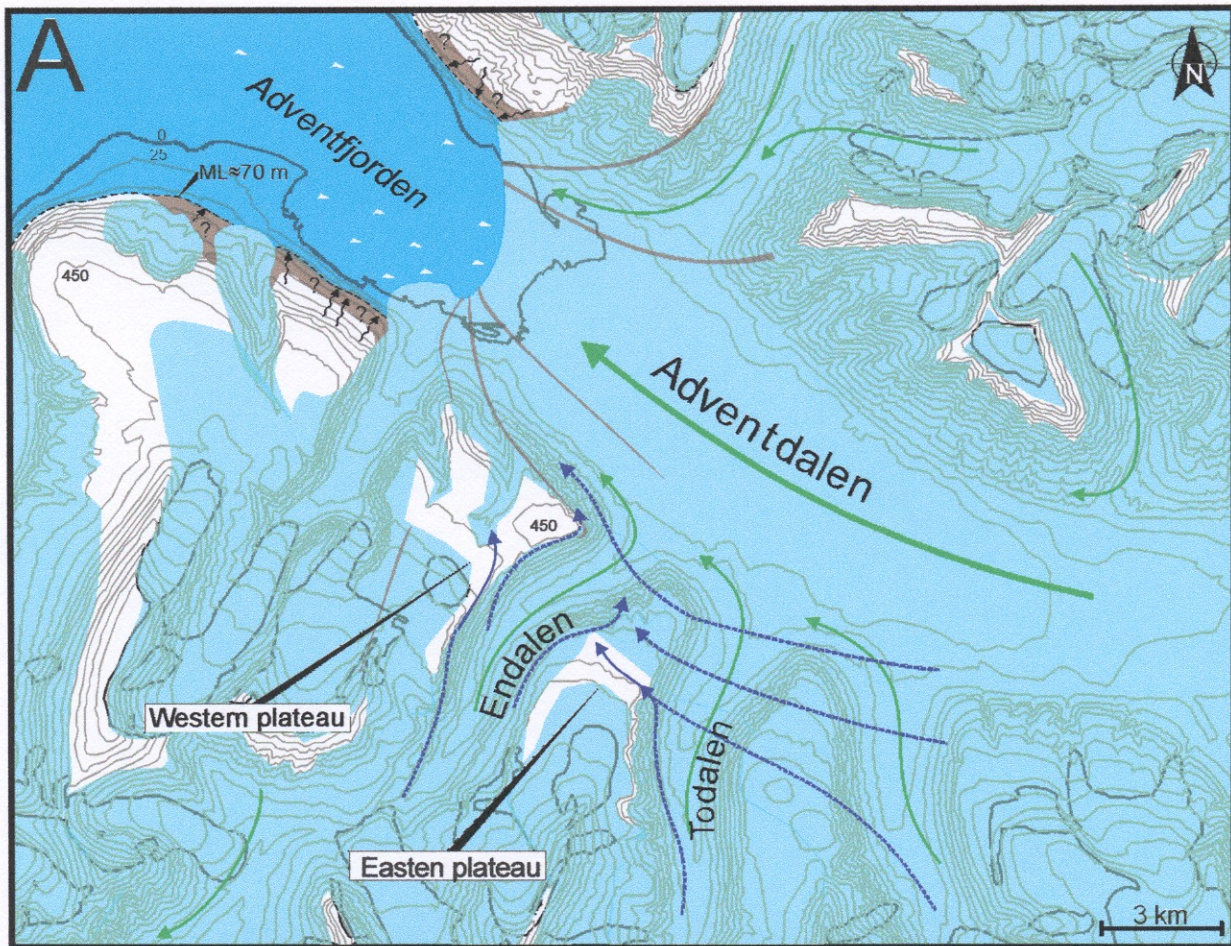
Fig. 6.1: (**A**) A tentative model for the deglaciation of the Adventdalen area (see legend at the bottom of the page). During the older Dryas the Adventdalen glacier retreated rapidly to a stage where it first became a grounded calving glacier. Small ice-cored lateral moraines were supposedly deposited, but these are erased by slope-wasting and are not recognizable in the present terrain. During this phase the first glaciofluvial channels, with meltwater drainage from the 2de-order Adventdalen glacier, on the eastern Endalen plateau were formed. At this time the sea level was probably around 70 m higher than today and slope processes rapidly reshaped the mountain slopes after the glacial retreat. (**B**) The supraglacial lateral meltwater draining the glaciers in Adventdalen and Todalen are thought to have formed the meltwater channels described in chapter 3, crossing the eastern plateau in glaciofluvial channels. In the same way the Adventdalen glacier was the catchment area for the valley west of Ugledalen. (**C**) As the thickness of the Adventdalen glacier decreased, the glacier front retreated rapidly up-valley during the Younger Dryas, making the 3rd-order glaciers calving in Adventfjorden. Minor lateral moraines, possible formed during the retreat, were reshaped by slope-wasting and alluvial fans were initiated by meltwater drainage from the plateaux. The lateral moraine at the eastern side of the Endalen valley mouth, formed by the 3rd-order glacier in Endalen, are interpreted from sediment analysis described in chapter 3. Morphologically similar features are interpreted as moraine relicts in the valley mouth area of Longyeardalen and Todalen. (**D**) In early Holocene time the glaciers in the 3rd-order basins melted *in situ*. Lateral ice-cored moraines were formed, but rapidly reshaped by slope processes forming additional gravel fans towards the climatic optimum.
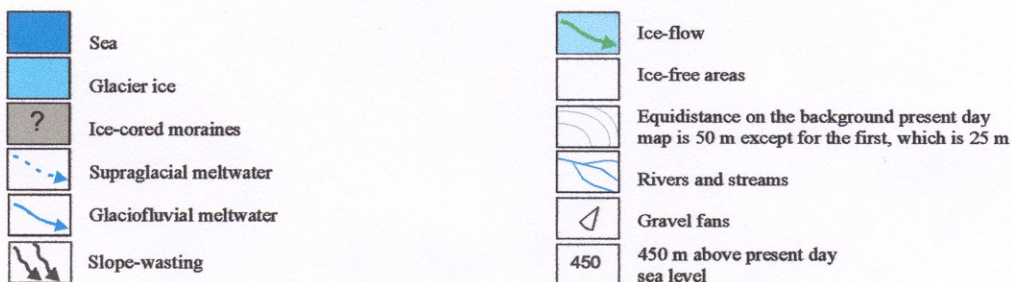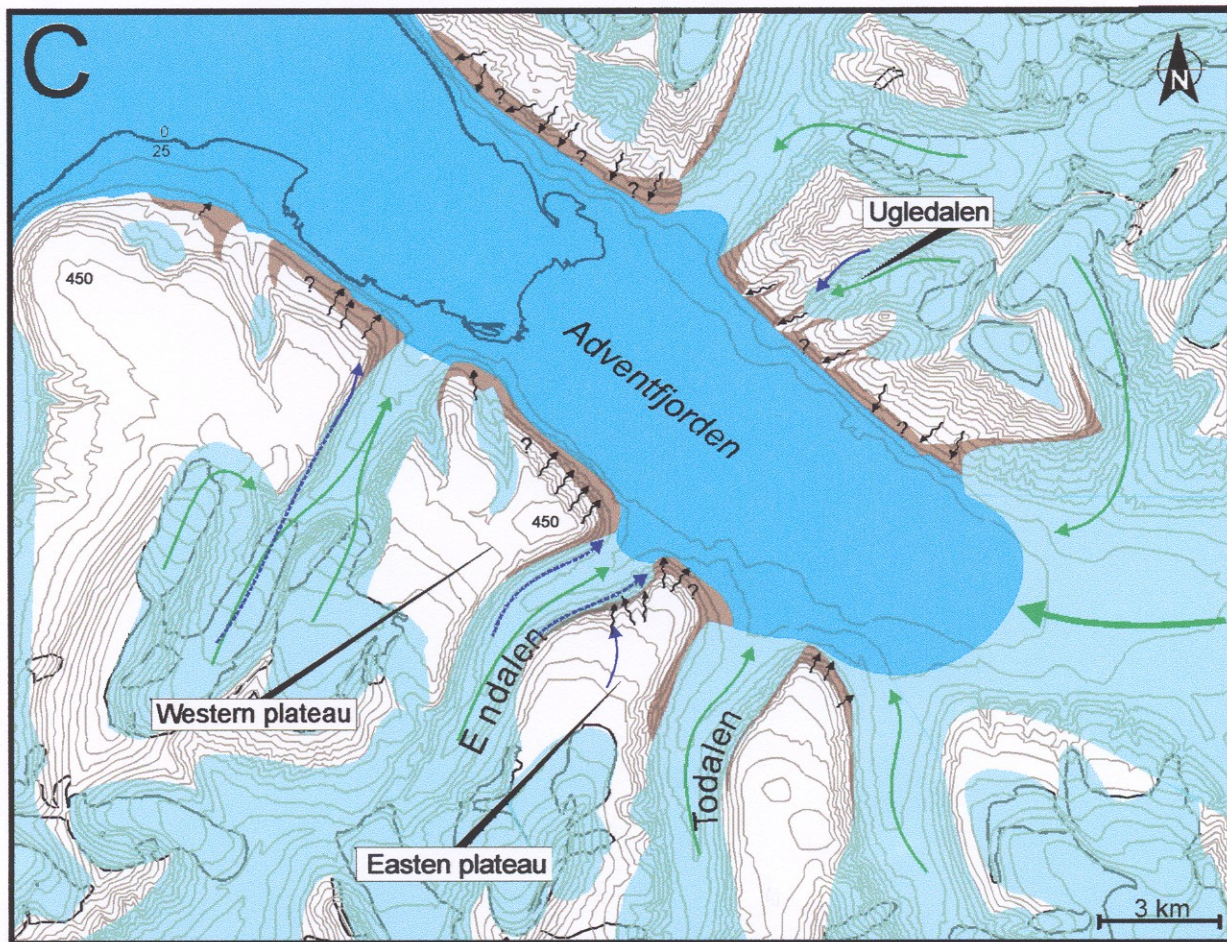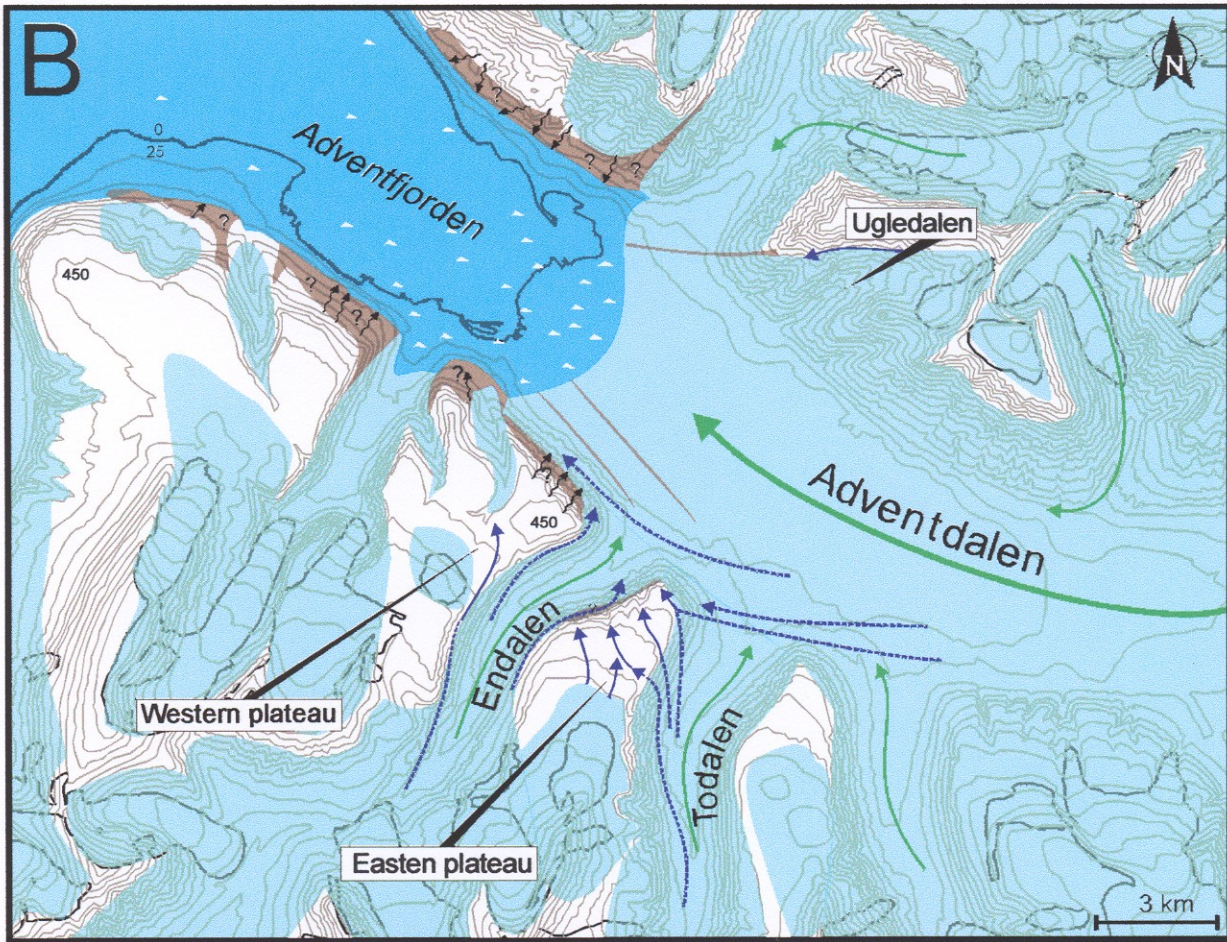
glacier occupied Endalen (Fig. 6.1 A & B). The orientation of the meltwater channels and linear scours on the plateau surface (see Chapter 3, Figs. 3.3, 3.4 & 3.5) is used to assess the ice-front position in Adventdalen. The west-trending channels on the plateau east of Endalen were likely formed during the glacier still-stand phase in Adventdalen shortly after 12.4 ka BP, whereas the north-trending channels were probably formed during the melting of the 3rd-order tributary glacier in the adjacent Todalen. The meltwater flow is thought to have scoured the ravines in area B (Fig. 3.1B, 3.8 & 6.1B) and deposited sediment on the glacier and its lateral moraine in Endalen. The remnant of the lateral moraine on the eastern side of the valley outlet was modified by slope processes and reworked by waves into beach terraces. A similar pattern of lateral meltwater drainage, attributable to the deglaciation phase, is recognizable on the northern side of Adventdalen (I. Lønne, pers. comm. 1998), where the geomorphic features scoured by meltwater flow include a small valley west of Ugledalen, with the Adventdalen glacier draining the area (Fig. 6.1B & C). The present day drainage area is not large enough to explain the formation of this small valley.

The calving rate of the Adventdalen glacier is thought to have increased with the general ablation and thinning of the ice mass. The glacier then rapidly retreated from the mouth of Adventdalen and turned into a completely land-based glacier. Mollusc shells (including *Mya truncata*) from the raised beach deposits at the mouth of Bolterdalen have yielded a radiocarbon date indicating ice-free conditions in the area around 10,025 (±125) yr. BP (sample T-13882, I. Lønne, pers. comm. 1999). Several raised-beach terraces are recognizable in the Adventdalen area, and the highest of them is directly outside the mouth of Endalen at an altitude of 63 m (Figs. 3.20 & 3.21). The raised beach at 62-m altitude at the mouth of Bolterdalen (I. Lønne, pers. comm. 1999), 5 km eastwards from the Endalen outlet, supports the notion of a rapid calving of the Adventdalen glacier. No beach terraces are recognizable within the 3rd-order valleys, such as Endalen and the adjacent Longyeardalen and Todalen, probably because they were still occupied by the glaciers during the sea-level highstand. However, it cannot be precluded that some palaeobeaches did exist in these tributary valleys, but have been destroyed by the postglacial slope-waste processes or covered by their deposits. Nevertheless, even if glaciers did not occupy these 3rd-order valleys, the sea would not have reached far into these relatively high-gradient valleys (Fig. 6.1).

Figure 6.1C shows the inferred position of the melting ice-sheet front during the formation of the highest recognizable beaches, based on the local marine limit and the lateral moraines at the mouth of Endalen (see earlier Figs. 3.17 & 3.18). On the valley-side slope of Adventdalen directly outside Endalen, late-glacial lateral moraine deposits and beach terraces are relatively well preserved due to the sparse sediment supply over the plateau edge. As the Endalen glacier melted and the relative sea-level fall occurred, the flow of meltwater from ice relicts on the eastern plateau
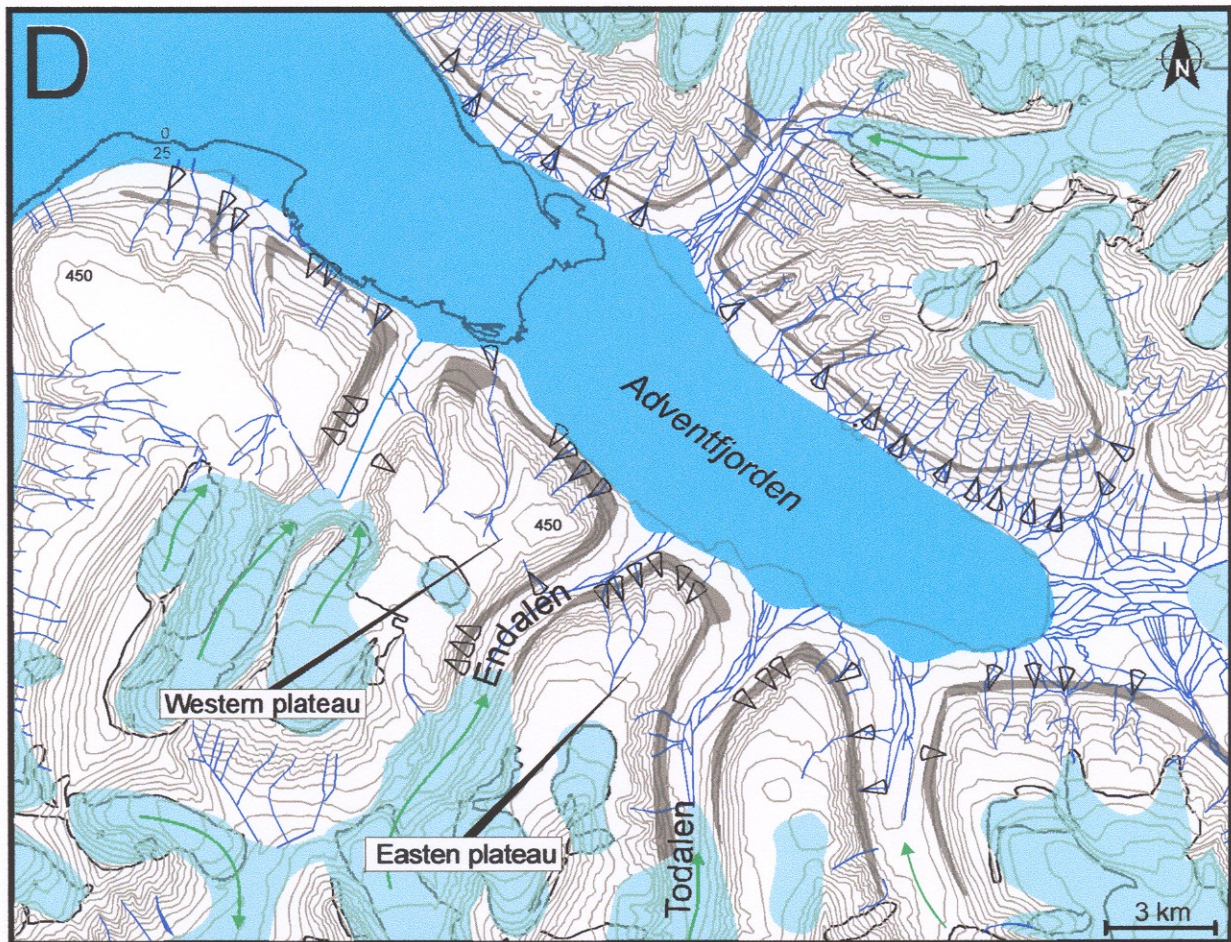
formed the mountain-slope ravine with which the colluvial fan Ee1 is associated (Fig. 3.8). The meltwater drained by the ravine has eroded the lateral moraine and the beach terraces, with the waterflow post-dating these deposits. The valley-side colluvial fans are thus clearly postglacial, formed in the Holocene time. It is clear also that the water runoff from the melting glaciers and subsequent slope-waste processes have strongly altered the valley-side slopes, erasing most of the glacial deposits and possible palaeobeaches (Fig. 6.1D). The side slopes of Adventdalen have been altered to a lesser extent and thus show local remnants of raised beaches and lateral moraine deposits.

At the latest stage of the deglaciation, small, low relief ice-cored lateral moraines were likely left in the 3rd-order valleys (Fig.6.1D), but have subsequently collapsed due to melting and become largely obliterated by slope-wasting processes (forming stage I deposits) during the early Holocene and further reshaped by the postglacial slope-waste processes (see earlier Fig. 3.1B).

The thickness of the late Weichselian Barents Sea ice-sheet is still debated. The glacioisostatic model by Lambeck (1995), supported by Landvik et al., (1998), suggests that the ice-sheet was extensive and had a maximum thickness of more than 800 m in the western Spitsbergen. However, Andersson et al., (1999) and Houmark-Nielsen & Funder (1999) have argued that the ice cover along the western coast of Spitsbergen was restricted to the larger valleys and fjords, with relatively

large areas, like the mountain plateaux around Adventdalen, virtually ice-free. The regional scope of the present study is too limited to contribute with any definitive answers to that debate, but the evidence from Endalen (including the record and pattern of meltwater drainage on the adjoining plateaux, the incision of ravines at the plateau edges, and the two-storied stratigraphy of the valley-side gravel fans) gives a reason to believe that these bedrock plateaux were covered by glacier, probably cold-based (see also Lægreid, 1999). The lack of recognizable till or erratic clasts on the eastern plateau does not necessarily preclude the presence of an ice cover in the late Weichselian time. It has been argued that the Arctic glaciers are capable of overriding even a soft sedimentary substratum without removing it or depositing any till layer (Landvik *et al.,* 1998). Notably, erratic boulders have been recognized by the present author on the western plateau of Endalen, beyond the direct catchment of the latter valley (see Figs. 3.1B & 6.1A,), and surface deposits on the mountain plateau west of Longyeardalen are interpreted to be till deposits (I. Lønne, pers. comm. 1998). However, even though interpreted so, the available field evidence does not necessarily prove that the glaciogenic features on the plateaux are products of the late Weichselian glaciation.

6.2. Postglacial sedimentation in Endalen

6.2.1. The development on valley-side fans

The valley-side gravel fans in the study area are postglacial deposits, whose development commenced at the time of the deglaciation in early Holocene time. The sediment has been derived by slope-wasting processes, but was supplied also by meltwater flowing from the adjoining mountain plateau during the deglaciation (Fig. 6.2). The drainage pattern on the plateau is thought to have resulted in differences in the size and shape of the valley-side postglacial fans in Endalen. The gravel fans whose formation involved direct meltwater flow from the plateau are larger, associated with well-incised ravines and often show two storeys of deposits (Lønne, 1998b), a broad lower alluvial storey (now vegetated, but locally dissected by young gullies) and an upper colluvial storey of lesser areal extent. The two storeys are thought to represent the syn-deglaciation and post-deglaciation Holocene sedimentation, respectively. Fans that have formed without significant meltwater input from the plateau are smaller and steeper, and are largely coeval with the upper (colluvial) storey of the former fans. In general, these postglacial valley-side fans seem to show three stages of deposition (Fig. 6.2, see Chapter 5).
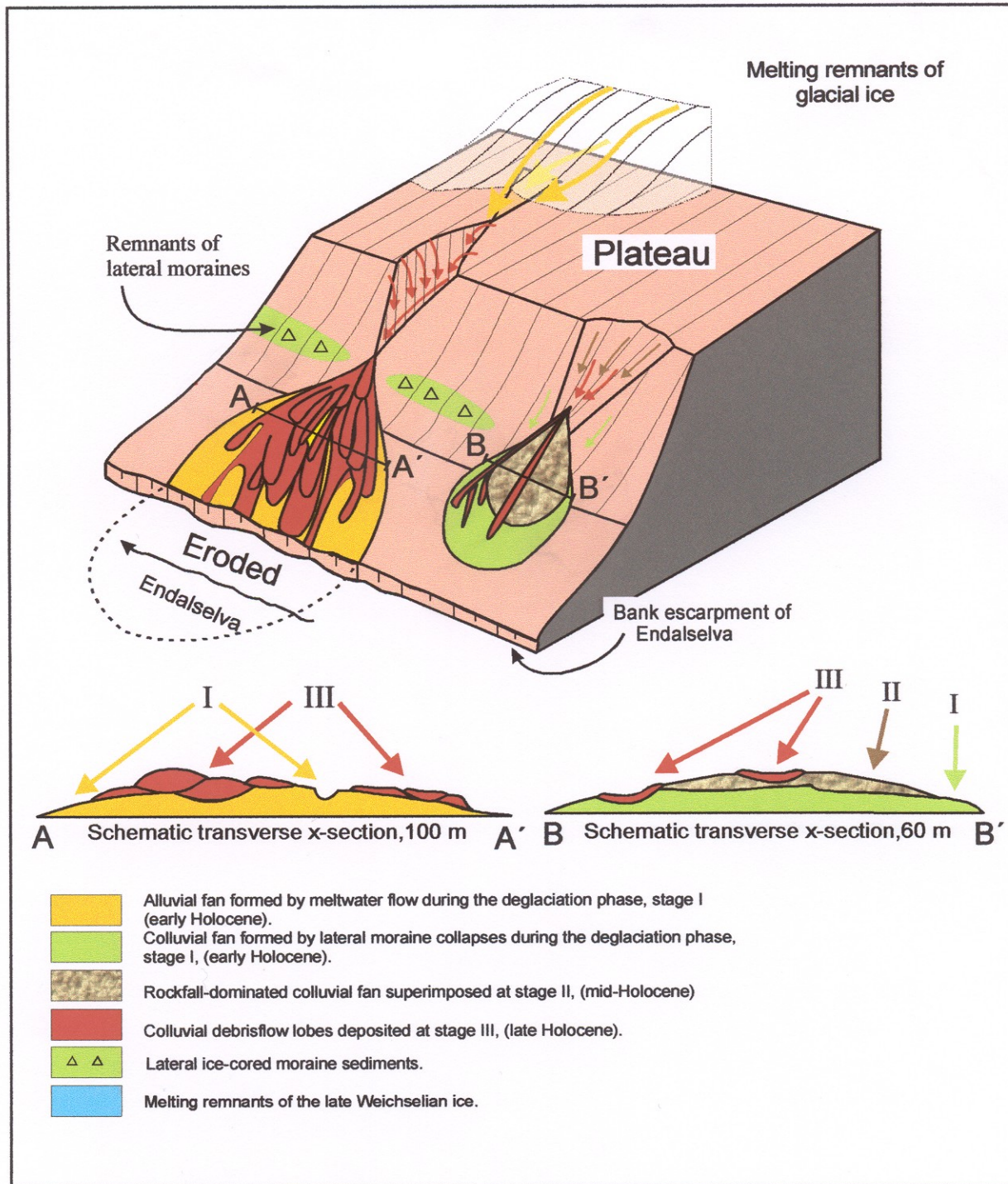
Fig. 6.2: Schematic stratigraphy of the valley-side gravel fans, eastern side of Endalen.

Stage I is represented by the oldest, relatively broad, low-relief mounds of gravelly base-of-slope deposits that are now covered with vegetation and have fairly smooth surfaces with poorly recognizable debrisflow levees. These oldest deposits are invariably associated with pronounced mountain-slope ravines scoured by plateau-derived meltwater flow, but the alluvium is thought to include debrisflow deposits generated directly by slope failures (resedimentation of lateral moraine

and the melting of permafrost). These earliest postglacial valley-side deposits, attributed tentatively to the early Holocene (Fig. 2.5), can probably be classified as alluvial fans (see lower segments of the fan profiles in Figs. 5.5D, 5.6C & 5.7D). The coeval slope-failures in other parts of the valley-side zone, between the waterflow ravines, are likely to have formed some incipient colluvial fans, but these are now hardly recognizable due to their further reworking and being covered by the subsequent slope-waste processes and products. The sedimentation stage I was probably of a relatively long duration, accompanying the deglaciation and continuing during the subsequent climatic optimum, and was likely characterized by the highest rate of sediment flux to the foot zone of the valley-side slope. Most of the glaciogenic deposits were probably eroded during this early postglacial stage, due to the maximum intensity of waterflow and highest instability of slope-hosted glaciogenic deposits. The most pronounced accumulation of gravel was also most localized, associated with the ravines, and the waterflow rendered the downslope transfer of sediment quite effective. These oldest fan deposits have the longest horizontal extent, defining the outer limit of the multistorey fans (e.g., see Figs. 5.7B & 6.2) and often extending far onto the valley floor, into the axial zone now scoured and occupied by Endalselva (see the logged section in Fig. 3.15).

A phase of climatic cooling then commenced about 4000 BP (Svendsen & Mangerud, 1992), and this change is thought to be reflected in the sedimentation of stage II, characterized by rockfall processes and little evidence of flowing water. The lower atmospheric temperatures lengthened the winters and favoured the formation of small, rockfall-dominated colluvial fans on top of the debrisflow-dominated colluvial fans of stage I (see Fig. 5.6). The rockfall deposits of stage II are rarely overlying the larger alluvial fans of stage I on the eastern side of Endalen, either because the ravines were short of debris after the phase of meltwater flow, or because the deposits of stage II on these fans have been completely reworked and/or buried by the more extensive debrisflow processes and deposits of stage III. The middle to late Holocene cooling led to a neoglacial advance, culminating in the Little Ice Age. In western Norway, the activity of rockfall processes increased recognizably around 3800 BP, presumably as a result of colder winters and increased summer precipitation (Blikra & Nesje, 1997).

The slope-derived deposits of stage III are recognizable as abundant fresh debrisflow scours with levees and elongate gravel lobes on the surfaces of the older fans. These young debrisflows have commonly scoured the rockfall-dominated colluvial deposits of stage II and occasionally also the oldest fan alluvium of stage I (e.g., Figs. 5.10A & 6.2). Most of the deposits of stage III were probably accumulated during the 20th century, after the Little Ice Age, and a local series of aerial photographs from 1936 to 1990 show the activity of debrisflow processes (Fig. 6.3A, B & C). For example, fan Ee3 shows clearly an increase in colluvial sedimentation from 1936, when one major
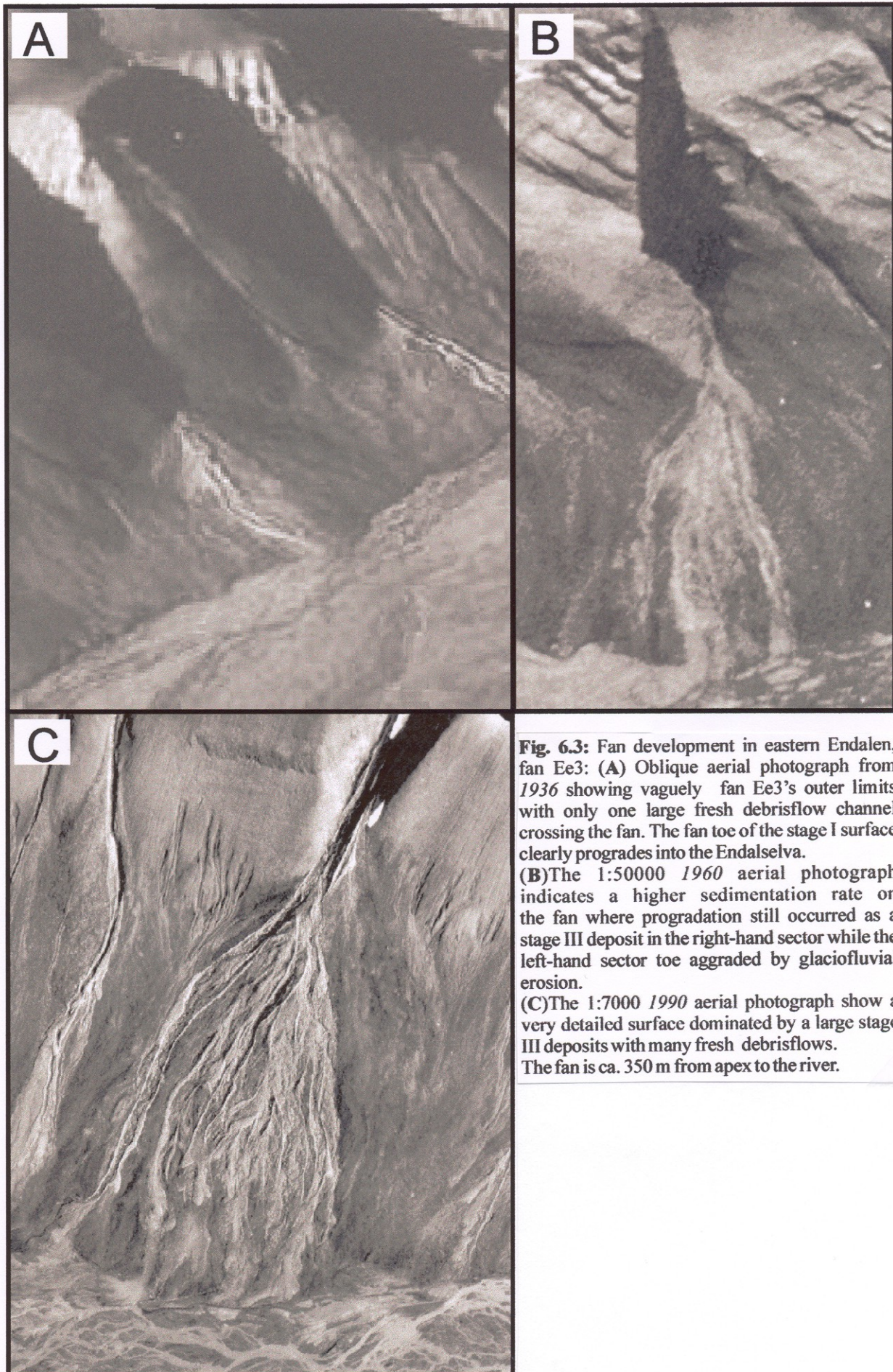
Fig. 6.3: Fan development in eastern Endalen, fan Ee3: **(A)** Oblique aerial photograph from *1936* showing vaguely fan Ee3's outer limits with only one large fresh debrisflow channel crossing the fan. The fan toe of the stage I surface clearly prograde into the Endalselva.

(B) The 1:50000 *1960* aerial photograph indicates a higher sedimentation rate on the fan where progradation still occurred as a stage III deposit in the right-hand sector while the left-hand sector toe aggraded by glaciofluvial erosion.

(C) The 1:7000 *1990* aerial photograph show a very detailed surface dominated by a large stage III deposits with many fresh debrisflows.
The fan is ca. 350 m from apex to the river.

channel in the fan central sector dominated the dispersal of debris, to 1990, when the fan surface has been completely altered and remoulded by the emplacement of fresh debrisflow deposits.

The meteorological observations in Spitsbergen area commenced in 1912, and a recognizable increase in atmospheric temperatures was noted after 1930 (Fig. 6.4A). A coeval temperature rise of similar magnitude was recorded also at the western coast of Greenland, where it changed the continuous permafrost to a discontinuous one (Humlum, 1999). The temperature rise in Spitsbergen presumably resulted in a similar change, destabilizing the active layer and increasing the intensity of slope-waste processes. After 1930, several episodes of abnormally warm weather, sometimes combined with heavy rainfalls, were recorded in the Adventdalen area (Fig. 6.4A & B).
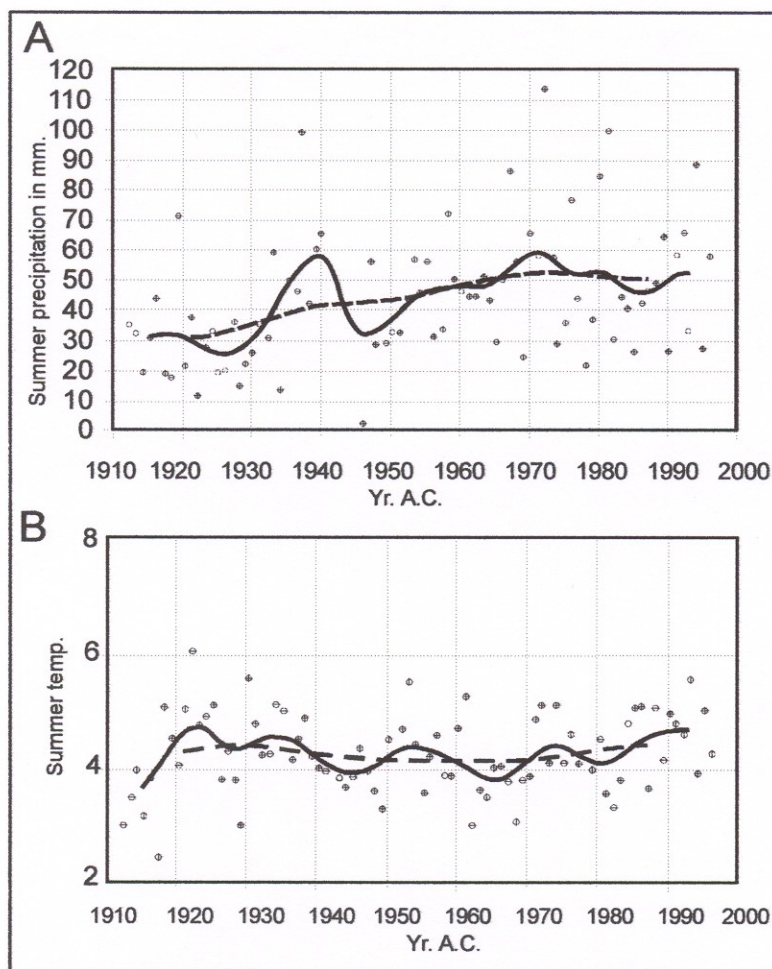
Fig. 6.4: (**A**) Average precipitation in mm during the summer months (June, July and August) with two different filters (hole line 3yr. and stippled line 9 yr.). A noticeable trend towards more frequent rainstorms is visible in the data with 1937, 1972 and 1981 as the most rainy summers. (**B**) Temperatures in C° (J u n e,   J u l y   a n d August). None of the extreme temperatures correlate with the extreme precipitation summers indicating that high summer do not cause debrisflows alone, but should becombined with precipitation to trigger larger slope avalanches (from Førland *et al.*, 1997).

The surficial changes shown by colluvial fan Ee3 between 1936 and 1960 may have occurred during the wet summer seasons in 1937 and 1958 (see Fig. 6.4A & B). The rainfall during summer seasons seems to have increased in frequency during the last 50 years (Fig. 6.4A). Between 1960 and 1990, several summers where rainy and caused the emplacement of new debrisflows on the

colluvial fan surfaces. The summer precipitation in Longyearbyen area was extremely high in 1972 and 1981, but since the triggering of debrisflows may involve a number of factors (Larsson, 1982), it is uncertain if these weather extrema have actually led to the emplacement of a significant number of debrisflows in the study area. In June 1953, for example, the summer temperatures were unusually high and increased the melting rate of permafrost and local snow patches, resulting in a large slushflow avalanche in Vannledningsdalen, a steep tributary of Longyeardalen (Jahn, 1967).

In the eastern part of Endalen, many of the fresh debrisflow deposits on the surfaces of colluvial fans in area B overlie wires and cables derived from the mining activity that ended in 1973 (P.O. Morken, pers. comm. 1999). This indicates that many of these debrisflows may be younger than the 1972 rainstorm, perhaps related to the summer rainfalls in 1981, 1990 and 1995 (Fig. 6.4A) or to a more subtle combination of factors, possibly involving slush.

It is interesting to compare the longitudinal profiles of fans A1, Ee2 and Ee3 (Fig. 6.5, for locations see Figs. 5.3, 5.6 & 5.7). In contrast to fan Ee3, associated with a large ravine and plateau catchment, the colluvial fans A1 and Ee2 were subject to little meltwater runoff from the mountain plateau. The latter two fans are characterized by a relatively steep and smooth depositional profile of stage I, whereas the profile of fan Ee3 is characterized by a pronounced deposition of stage III around the altitude of 300 m and smaller debrisflow lobes around 200 and 100 m (Fig. 6.5).
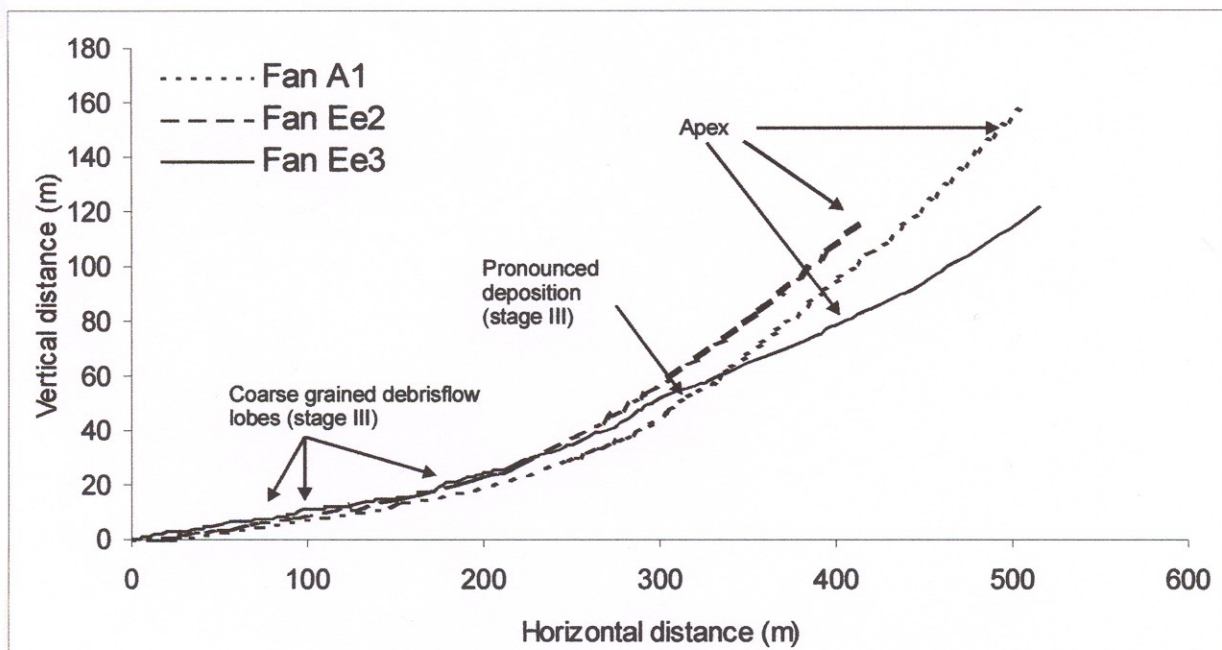
Fig. 6.5: Comparison of the longitudinal fan profiles (fans A1, Ee2 and Ee3), eastern side of Endalen, using the fan toe as reference point .The horizontal length of the profiles are different due to difficulties in measuring the steep slopes in field. Note the pronounced stage III deposits near 300 m on fan Ee3.

An abundant coarse debris is presently stored in the steep ravine above fan Ee3, and is likely to be released by a rainstorm or rich accumulation of slush. The deposits of stage II are rather poorly recognizable in the profile of fan Ee2, marked a subtle break in gradient at the altitude of 220 m. The deposits of stage III are hardly recognizable in the profile of fan A1, where they have apparently been distributed rather evenly, without visibly disturbing the gradient. The lower segment of the fan profile in all three cases is the smooth, old depositional surface of stage I, partly covered conformably with the younger debrisflow deposits of stage III.

6.2.2. Rockfall processes and slope failures

In Spitsbergen, rockfalls occur both in winter and during the summer, contributing to the sediment accumulation in the slope ravines and on the base-of-slope colluvial fans (Jahn, 1967; Åkerman 1984; Sollid & Sørebel, 1988). These processes are common also in the present study area, due the steep and frost-shattered rockwalls. During the summer, rockfalls may lead to the temporal accumulation of debris in local depocentres on the mountain slope (Lægreid, 1999), and these metastable accumulations subsequently tend to collapse under the influence of slush and meltwater, due to rainstorms or the melting of the active layer, or sometimes due to the slow creep processes driven by diurnal freeze-and-thaw cycles (Larsson, 1982). No such failures were observed in the study area during the 1998 field season, but the colluvial processes are inherently low-frequency phenomena that require longer-term continuous observation of a mountain slope to be spotted.

On the hard surface of a windblown snowpack, cobbles and boulders derived by rockfalls are able to roll and bounce, thus often moving down to the fan surface or the adjacent valley floor. In the summer, when snowpack is lacking, the rockfall clasts often come to rest in the ravines or fan-head channels.

The relative frequency of rockfalls and the areal distribution of their deposits on the eastern side-slope of Endalen have not been assessed in details, but it has been suggested by Åkerman (1984) on the basis of the aerial photographs of Adventdalen area that the highest frequency of small rockfalls is associated with the west-facing mountain cliffs, subject to maximum solar radiation. If this rule applies to the eastern slope of Endalen, then the rockfall products here are mainly redeposited as debrisflows or obliterated by the latter. Surficial observations suggest, in fact, that the rule may be quite opposite in the inner part of Endalen, where the east-facing slope, remaining in a shadow through most of the day, hosts well-developed colluvial fans dominated by rockfall processes (see Lægreid, 1999). The west-facing colluvial slope, more exposed to the sun, is

dominated by debrisflow processes and deposits. Although, Åkerman's study did include aerial photographs from the 3rd-order Endalen valley, it did not take into consideration that in Endalen the slope-waste processes are to a great extent pre-conditioned by the plateau-edge morphology inherited from the deglaciation stage and sculptured by the associated pattern of local meltwater drainage. Furthermore, the slope ravines here have a high capacity to accumulate snowdrift, which means an abundance of slush and meltwater and a higher potential for debrisflows in the west-facing slope. Åkerman's observation are chiefly from Linnédalen area, where the mountain slopes were unaffected by the plateau drainage, and his tentative estimates cannot thus be considered to provide a general rule for the areal variation in rockfall intensity in the central Spitsbergen. Furthermore, the bedrock stratigraphy on the western side of Endalen includes steep cliffs of the Basilika Fm. and Grumantbyen Fm., which favors rockfalls. These sandstone-rich formations are removed by erosion on the eastern side of Endalen (Fig. 3.2). Therefore, it would appear that the local bedrock geology and the geomorphic impact of the deglaciation phase of meltwater drainage may play a particularly important role in controlling slope-waste processes in the 3rd-order valleys in Spitsbergen.

The permafrost table and the summer rainfall are other factors that probably have an important effect on the colluvial sedimentation in a high-Arctic valley such as Endalen. A shear plane of detachment and sliding tends to develop between the water-saturated surficial layer of debris and the permafrost below (Larsson, 1982). Heavy rainfalls and spells of warm weather cause deeper melting of the active layer, which may lead to large slope failures more readily than in other climatic settings (Larsson, 1982). For example, the July 1972 slope-failure event in Longyearbyen was caused a heavy rainstorm on the 10th and 11th of July, after a prolonged period of dry summer weather (Larsson, 1982). A recalculation of the data given by Larsson (1982) indicates a rainfall intensity of 1.3 mm/hr (Lægreid, 1999). The rainstorm have triggered about 80 debrisflows in Longyeardalen and many more similar massflows in the adjacent valleys (Larsson, 1982). Notably, a rainfall rate of 1.3 mm/hr is an extremely low value compared to the threshold values reported for other climatic settings, and it is the impermeable permafrost combined with an abrupt oversaturation of the surficial layer of loose debris that play a crucial role in triggering slope failures in this high-Arctic region. For comparison, the July and August 1976 were almost continuously rainy, with a cumulative monthly precipitation of 23 and 63 mm, respectively, but no debrisflows occurred in Longyeardalen or the adjacent valleys. Hence, it is rather a rainstorm and abrupt oversaturation that tend to trigger slope failures.

Similar observations have been reported from other climatic settings. Sandersen *et al.,* (1996) have examined more than 30 historical debrisflow events in sub-Arctic Norway and concluded that

the triggering factor was typically an episode of heavy rainfall of approximately one-day duration and intensity between 5 and 30 mm/hr, accompanied by a 1- to 4-hour rainstorm or combined with rapid snowmelt. In the humid North Island of New Zealand, landslides occur typically after an episode of heavy rainfall with an intensity of 85 mm/hr or more (Rogers & Selby, 1980), but a peak precipitation of 8.5 mm/hr was enough to trigger a series of debrisflows on a water-saturated sedimentary slope in North Canterbury after a rainfall of 310 mm during the preceding three days (Pierson, 1980). In the western part of the semiarid American Great Basin, a rainfall intensity of 50-70 mm/hr is generally required to trigger debrisflows (Beaty, 1974).

The colluvial fans outside the mouth of Endalen, on the adjoining side-slope of Adventdalen, stay persistently in a solar shadow and receive no significant runoff from the mountain plateau, and these fans are thus not particularly active at present. This relationship highlights the important role of the controlling factors discussed in this chapter. Some fresh debrisflow gullies and lobes are observed in this area, particularly on fan A3 (Fig. 5.3), and although these features seem to be of approximately the same relative age as many of the debrisflows in Endalen, they are clearly unrelated to any water runoff from the mountain plateau. The ravines here are small and do not reach the plateau edge, and the small slope catchments of the fans are nearly devoid of snow through most of the winter. The sporadic debrisflows are most probably related to episodic heavy rainfalls and a seasonal deep melting of the active layer (cf. Fig. 6.3).

6.2.3. Rock glaciers or ice-cored lateral moraine relicts

A range of rock glacier types have been described from Spitsbergen, and the most common is the talus-foot lobate type, with a length much shorter than the width (André, 1994). In contrast, tongue-shaped rock glaciers occur at several localities in the Adventdalen area, with lengths greater than widths, similar to the rock glacier varieties described by Giardino & Vick (1987). The rock glaciers in the Adventdalen area are not associated with strandflats, unlike most of the rock glaciers described in Sollid & Sørbel (1992), and occur in ravine escarpments or cirques at an altitude of 500-600 m, some extending several hundred metres downslope.

The two rock glaciers in Endalen, one near the entrance to Coal Mine 5 and the other at the valley floor opposite of the cirque in area C (Fig. 3.10; Lægreid 1999), differ in morphology, although may be of similar origin. It is uncertain if the latter rock glacier is of a talus (Barsch, 1988) or a protalus type (Walley & Martin, 1992), or merely a relict of an ice-cored lateral moraine (Lægreid, 1999). The topographic position and morphology of the rock glacier near Coal Mine 5

are different from those of the lobate rock glaciers described from the north-western Spitsbergen by André (1994), although the glacier's length/width ratio of 1 is similar as in many lobate rock glaciers (cf. Giardino & Vick, 1987). The rock glacier in the present case is situated in the middle of the valley-side mountain slope, with the debris derived from a high rockwall. The relatively high altitude and the fact that the upper part of the rock glacier is partly covered by small, rockfall-dominated, postglacial colluvial fans suggest that the rock glacier itself may be an older feature. It is likely that this rock glacier is a remnant of an ice-cored lateral moraine, deposited during the last deglaciation (see Fig 6.1 B), that has creeped downslope due to a partial melting of the ice core, the seasonal melting of the slope's active layer and the load of the overlying debris. Neoglacial permafrost processes may have contributed to the remoulding of the moraine relict and make it look like a typical rock-glacier lobe. It should be noted that this genetic type of rock glaciers has been little described from Svalbard and the model for ice-cored moraines evolving into rock glaciers is still disputed (Barsch, 1987; Hamilton & Whalley, 1995).

Based on the assumption that the rock glaciers in Svalbard are true periglacial features, formed in permafrost conditions after the climatic optimum (Barsch, 1987), an age of around 3500 BP have been suggested for the rock glaciers in northern Spitsbergen, dated partly by lichenometry (André, 1994). The rockfall taluses covering the rock glacier in the present case is probably of an middle Holocene age (earlier mentioned as stage II), thus the formation of the rock glacier itself, by the transformation of a primary moraine relict, must have occurred in middle to late Holocene time. A lateral moraine at this location fits well in the deglaciation model (Fig. 6.1B).

6.3. Snow conditions and the role of meltwater flow: implications from Endalen

Due to the low precipitation that characterizes the "Arctic desert" region, the snow cover in Spitsbergen is generally thin and discontinuous. Snowdrift is important, not least because 35-45 % of the days every year have winds stronger than 6 in the Beaufort scale. The mean precipitation measured at Longyearbyen airport is merely 190 mm/yr. (Førland *et al.,* 1997), less than 10 times lower than the corresponding value at the sea level in western Norway (ca. 2000 mm/yr.). However, the strong winds render the local measurements somewhat unreliable, because much of the snow simply bypasses the snow-collecting devices (Førland *et al.,* 1997). Measurements from Endalen t he 1998 winter season (Table 4.1) support this reservation by Førland et al. (1997). In the mountain slope ravines and fan channels in the study area, the thickness of wind-derived snow cover commonly reaches several metres. The snow cover is much thinner (0-25 cm) on the flat

surfaces exposed to wind (see earlier Figs. 4.3 & 4.4), but the lee sides of gravelly levees and other protruding features invariably tend to accumulate more snow (Fig.4.5). Likewise, abundant snow tends to accumulate in the open interstices of bouldery scree gravel.

The high frequency of strong winds and the changes in wind direction, along with the varied surface morphology, are probably the main reason of the variable thickness of a local snow cover over relatively short periods of time (Fig. 4.3). In short, wind is a key agent controlling the thickness distribution and local excessive accumulation of snow in Spitsbergen.

In western Norway, for comparison, both the annual precipitation and the air temperatures are much higher. Wind is still an important factor, but the conditions of low atmospheric pressure and high precipitation reach western Norway mainly in connection with south-westerly winds, forming large cornices above the lee slopes during the winter and causing snow avalanches. The avalanches derive debris from the sedimentary substratum, often non-frozen or water-soaked in the springtime, and generally play an important role as an agent of local colluvial sedimentation. No comparable conditions occur in the high-latitude Arctic region.

The meteorological data from the Longyearbyen airport show that the air temperature there seldom rises above 0º C before late May (Appendix A). In the spring 1998, after more than a month of midnight sun, the snow-free areas in Endalen visibly expanded, without any significant surficial runoff of meltwater. The solar radiation on sunny days is strong enough to instigate the process of snow sublimation, although the permafrost and the radiation-reflecting effect of the surrounding snow cover cause the wet snow and the meltwater to freeze during the night hours. Where the snow cover is thin and the exposure to sun sufficiently long, the sublimation makes the snow disappear. Measurements by Takeuchi *et al.,* (1995) in Ny Ålesund area from October to June 1993 have indicated a sublimation rate of 7-20 cm/yr. (Winther *et al.,* 1998).

It is worth noting that the process of sublimation is important in areas where the solar radiation is high, but the air temperatures are low. In western Norway, sublimation thus plays a minor role in the removal of snow cover, because (1) the sub-Arctic climate is warmer, the snow melts faster and the meltwater percolates into the unfrozen substratum, and (2) the lack of midnight sun renders the daily phases of active sublimation much shorter. Consequently, the meltwater runoff in sub-Arctic Norway is far more pronounced and much more effective as an agent of sediment transport.

However, short summer peaks of meltwater runoff of 2- to 3-week duration may occasionally erode the bedrock in mountain-slope ravines and rejuvenate fan channels, flushing some of the frost-shattered shale debris to the lower colluvial slope (see earlier Fig. 4.6). When the active layer thaws, by ca. 70 cm during the summer, the weathered shaley bedrock on the steep sides of a ravine tends to collapse and either avalanches further downslope or contributes to the ravine's latent stock

of debris. A rainstorm or a spell of warm weather causing deeper thaw of the active layer can trigger debrisflows or debris-laden slushflow avalanches that transfer sediment to the lower colluvial slope or valley floor (Larsson, 1982; André, 1990). Sandstone debris is generally much coarser, less mobile and lagging behind. One may speculate that only an abundant admixture of slush is probably capable of lubricating such a mass of angular, blade-shaped bouldery debris (see Figs. 5.9A & 5.11). The sediment transport processes are thus dependent on the slope snow conditions, seasonal atmospheric conditions and the amount of available surficial water. July is generally characterized by the highest precipitation (Førland *et al.,* 1997) and the highest probability of debrisflow occurrence, whereas slushflow avalanches are more likely to occur in the early June, in connection with the peak of snow melting (André, 1990). The summer in 1998 was relatively warm (see Appendix A), but no debrisflows occurred on the slopes in Endalen, probably due to the lack of rainfall and/or a temporal lack of any critically unstable accumulation of debris in the slope ravines.

It is very unlikely that the large masses of immature cobble and boulder gravel that constitute the colluvial fans may have been transported downslope by flowing water. The large bladed clasts are highly immobile, whereas the occurrence of powerful flash flows is virtually unlikely in the study area. The meltwater runoff from the mountain plateau is very limited and incapable of removing large amounts of debris from the ravines, except for the fine-grained sediment, rarely coarser than granule or fine-pebble gravel. However, the percolating water almost certainly has the capacity to infiltrate the coarse gravel with fine sediment, and this watery matrix might then lubricate the gravel mass and turn it into a debrisflow. The rainwater and the meltwater from snow cover might subsequently remove much of the fine-grained matrix from a debrisflow lobe resting on a colluvial fan surface. In short, the surficial runoff on the valley-side slopes is sparse, but its role in modifying the gravel texture and mobility may be very important.

The water discharge is seasonally high in the valley-floor river, which derives its water from the valley-head glacier and is capable of rolling boulders up to 50 cm in diameter during summer floods. The permafrost maximizes the river discharge, while minimizing the runoff on the adjacent mountain slopes, where a substantial portion of the limited meltwater tends to be retained in the permeable active layer and drain very slowly downslope. These recent conditions are different than during the deglaciation, when the meltwater yield on the mountain plateaux was incomparably higher and the sediment-transport capacity of the flowing water in the slope ravines was probably much higher (see earlier Chapter 6.2.1.).

It has been suggested above that slush may play an important role in mobilizing and lubricating coarse debris in ravines (see also André, 1990), but the possible role of dry, powder-snow

avalanches in the colluvial sedimentation in the study area is very uncertain. Although snow cornices have been observed to form at the plateau edges in Endalen during the winter, these snow masses were never observed to collapse and avalanche downslope. Similarly, snowflow deposits have not been recognized on the colluvial slopes in the study area during the summer fieldwork season. The cornices there persisted into the melting season and were probably frozen to the rockwall, while melting *in situ* by sublimation, instead of collapsing into avalanches. Powder-snow avalanches are know to occur locally on the mountain slopes in Spitsbergen during the winter, but they do not seem to transport significant amounts of debris, probably due to the permafrozen substratum (I. Lønne, pers. comm. 1999). In the sub-Arctic western Norway, in contrast, large snow avalanches are common during the winter, eroding and transporting significant amounts of debris on the colluvial slopes and acting as an important agent of colluvial sedimentation (Blikra & Nemec, 1998).

7. CONCLUSION

The present study, focused in the valley-side gravel fans in the eastern part of Endalen and the adjoining side-slope of Adventdalen, has contributed to an understanding of the spatial pattern of the last (late Weichselian) deglaciation and associated meltwater drainage in a 3rd-order and a 2nd-order valley and adjacent mountain plateau in the high-Arctic region of central Spitsbergen. The study methods included geomorphological mapping, sedimentological field observations and an analysis of both conventional and infrared aerial photographs. The fieldwork in 1998 was focused in the following main topics: (1) the mapping and chronology of sediment accumulations, (2) the assessment of the intensity, routes and controlling factors of the downslope transfer of sediment and water, including the recognition and spatial pattern of meltwater palaeodrainage traces (linear scours) and their significance for the reconstruction of the last glacial retreat; (3) the development history and depositional processes of the valley-side gravel fans; and (4) the snow-cover conditions on the valley-side slopes during the whole melting to freezing season in 1998, including comparative photographic documentation and fixed-point snow thickness measurements.

The analysis of infrared aerial photographs has proved to be very useful in deciphering the areal pattern of meltwater palaeodrainage and other geomorphic features of the deglaciation stage. Arrays of surficial palaeochannels are recognizable on the eastern plateau of Endalen, trending NW and lacking any obvious water catchment today, and these scours are thus attributed to the meltwater runoff during the early Holocene deglaciation. Notably, the palaeochannels are mainly bedrock scours that lack associated deposits, which indicates that the scouring occurred during a period of high water discharges and the sediment transported by the waterflow has apparently been carried off the plateau area and transferred down to the adjacent valleys. Endalen itself must have concurrently conveyed large meltwater discharges from glacial ice in the upper part of the valley.

The morphological mapping failed to recognize any preserved glacigenic diamicton deposits on the eastern plateau of Endalen, but erratic cobbles and boulders have been found on the western plateau, directly outside the Endalen drainage basin, which indicates that the mountain plateaux were covered by the ice-sheet. Long-transport erratics have also been identified in Endalen, including the valley's eastern slope. Based on the aerial photographs

and direct field observations, a tentative spatial model has been suggested for the deglaciation of the Adventdalen area (Fig. 6.1).

The meltwater drainage from the plateau, localized by mountain slope ravines, is thought to have resulted in differences in the size and shape of the valley-side postglacial fans in Endalen. The gravel fans whose formation involved direct meltwater flow from the plateau are larger, associated with well-incised ravines and often show two storeys of deposits recognizable in geomorphic terms: a broad mound of older, vegetated base-of-slope deposits (alluvial fan), distinguished as sedimentation stage I, and a smaller, steeper accumulation of relatively fresh younger deposits (colluvial fan) superimposed onto the upper/apical part of the former and distinguished as sedimentation stages II and III. The three stages of deposition are interpreted as: (I) an early Holocene, early postglacial stage dominated by the meltwater runoff from the plateaux and coeval high-viscosity debrisflows on the mountain-slopes between the ravines; (II) a middle Holocene stage dominated by rockfall processes and minor debrisflows; and (III) the late Holocene stage dominated by the more mobile, watery or slush-laden debrisflows. The low-viscosity debrisflows of stage III have commonly caused strong incision in the fan apex and upper segment, with channels up to a few metres deep and the associated intersection-point deposits making the fan prograde in a "telescoping" style and aggrade in the lower segment. This tripartite fan stratigraphy is thought to reflect the Holocene climatic changes, as interpreted by Svendsen & Mangerud (1997).

The deglaciation phase was characterized by an abundant meltwater runoff, with the deposition of waterlain fans, of sedimentation stage I, at the toes of the bedrock ravines accompanied slope-wasting processes and a removal of much of the glaciogenic deposits from the valley-side slope. The colluvial sedimentation of stage I followed directly the deglaciation phase, when the valley-side slope was still charged with glacial debris. The deposits of stage I are base-of-slope accumulations that have been mainly smoothened and covered by vegetation, with some recognizable surficial traces of levees and broad, matrix-supported gravel lobes, indicating deposition by cohesive, high-viscosity debrisflows. Most of the glacier ice had melted during the climatic optimum, around 8000 yrs BP, and the slope-waste processes had removed most of the unstable mantle glaciogenic debris. The subsequent stage II, dominated by rockfall processes, reflected colder climatic conditions and a temporal exhaustion of the slope sedimentary mantle. The rockfall colluvium consists mainly of coarse angular debris derived by frost action form the steep sandstone cliff of the Firkanten Formation. Some of the rockfall deposits were probably accumulated in the slope ravines, and have later been removed as debrisflows in the late Holocene time, during the sedimentation

stage III. These deposits are highly elongate channel-and-lobe features with bouldery channel-flank levees, superimposed "imbricate" lobes (overridden by one another) and runout distances of 200-500 m on fan slopes of 15° to 2°, which is a clear evidence of a high mobility (low viscosity) of the depositing debrisflows. Some of the debrisflow lobes consist of a matrix-supported gravel, rich in muddy sand, but the majority are openwork or containing matrix in the lower parts only. The gravel is blade-shaped cobble and boulder debris, and the debrisflows must have been lubricated by some interstitial medium. There are two possibilities, not necessarily mutually exclusive: (a) the debrisflows may have originally contained an abundant fine-grained watery matrix, which was subsequently washed out from the deposits; or (b) the debrisflows may have contained an abundant admixture of wet snow or slush, which subsequently melted and left an openwork gravel.

The ravines collect coarse rockfall debris, but are prone also to the accumulation of both fine sediment and snow, and thus seem to be capable of generating either type of debrisflow in the summer. Debrisflows may be triggered by the early-summer melting of a ravine-hosted snowpack, by a summer event of heavy rainfall and/or by a summer episode of a deeper melting of the active layer.

The snow cover is generally sparse, due to the low precipitation in the Arctic desert, but the predominance of strong and variable winds renders them a key agent controlling the thickness distribution and local excessive accumulation of snow in Spitsbergen. In Endalen, the winter winds are capable of filling ravines with several metres of snow and forming large snow cornices. No snow avalanches were observed on the valley slopes during the weekly visits in the winter 1998, but this does not preclude, of course, the occurrence of such processes. No debrisflows and no large rockfalls were observed either in 1998, but the slopes show clearly that these processes do occur in Endalen. However, parts of the snow cover, especially where thin, seems to disappear due to the processes of sublimation and gradual melting, with the main phase of melting in the early June. The surficial runoff on the valley-side slopes is very limited, but its role in modifying the gravel texture and mobility may be very important for the postglacial sedimentation on the mountain-side slopes.

The meteorological record from this part of Spitsbergen, with data since 1912, indicates the occasional occurrence of an unusually warm and rainy summer weather, which might explain episodes of debrisflow activity. The available aerial photographs suggest an increased frequency of debrisflows on the colluvial fans in Endalen during the last 70 years.

It has been suggested by Åkerman (1984), on the basis of the aerial photographs of Adventdalen area, that the highest frequency of small rockfalls is associated with the west-

facing bedrock cliffs, most exposed to the solar radiation. If this rule applies to the eastern slope of Endalen, then the rockfall products here are mainly redeposited as debrisflows or obliterated by the deposits of the latter. Surficial evidence indicates that the rule may actually be opposite in the inner part of Endalen, where the east-facing slope, remaining in a shadow through most of the day, hosts well developed colluvial fans dominated by rockfall processes. The west-facing colluvial slope is clearly dominated by debrisflow processes.

Based on a relative dating, the rock glacier near the entrance to Coal Mine 5 in the study area is interpreted to be a remnant of an ice-cored lateral moraine left by the last deglaciation. The primary glaciogenic deposit is thought to have creeped downslope due to a partial melting of the ice core, the seasonal melting of the slope's active layer and the load of the overlying, rockfall-dominated, postglacial colluvial fans.

References

Andersson, T., Forman, S. L., Ingolfson, O. & Manley, W. F. (1999) Late Quaternary environmental history of central Prins Karl Forland, Western Svalbard. Boreas, 28, 292-307.

André, M.-F. (1986) Dating slope deposits and estimating rates of rock wall retreat in northwest Spitsbergen by lichenometry. Geografiska Annaler, 68A(1-2).

André, M.-F. (1990) Geomorphic impact of spring avalanches in northwest Spitsbergen. Permafrost and Periglacial Processes, 1, 97-110.

André, M.-F. (1994) Rock glaciers in Svalbard: Tentative dating and inferred long-term velocities. Geografiske Annaler, 76 A, 235-245.

Astakhov, V. I., Svendsen, J. I., Mathiouchkov, A., Mangerud, J., Maslenikova, O. & Tverranger, J. (1999) Marginal formations of the last Kara and Barents ice sheet in northern European Russia. Boreas, 28, 23-45.

Baas, J. H. (2000) EZ-ROSE: a computer program for equal-area circular histograms and statistical analysis of two-dimensional vectorial data. Computers & Geosciences, 26, Nr.2, 153-166.

Barsch, D. (1987) The problem of the ice-cored rock glacier. Allen & Unwin, Boston, 355 pp.

Barsch, D. (1988) Rockglaciers. In: Advances in Periglacial Geomorphology (Ed. by M. J. Clark). John Wiley & Sons Ltd, New York.

Beaty, C. B. (1974) Debris flows, alluvial fans, and a revitalized catastrophism. Z. Geomorphology N. F., Suppl. Bd. 21, 39-51.

Berger, A., Imbrie, J., Hays, J., Kukla, G. & Saltzman, B. (1984) Understanding the Response to Astronomical Forcing. In: Milancovitch and Climate. Riedel, Dordrecht.

Birks, H. H., Paus, A., Svendsen, J. I., Alm, T., Mangerud, J. & Landvik, J. Y. (1994) Late Weichselian environmental-change in Norway, including Svalbard. Journal of Quaternary Science, 9(2), 133-145.

Blikra, L. H., Hole, P. A. & Rye, N. (1989) Rapid mass movements and related deposits in alpine areas, indre Nordfjord, Western Norway. Norges Geologiske Undersøkelse Skrifter, 92, 1-17.

Blikra, L. H. (1994) Colluvial Sedimentary Processes and Facies: Postglacial Avalanche Sedimentation in Western Norway. Postglacial Colluvium in Western Norway: Sedimentology, Geomorphology and Palaeoclimatic Record. Unpubl. Dr. Scient. thesis, University of Bergen.

Blikra, L. H. & Nesje, A. (1997) Holocene avalanche activity in western Norway: Chronostratigraphy and palaeoclimatic implications. Palaoklimaforchung, 19, 299-312.

Blikra, L. H. & Nemec, W. (1998) Postglacial colluvium in western Norway: depositional processes, facies and palaeoclimatic record. Sedimentology, 45, 909-959.

Blissenbach, E. (1954) Geology of alluvial fans in semiarid regions. Bulletin of the Geological Society of America, 65, 175-190.

Bluck, B. J. (1967) Sedimentation of beach gravels: examples from South Wales. Journal of Sedimentary geology, 37, 128-156.

Bowman, D. (1978) Determination of intersection points within a telescopic alluvial fan complex. Earth surface processes, 3, 265-276.

Bull, W. B. (1972) Recognition of alluvial fan deposits in the stratigraphic record. In: Recognition of Ancient Sedimentary Environments, Vol. Secial Publication 16 (Ed. by W. K. Hamblin and J. K. Rigby), pp. 63-83. Soc. Econ. Paleont., Tulsa.

Bull, W. B. (1977) The alluvial fan environment. In: Progress in Physical Geography, Vol. 1, pp. 222-270.

Caine, N. (1980) The rainfall intensity - duration control of shallow landslides and debris flows. Geografiske Annaler, 62A, 23-27.

Dalland, A. (1977) Erratic clast in the Lower Tertiary deposits of Svalbard - evidence of transport by winter ice. Norsk Polarinstitutts Årbok 1976, 151-166.

Dallmann, W. K. ((ed.) (in press)) Lithostratigraphic Lexicon of Svalbard. Review and recommendations for nomenclature use. Upper Paleozoic to Quaternary bedrock. Committee on Stratigraphy of Svalbard. Norwegian Polar Institute, Tromsø.

Eisbacher, G. H. & Clauge, J. J. (1984) Destructive mass movements in high mountains: Hazards and management. Geological survey of Canada, paper, 84-16, 230 pp.

Folk, R. L. (1968) Petrology of Sedimentary Rocks. Hemphill Publishing Co., Austin.

Fowler, A. C. (1987) A theory of glacier surges. Journal of geophysical research, 92, 9111-9120.

Førland, E. J., Hanssen-Bauer, I. & Nordli, P. Ø. (1997) Climate statistics and longterm series of temperature and precipitation at Svalbard and Jan Mayen. In: Klima. DNMI.

Giardino, J. R. & Vick, S. G. (1987) Geological engineering aspects of rock glaciers. Allen & Unwin, Boston, 355 pp.

Hagen, J. O., Liestøl, O., Roland, E. & Jørgensn, T. (1993) Glacier atlas of Svalbard and Jan Mayen. Norsk Polarinstitutt meddelelser, Nr. 129.

Hambrey, M. J., Dowdeswell, J. A., Murray, T. & Porter, P. R. (1996) Thrusting and debris entrainment in a surging glacier: Bakaninbreen, Svalbard. Annals of Glaciology, 22.

Hamilton, S. J. & Whalley, W. B. (1995) Rock Glacier nomenclature: A re-assessment. Geomorphology, 14, 73-80.

Hamilton, G. & Dowdeswell, J. A. (1996) Controls on glacier surging in Svalbard. Journal of glaciology, 42 No. 140, 157-168.

Harvey, A. M. (1984) Debris flows and fluvial deposits in spanish Quaternary alluvial fans: implications for fan morphology. Canadian Society of Petroleum Geologists, Memoir, 123-132 pp.

Harvey, A. M. (1989) The occurrence and role of arid zone alluvial fans. Frances Pinter, Belhaven, 136-158.

Harvey, A. M. (1992) Controls on sedimentary style on Alluvial fans. John Wiley & Sons Ltd.

Hooke, R. L. B. (1967) Processes on arid-region alluvial fans. The Journal of Geology, 75, 438-460.

Hooke, R. L. & Rohrer, W. L. (1977) Relative erodibility of source-area rock types, as determined from second-order variations in alluvial-fan size. Geological Society of America Bulletin, 88, 1177-1182.

Hooke, R. L. & Rohrer, W. L. (1979) Geometry of alluvial fans: effect of discharge and sediment size. Earth surfaces processes, 4, 147-166.

Houmark-Nielsen, M. & Funder, S. (1999) Pleistocene stratigraphy of Kongsfjordhallet, Spitsbergen, Svalbard. Polar Research, 18(1), 39-49.

Hubert, J. F. & Filipov, A. L. (1989) Debris-flow deposits in alluvial fans on the west flank of the White Mountains, Owens Valley, California, U.S.A. Sedimentary Geology, 61, 177-205.

Humlum, O. (1999) Late-Holocene climate in central West Greenland: meteorological data and rock-glacier isotope evidence. The Holocene, 9, 4, 581-594.

Jahn, A. (1967) Some features of mass movement on Spitsbergen slopes. Geografiske Annaler, 49A(2-4), 213-225.

Johnson, A. M. (1970) Physical Processes in Geology. Freeman, Cooper & Co., San Francisco.

Johnson, A. M. & Rodine, J. R. (1984) Debris flow. John Wiley & Sons, New York, 257-361.

Krumbein, W. C. (1941) Measurement and geological significance of shape and roundness of sedimentary particles. Journal of Sedimentary Petrology, 11 No. 2, 64-72.

Lambeck, K. (1995) Constraints on the Late Weichselian ice sheet over the Barents Sea from observations of raised shorelines. Quaternary Science Reviews, 14, 1-16.

Landvik, J. Y., Bondevik, S., Elverhøi, A., Fjeldskaar, W., Mangerud, J., Salvigsen, O., Siegert, M. J., Svendsen, J. I. & Vorren, T. O. (1998) The last glacial maximum of Svalbard and the Barents sea area: Ice sheet extent and configuration. Quaternary Science Reviews, 17, 43-75.

Larsson, S. (1982) Geomorphological effects on the slopes of Longyear valley, Spitsbergen, after a heavy rainstorm in July 1972. Geografiske Annaler, 64 A, 105-125.

Lawson, D. E. (1982) Mobilization, movement and deposition of active subaerial sediment flows, Matanuska Glacier, Alaska. journal of geology, 90, 279-300.

Lægreid, A. K. (1999) Postglacial sedimentation in a high-arctic valley: slope processes and geomorphic development in Endalen, Spitsbergen. Cand. Scient. Thesis, University of Bergen.

Lecce, S. A. (1991) Influence of lithologic erodibility on alluvial fan area, Western White Mountains, California and Nevada. Earth Surface Processes and Landforms, 16, 11-18.

Lehman, S. J. & Forman, S. L. (1992) Late Weichselian glacier retreat in Kongsfjorden, west Spitsbergen, Svalbard. Quaternary Research, 37, 139-154.

Lønne, I. (1998a) The effect of glacial meltwater in shaping the land-scape on high latitudes, as seen from Svalbard (78oN). In: 28th Arctic Workshop. Institute of Arctic and Alpine Research, University of Colorado, Boulder, CO USA, Colorado.

Lønne, I. (1998b) The development of talus slopes and alluvial fans at Svalbard- A new approach. In: 28th Arctic Workshop. Institute of Arctic and Alpine Research, University of Colorado, Boulder, CO USA, Colorado.

Major, H. & Nagy, J. (1972) Geology of the Adventdalen map area. Norsk Polarinstitutt Skrifter, 138.

Major, J. J. (1998) Pebble orientation on large, experimental debris-flow deposits Sedimentary Geology, 117, 151-164. Sedimentary Geology, 117, 151-164.

Major, J. J. & Iverson, R. M. (1999) Debris-flow deposition: Effects of pore-fluid pressure and friction concentrated at flow margins. GSA Bulletin, 111, no.10, 1424-1434.

Mangerud, J. & Svendsen, J. I. (1992) The last interglacial-glacial period on Spitsbergen, Svalbard. Quaternary Science Reviews, 11, 633-664.

Mangerud, J., Dokken, T., Hebbeln, D., Heggen, B., Ingòlfsson, Ò., Landvik, J. Y., Mejdahl, V., Svendsen, J. I. & Vorren, T. O. (1998) Fluctuations of the Svalbard-Barents sea ice sheet during the last 150 000 years. Quaternary Science Reviews, 17, 11-42.

Mangerud, J., Svendsen, J. I. & Astakhov, V. I. (1999) Age and extent of the Barents and Kara ice sheet in Northern Russia. Boreas, 28, 46-80.

McArthur, J. L. (1987) The characteristics, classification and origin of late Pleistocene fan deposits in the Cass Basin, Canterbury, New Zealand. Sedimentology, 34, 459-471.

Nemec, W. & Steel, R. J. (1984) Alluvial and coastal conglomerates: their significant features and some comments on gravely mass-flow deposits. Canadian Society of Petroleum Geologists, 1-31 pp.

Nemec, W. (1992) Depositional control on plant growth and peat accumulation in a braidplain delta environment: Helvetiafjellet Formation (Barremian-Aptian), Svalbard. Geological Society of America, Boulder, Colorado,.

Nemec, W. & Kazanci, N. (1999) Quaternary colluvium in west- central Anatolia: sedimentary facies and palaeoclimatic significance. Sedimentology, 46, 139-170.

Parson, A. J. & Abrahams, A. D. (1987) Gradient-particle size relations on quartz monzonite debris slopes in the Mojave Desert. Journal of Geology, 95, 423-452.

Pierson, T. C. (1980) Erosion and deposition by debris flows at Mt Thomas, North Canterbury, New Zealand. Earth surface processes, 5, 227-247.

Postma, G. & Nemec, W. (1990) Regressive and transgressive sequences in a raised Holocene gravely beach, southwestern Crete. Sedimentology, 37, 907-920.

Rachocki, A. H. (1981) Alluvial fans: A field approach, pp. 161. John Wiley & Sons, New York.

Rapp, A. (1960) Talus slopes and mountain walls at Tempelfjorden, Spitsbergen; a geomorphological study of the denudation of slopes in an Arctic locality. Norsk Polarinstitutt Skrifter, 119.

Rapp, A. & Nyberg, B. (1981) Alpine debris flows in northern Scandinavia. Morphology and dating by lichenometry. Georafiske Annaler, 63 A (3-4), 183-196.

Rogers, N. W. & Selby, M. J. (1980) Mechanisms of shallow translational landsliding during summer rainstorms: North Island, New Zealand. Geografiske Annaler, 62A, 11-21.

Sandersen, F., Bakkehøi, S., Hesynes, E. & Lied, K. (1996) The influence of meteorological factors on the initiation of debris flows, rockfalls, rockslides and rockmass instability. Norwegian Geotechnical Institute, 585910, 21pp.

Sollid, J. L. & Sørebel, L. (1988) Utbedelsesmønsteret av løsmateriale og landformer på Svalbard- noen hovedtrekk. Norsk Geografisk Tidsskrift, 42, 265-270.

Svendsen, J. I. & Mangerud, J. (1992) Paleoclimatic inferences from glacial fluctuations on Svalbard during the last 20 000 years. Climate Dynamics, 6, 213-220.

Svendsen, J. I., Elverhøi, A. & Mangerud, J. (1996) The retreat of the Barents Sea Ice Sheet on the western Svalbard margin. Boreas, 25, 244-256.

Svendsen, J. I. & Mangerud, J. (1997) Holocene glacial and climatic variations on Spitsbergen, Svalbard. The Holocene, 7, 45-57.

Svendsen, J. I., Astakhov, V. I., Bolshiyanov, D. Y., Demidov, I., Dowdeswell, J. A., Gatuallin, V., Hjort, C., Hubberten, H. W., Larsen, E., Mangerud, J., Melles, M., Møller, P., Saarnisto, M. & Siegert, M. J. (1999) maximum extent of the Eurasian ice sheet in the Barents and Kara Sea region during the Weichselian. Boreas, 28, 234-242.

Takeuchi, Y., Kodoma, Y. & Nakabayashi, H. (1995) Characteristics of evaporation from snow and tunda surface in Spitsbergen in the snowmelt season 1993. Glaciology, 9(Proc. NIPR Symp. Polar Meteorol.), 54-65.

Tverranger, J., Astakhov, V., Mangerud, J. & Svensen, J. I. (1999) Surface form of the south-western sector of the last Kara Sea Ice Sheet. Boreas, 28, 81-91.

Wasson, R. J. (1974) Intersection point deposition on alluvial fans: An Australian example. Geografiske Annaler, 56 A, 1-2, 83-92.

Whalley, W. B. & Martin, H. E. (1992) Rock glaciers. II. models and mechanisms. Program of Physical Geography, 16, 127-186.

Whipple, K. X. & Dunne, T. (1992) The influence of Debris-flows rheology on fan morphology, Owens Valley, California. Geological society of America Bulletin, 104, 887-900.

Winther, J.-G., Bruland, O., Sand, K., Killingtveit, Å. & Marechal, D. (1998) Snow accumulation distribution on Spitsbergen, Svalbard, in 1997. Polar Research, 17(2), 155-164.

Åkerman, H. J. (1984) Notes on talus morphology and processes in Spitsbergen. Geografiske Annaler, 66 A (4), 267-284.

Appendix A

Meteorological data from Longyear Airport

WEEK 8

Date	Time	Temp. (ºC)	Temp.max (ºC)	Temp.min (ºC)	Windspeed (knot)	Wind direction (º)	Precipitation (mm)
16.02.98	00.00						
	06.00	-15		-15,3			0
	12.00						
	18.00	-12,5	-13,3				0
17.02.98	00.00						
	06.00	-10,6		-19,5			0,5
	12.00						
	18.00	-12,6	-10,0				0,1
18.02.98	00.00						
	06.00	-14,8		-15,5			0,1
	12.00						
	18.00	-17,2	-13,6				0
19.02.98	00.00						
	06.00	-21.5		-21,8			0
	12.00						
	18.00	-23,9	-20,9				0
20.02.98	00.00						
	06.00	-29,1		-29,5			0
	12.00						
	18.00	-30,6	-27,3				0
21.02.98	00.00						
	06.00	-32,5		-29,7			0
	12.00						
	18.00	-29,7	-29,3				0
22.02.98	00.00						
	06.00	-28,9		-30,3			0
	12.00						
	18.00	-28,8	-26,6				0

WEEK 9

Date	Time	Temp. (ºC)	Temp.max (ºC)	Temp.min (ºC)	Windspeed (knot)	Wind direction (º)	Precipitation (mm)
23.02.98	00.00						
	06.00	-29,8		-31,4			0
	12.00						
	18.00	-26,9	-24,8				0
24.02.98	00.00						
	06.00	-25,5		-31,4			0,4
	12.00						
	18.00	-27,9	-23,1				0
25.02.98	00.00						
	06.00	-33,5		-34,3			0
	12.00						
	18.00	-31,6	-28,8				0
26.02.98	00.00						
	06.00	-28,1		-32,8			0
	12.00						
	18.00	-16,2	-15,3				0
27.02.98	00.00						
	06.00	-19,7		-20,6			0
	12.00						
	18.00	-28,1	-18,9				0
28.02.98	00.00	-27,6			21	040	
	06.00	-28,7	-27,9	-29,9	15	100	0
	12.00	-27,0			15	030	
	18.00	-29,1	-26,3	-29,5	11	050	0
01.03.98	00.00	-30,5			1	110	
	06.00	-32,4	-28,6	-32,8	10	120	0
	12.00	-31,3			7	110	
	18.00	-30,5	-29,6	-30,5	7	110	0

WEEK 10

Date	Time	Temp. (ºC)	Temp.max (ºC)	Temp.min (ºC)	Windspeed (knot)	Wind direction (º)	Precipitation (mm)
02.03.98	00.00	-30,2			3	100	
	06.00	-29,0	-27,6	-33,5	6	110	0
	12.00	-29,8			6	100	
	18.00	-30,1	-27,8	-32,0	5	110	0
03.03.98	00.00	-29,9			4	110	
	06.00	-29,8	-27,6	-32,5	3	160	0
	12.00	-29,5			5	120	
	18.00	-30,8	-27,8	-32,3	5	100	0
04.03.98	00.00	-30,9			1	100	
	06.00	-31,7	-30,1	-33,5	4	080	0
	12.00	-28,0			0	000	
	18.00	-25,1	-23,5	-32,3	4	240	0
05.03.98	00.00	-21,6			2	090	
	06.00	-21,1	-19,5	-27,5	10	130	0
	12.00	-23,2			7	120	
	18.00	-24,0	-20,3	-24,7	6	260	0
06.03.98	00.00	-27,1			0	000	
	06.00	-24,7	-23,2	-28,0	0	000	0
	12.00	-24,3			5	250	
	18.00	-26,1	-23,0	-27,0	8	250	0
07.03.98	00.00	-26,4			2	270	
	06.00	-25,0	-24,2	-28,4	1	230	0
	12.00	-26,1			0	000	
	18.00	-24,9	-23,9	-28,6	0	000	0
08.03.98	00.00	-26,7			5	100	
	06.00	-27,1	-24,3	-30,4	2	110	
	12.00	-26,8			3	120	
	18.00	-25,1	-24,8	-28,9	0	000	

WEEK 11

Date	Time	Temp. (ºC)	Temp.max (ºC)	Temp.min (ºC)	Windspeed (knot)	Wind direction (º)	Precipitation (mm)
09.03.98	00.00	-26,1			2	120	
	06.00	-24,2	-24,0	-28,8	0	000	0
	12.00	-23,3			0	000	
	18.00	-20,3	-19,6	-27,2	1	130	0
10.03.98	00.00	-16,2			9	250	
	06.00	-18,3	-12,5	-20,5	3	250	2,0
	12.00	-24,1			3	260	
	18.00	-25,6	-18,1	-25,9	4	320	0
11.03.98	00.00	-20,3			5	250	
	06.00	-19,9	-18,1	-26,1	4	250	0,1
	12.00	-19,3			4	250	
	18.00	-7,7	-6,5	-22,0	12	130	0
12.03.98	00.00	-6,7			11	130	
	06.00	-10,2	-6,3	-10,2	19	130	0
	12.00	-8,4			25	120	
	18.00	-8,3	-7,4	-10,6	20	110	0
13.03.98	00.00	-8,8			22	130	
	06.00	-8,4	-7,5	-9,3	26	140	0,1
	12.00	-7,4			19	120	
	18.00	-6,8	-5,5	-9,0	13	150	0
14.03.98	00.00	-6,2			10	130	
	06.00	-4,4	-4,1	-9,3	17	120	0
	12.00	-3,3			15	120	
	18.00	-3,5	-2,3	-5,1	11	170	0
15.03.98	00.00	-2,4			11	200	
	06.00	-3,5	-2,3	-5,8	12	120	0
	12.00	-2,1			19	120	
	18.00	0,8	1,6	-3,8	20	140	0,1

WEEK 12

Date	Time	Temp. (ºC)	Temp.max (ºC)	Temp.min (ºC)	Windspeed (knot)	Wind direction (º)	Precipitation (mm)
16.03.98	00.00	-1,5			31	140	
	06.00	-3,2	0,8	-4,0	18	120	0,1
	12.00	-2,1			22	140	
	18.00	-2,4	-1,3	-4,4	16	130	0
17.03.98	00.00	-2,7			13	150	
	06.00	-1,5	-0,6	-5,8	24	090	0,1
	12.00	-5,9			30	220	
	18.00	-6,4	0,0	-7,1	7	190	1,0
18.03.98	00.00	-6,6			8	110	
	06.00	-4,3	-3,3	-9,3	16	120	0,2
	12.00	-1,5			21	130	
	18.00	-1,9	0,0	-4,4	19	110	0
19.03.98	00.00	-3,3			11	120	
	06.00	-5,5	-1,3	-5,8	9	100	0
	12.00	-2,9			9	110	
	18.00	-5,0	-2,4	-6,4	6	060	0
20.03.98	00.00	-7,9			3	250	
	06.00	-12,5	-3,7	-13,0	8	250	
	12.00	-9,8			3	250	
	18.00	-14,5	-9,4	-15,9	1	110	
21.03.98	00.00	-12,0			1	270	
	06.00	-11,6	-11,5	-17,9	0	000	0,2
	12.00	-13,4			4	260	
	18.00	-12,3	-10,9	-19,3	0	000	0,1
22.03.98	00.00	-5,7			21	120	
	06.00	-3,3	-2,8	-13,0	28	130	0,4
	12.00	-2,4			13	210	
	18.00	-4,0	-0,5	-4,0	13	220	2,1

WEEK 13

Date	Time	Temp. (ºC)	Temp.max (ºC)	Temp.min (ºC)	Windspeed (knot)	Wind direction (º)	Precipitation (mm)
23.03.98	00.00	-1,9			10	180	
	06.00	2,8	3,1	-4,2	14	160	0,2
	12.00	-4,9			26	250	
	18.00	-6,8	3,2	-7,0	9	270	0,5
24.03.98	00.00	-11,3			2	310	
	06.00	-6,2	-6,2	-12,0	6	270	0
	12.00	-1,9			22	140	
	18.00	-1,7	-1,0	-7,4	13	120	0
25.03.98	00.00	-2,2			22	140	
	06.00	-2,1	-0,8	-2,8	30	140	0
	12.00	-1,8			17	120	
	18.00	-2,9	-1,5	-3,7	22	130	0
26.03.98	00.00	-2,2			23	140	
	06.00	-1,3	-0,9	-3,6	16	130	0
	12.00	-1,5			13	140	
	18.00	-2,5	-1,1	-3,1	21	140	0
27.03.98	00.00	-3,4			23	130	
	06.00	-3,1	-1,9	-4,0	20	130	0
	12.00	-3,8			23	140	
	18.00	-6,5	-1,9	-6,6	25	120	0
28.03.98	00.00	-9,0			24	150	
	06.00	-10,9	-5,6	-11,5	27	140	0
	12.00	-12,2			21	130	
	18.00	-11,2	-10,2	-12,5	28	130	0
29.03.98	00.00	-15,2			35	120	
	06.00	-13,3	-11,0	-15,8	35	110	0
	12.00	-12,1			29	120	
	18.00	-12,7	-11,0	-13,7	26	120	

WEEK 14

Date	Time	Temp. (ºC)	Temp.max (ºC)	Temp.min (ºC)	Windspeed (knot)	Wind direction (º)	Precipitation (mm)
30.03.98	00.00	-13,8			18	120	
	06.00	-13,4	-12,4	-14,6	20	120	0
	12.00	-12,2			20	120	
	18.00	-12,1	-11,1	-13,7	14	140	0
31.03.98	00.00	-11,6			11	130	
	06.00	-12,3	-10,6	-13,1	12	100	0
	12.00	-10,2			3	250	
	18.00	-13,1	-8,4	-13,1	2	280	0
01.04.98	00.00	-18,1			1	340	
	06.00	-20,0	-13,0	-22,4	2	270	0
	12.00	-15,3			4	230	
	18.00	-15,4	-13,4	-20,0	8	080	0
02.04.98	00.00	-14,5			1	330	
	06.00	-13,7	-9,4	-16,2	3	260	0,6
	12.00	-2,5			13	240	
	18.00	-8,7	-2,2	-14,0	0	000	0
03.04.98	00.00	-11,6			2	020	
	06.00	-10,7	-7,2	-14,2	4	250	0
	12.00	-9,0			4	240	
	18.00	-8,3	-7,8	-10,7	4	240	0
04.04.98	00.00	-9,9			2	310	
	06.00	-13,2	-8,0	-13,4	15	330	0
	12.00	-14,8			18	330	
	18.00	-15,7	-12,5	-15,8	20	330	0
05.04.98	00.00	-17,6			6	300	
	06.00	-19,9	-15,2	-19,8	2	230	
	12.00	-18,0			10	010	
	18.00	-19,6	-17,4	-19,6	11	010	

WEEK 15

Date	Time	Temp. (ºC)	Temp.max (ºC)	Temp.min (ºC)	Windspeed (knot)	Wind direction (º)	Precipitation (mm)
06.04.98	00.00	-21,0			6	260	
	06.00	-21,1	-19,3	-22,1	2	250	0
	12.00	-19,2			7	350	
	18.00	-20,0	-18,0	-21,3	5	010	0
07.04.98	00.00	-23,7			2	160	
	06.00	-23,9	-19,9	-25,8	2	070	0
	12.00	-20,0			5	230	
	18.00	-18,6	-17,5	-25,0	3	110	0
08.04.98	00.00	-21,1			8	100	
	06.00	-19,7	-18,0	-23,2	7	110	0
	12.00	-15,0			10	020	
	18.00	-15,8	-14,4	-20,8	3	060	0
09.04.98	00.00	-18,7			2	310	
	06.00	-20,3	-15,6	-22,7	5	100	0
	12.00	-18,0			10	110	
	18.00	-15,8	-14,1	-20,7	7	070	0
10.04.98	00.00	-20,9			5	090	
	06.00	-20,2	-15,0	-23,0	3	110	0
	12.00	-16,7			2	080	
	18.00	-16,4	-15,0	-20,6	8	120	0
11.04.98	00.00	-20,6			10	110	
	06.00	-19,3	-16,4	-22,6	2	210	0
	12.00	-18,4			3	240	
	18.00	-17,7	-16,8	-20,2	1	240	0
12.04.98	00.00	-21,7			0	000	
	06.00	-21,4	-16,9	-24,1	0	000	0
	12.00	-16,7			0	000	
	18.00	-16,7	-14,8	-21,6	4	240	0

WEEK 16

Date	Time	Temp. (ºC)	Temp.max (ºC)	Temp.min (ºC)	Windspeed (knot)	Wind direction (º)	Precipitation (mm)
13.04.98	00.00	-20,6			2	110	
	06.00	-19,1	-16,5	-21,9	2	110	0
	12.00	-14,4			0	000	
	18.00	-14,6	-13,0	-19,4	1	200	0
14.04.98	00.00	-16,8			0	000	
	06.00	-18,4	-13,9	-20,3	0	000	0
	12.00	-14,0			4	250	
	18.00	-12,4	-12,4	-19,3	1	250	0
15.04.98	00.00	-14,0			2	060	
	06.00	-13,1	-10,3	-14,2	1	080	0,1
	12.00	-10,0			3	090	
	18.00	-1,8	-1,5	-13,6	4	280	0
16.04.98	00.00	-4,1			1	330	
	06.00	-7,0	-1,5	-8,1	3	250	0,1
	12.00	-6,2			2	250	
	18.00	-4,9	-2,5	-7,3	2	230	0
17.04.98	00.00	-9,4			0	000	
	06.00	-12,1	-4,6	-13,4	2	260	0
	12.00	-10,8			3	120	
	18.00	-10,9	-8,5	-14,9	1	250	0
18.04.98	00.00	-16,2			0	000	
	06.00	-15,4	-10,5	-18,1	0	000	0
	12.00	-11,0			2	270	
	18.00	-10,9	-7,9	-15,6	0	000	0
19.04.98	00.00	-15,1			1	250	
	06.00	-12,0	-10,3	-17,1	0	000	
	12.00	-11,6			4	250	
	18.00	-12,4	-9,9	-15,7	0	000	

WEEK 17

Date	Time	Temp. (ºC)	Temp.max (ºC)	Temp.min (ºC)	Windspeed (knot)	Wind direction (º)	Precipitation (mm)
20.04.98	00.00	-16,7			0	000	
	06.00	-14,1	-12,0	-18,8	0	000	0
	12.00	-11,9			1	280	
	18.00	-11,8	-9,0	-16,4	0	000	0
21.04.98	00.00	-17,2			0	000	
	06.00	-14,9	-10,8	-18,2	4	110	0
	12.00	-11,2			0	000	
	18.00	-8,9	-8,7	-15,3	0	000	0
22.04.98	00.00	-9,2			1	060	
	06.00	-8,6	-8,1	-9,4	2	280	0
	12.00	-5,5			6	230	
	18.00	-5,2	-4,6	-8,7	13	240	0
23.04.98	00.00	-6,3			8	240	
	06.00	-6,5	-5,2	-7,5	1	100	0,1
	12.00	-1,0			9	260	
	18.00	0,0	0,1	-6,9	16	220	0
24.04.98	00.00	-1,1			14	250	
	06.00	-1,8	0,1	-1,9	11	240	0,2
	12.00	-4,1			8	020	
	18.00	-4,6	-1,8	-4,8	2	060	0
25.04.98	00.00	-7,3			6	240	
	06.00	-5,5	-4,0	-9,2	1	310	0
	12.00	-5,1			4	260	
	18.00	-7,1	-5,0	-7,3	3	270	0
26.04.98	00.00	-10,7			2	240	
	06.00	-10,5	-6,9	-12,4	7	250	0
	12.00	-9,6			3	280	
	18.00	-11,0	-7,9	-11,2	4	210	0

WEEK 18

Date	Time	Temp. (ºC)	Temp.max (ºC)	Temp.min (ºC)	Windspeed (knot)	Wind direction (º)	Precipitation (mm)
27.04.98	00.00	-12,7			12	110	
	06.00	-12,8	-10,6	-14,5	5	240	0
	12.00	-10,2			5	250	
	18.00	-9,1	-8,7	-13,8	6	250	0
28.04.98	00.00	-10,7			1	260	
	06.00	-10,1	-8,7	-12,6	3	240	0
	12.00	-9,6			5	260	
	18.00	-9,0	-7,8	-10,1	4	250	0
29.04.98	00.00	-13,6			3	260	
	06.00	-11,2	-8,6	-14,7	5	250	0
	12.00	-4,6			12	140	
	18.00	-4,3	-3,7	-12,9	16	130	0
30.04.98	00.00	-5,0			16	120	
	06.00	-4,2	-4,2	-5,5	17	140	0
	12.00	-3,9			9	110	
	18.00	-4,9	-3,3	-5,2	8	110	0
01.05.98	00.00	-8,8			0	000	
	06.00	-7,2	-4,7	-10,5	1	010	0
	12.00	-5,8			2	240	
	18.00	-6,6	-5,2	-7,6	2	280	0
02.05.98	00.00	-10,0			1	010	
	06.00	-9,1	-6,4	-10,4	0	000	0
	12.00	-6,8			2	240	
	18.00	-5,2	-4,3	-9,1	2	240	0
03.05.98	00.00	-5,3			6	170	
	06.00	-4,7	-3,5	-6,4	4	110	0,2
	12.00	-1,5			12	110	
	18.00	-1,1	-0,9	-4,7	8	170	0,1

WEEK 19

Date	Time	Temp. (ºC)	Temp.max (ºC)	Temp.min (ºC)	Windspeed (knot)	Wind direction (º)	Precipitation (mm)
04.05.98	00.00	-2,8			13	110	
	06.00	-2,7	-0,5	-3,0	11	120	0,1
	12.00	-2,2			11	100	
	18.00	-4,2	-1,8	-4,4	16	020	0
05.05.98	00.00	-7,4			11	030	
	06.00	-7,2	-3,6	-8,4	14	040	0
	12.00	-6,3			10	040	
	18.00	-6,4	-5,8	-7,3	13	030	0
06.05.98	00.00	-9,4			7	040	
	06.00	-9,1	-6,4	-10,9	5	050	0
	12.00	-8,3			3	250	
	18.00	-8,0	-6,5	-9,2	5	250	0
07.05.98	00.00	-11,4			4	240	
	06.00	-9,3	-7,7	-13,7	1	350	0
	12.00	-9,8			2	280	
	18.00	-8,8	-7,5	-11,7	3	280	0
08.05.98	00.00	-11,0			5	230	
	06.00	-8,6	-7,1	-12,3	7	120	0
	12.00	-6,4			6	360	
	18.00	-5,9	-4,7	-8,8	2	040	0,2
09.05.98	00.00	-2,6			11	210	
	06.00	-3,2	-1,2	-6,1	11	260	0,1
	12.00	-4,4			3	300	
	18.00	-4,8	-2,6	-5,2	11	240	0
10.05.98	00.00	-9,8			4	340	
	06.00	-7,6	-4,4	-10,2	4	260	0
	12.00	-7,3			7	240	
	18.00	-7,1	-6,6	-8,4	2	300	0

WEEK 20

Date	Time	Temp. (ºC)	Temp.max (ºC)	Temp.min (ºC)	Windspeed (knot)	Wind direction (º)	Precipitation (mm)
11.05.98	00.00	-8,8			5	130	
	06.00	-8,4	-6,9	-9,1	4	010	0,2
	12.00	-8,5			4	340	
	18.00	-8,5	-6,9	-9,3	5	240	0
12.05.98	00.00	-10,3			9	250	
	06.00	-11,1	-8,0	-12,3	7	250	0
	12.00	-9,8			3	250	
	18.00	-9,7	-8,4	-11,5	3	310	0
13.05.98	00.00	-12,1			4	290	
	06.00	-12,2	-9,4	-14,3	1	270	0
	12.00	-7,8			10	100	
	18.00	-8,6	-6,1	-12,3	6	260	0,9
14.05.98	00.00	-6,3			4	260	
	06.00	-5,9	-5,3	-9,4	3	250	0,2
	12.00	-5,3			8	120	
	18.00	-6,0	-5,1	-6,1	7	130	0
15.05.98	00.00	-4,3			6	250	
	06.00	-3,5	-3,1	-6,0	18	130	0
	12.00	-1,4			14	130	
	18.00	-0,7	0,4	-4,2	4	250	0,2
16.05.98	00.00	-0,1			7	240	
	06.00	1,9	2,3	-1,0	13	230	0,4
	12.00	0,0			13	250	
	18.00	-1,7	2,1	-1,7	8	260	2,1
17.05.98	00.00	-2,4			7	230	
	06.00	-4,6	-1,0	-4,8	6	300	0
	12.00	-6,3			11	290	
	18.00	-6,4	-4,4	-6,9	17	250	0,3

WEEK 21

Date	Time	Temp. (°C)	Temp.max (°C)	Temp.min (°C)	Windspeed (knot)	Wind direction (°)	Precipitation (mm)
18.05.98	00.00	-6,9			12	250	
	06.00	-7,0	-6,3	-7,6	12	240	0
	12.00	-6,7			4	280	
	18.00	-5,7	-5,5	-7,3	6	250	0
19.05.98	00.00	-8,0			1	220	
	06.00	-8,2	-5,2	-9,2	3	250	0
	12.00	-5,2			8	250	
	18.00	-5,6	-4,3	-8,8	6	250	0
20.05.98	00.00	-7,8			9	020	
	06.00	-7,8	-5,2	-10,1	4	260	0
	12.00	-5,1			5	270	
	18.00	-5,4	-3,8	-7,9	6	340	0
21.05.98	00.00	-9,0			7	010	
	06.00	-7,6	-4,6	-9,9	9	250	0
	12.00	-6,2			11	290	
	18.00	-5,8	-5,2	-8,0	5	240	0
22.05.98	00.00	-5,9			7	240	
	06.00	-5,0	-3,8	-6,7	6	250	0
	12.00	-5,1			5	250	
	18.00	-4,7	-4,3	-5,8	5	240	0
23.05.98	00.00	-8,0			4	250	
	06.00	-6,5	-3,9	-9,4	9	220	0
	12.00	-5,0			13	240	
	18.00	-5,3	-4,4	-6,6	10	220	0
24.05.98	00.00	-5,4			4	260	
	06.00	-5,5	-4,9	-5,7	5	280	0
	12.00	-3,8			8	240	
	18.00	-3,4	-2,7	-5,6	8	240	0

WEEK 22

Date	Time	Temp. (ºC)	Temp.max (ºC)	Temp.min (ºC)	Windspeed (knot)	Wind direction (º)	Precipitation (mm)
25.05.98	00.00	-4,1			3	290	
	06.00	-4,5	-3,0	-4,5	2	300	
	12.00	-3,3			1	320	
	18.00	-2,6	-2,2	-2,6	4	030	
26.05.98	00.00	-3,9			2	300	
	06.00	-0,6	-0,4	-0,6	5	140	
	12.00	-0,8			3	250	
	18.00	-0,0	1,6	-0,0	4	140	
27.05.98	00.00	-2,3			12	120	
	06.00	-2,1	0,2	-2,1	10	110	
	12.00	-1,0			3	280	
	18.00	-2,2	0,6	-2,2	9	110	
28.05.98	00.00	-2,7			6	120	
	06.00	-2,4	-1,9	-2,1	2	270	
	12.00	-0,9			2	020	
	18.00	-0,3	-0,4	-0,3	6	250	
29.05.98	00.00	-1,9			1	320	
	06.00	-2,1	-0,1	-2,1	6	110	
	12.00	-1,9			10	120	
	18.00	-2,1	-1,3	-2,1	5	130	
30.05.98	00.00	-3,2			0	000	
	06.00	-4,8	-1,9	-4,8	3	360	
	12.00	-2,5			5	270	
	18.00	-0,6	-0,4	-0,6	12	240	
31.05.98	00.00	-2,6			5	250	
	06.00	-2,7	-0,3	-2,7	2	240	
	12.00	-1,1			3	250	
	18.00	-0,6	-0,2	-0,6	9	250	

WEEK 23

Date	Time	Temp. (ºC)	Temp.max (ºC)	Temp.min (ºC)	Windspeed (knot)	Wind direction (º)	Precipitation (mm)
01.06.98	00.00	-0,3			13	240	
	06.00	0,3	0,9	-1,2	13	250	0
	12.00	-0,8			6	260	
	18.00	0,2	1,5	-1,4	3	280	0
02.06.98	00.00	-0,4			6	260	
	06.00	-0,8	0,7	-3,3	4	250	0
	12.00	0,7			3	240	
	18.00	1,0	1,9	-0,9	4	260	0
03.06.98	00.00	0,4			5	250	
	06.00	-0,1	1,4	-0,4	4	010	0
	12.00	0,3			6	260	
	18.00	0,2	1,1	-0,5	1	280	0
04.06.98	00.00	1,0			4	260	
	06.00	0,0	1,6	-0,7	3	280	0
	12.00	0,8			3	220	
	18.00	0,0	1,8	-0,3	3	280	0
05.06.98	00.00	-0,7			1	240	
	06.00	-0,3	0,2	-1,2	4	280	0
	12.00	0,7			4	290	
	18.00	1,8	2,1	-0,6	8	250	0
06.06.98	00.00	0,6			9	240	
	06.00	0,1	2,7	0,0	7	250	0
	12.00	1,6			8	250	
	18.00	0,7	3,2	0,0	3	280	0
07.06.98	00.00	1,0			4	060	
	06.00	2,7	3,5	-1,2	6	260	0
	12.00	2,3			8	250	
	18.00	2,3	4,1	1,3	6	250	0

WEEK 24

Date	Time	Temp. (ºC)	Temp.max (ºC)	Temp.min (ºC)	Windspeed (knot)	Wind direction (º)	Precipitation (mm)
08.06.98	00.00	0,9			5	260	
	06.00	0,7	2,4	0,1	5	250	0,2
	12.00	1,6			2	050	
	18.00	1,8	2,9	0,6	4	310	0,1
09.06.98	00.00	0,8			2	060	
	06.00	0,6	1,8	-0,2	5	260	0
	12.00	2,9			5	260	
	18.00	2,5	3,6	0,5	3	080	0
10.06.98	00.00	2,3			7	020	
	06.00	1,5	3,5	0,6	1	120	0
	12.00	3,8			8	250	
	18.00	4,7	5,1	1,2	13	250	0
11.06.98	00.00	2,0			18	250	
	06.00	0,9	5,0	0,7	13	240	0
	12.00	3,2			14	250	
	18.00	2,3	3,8	0,6	14	240	0
12.06.98	00.00	1,2			12	240	
	06.00	1,8	2,8	0,9	13	240	0
	12.00	0,8			7	260	
	18.00	0,5	3,2	0,0	2	050	1,2
13.06.98	00.00	0,9			0	000	
	06.00	0,8	1,3	0,0	1	350	0
	12.00	1,0			4	280	
	18.00	2,1	2,3	0,6	10	260	0,8
14.06.98	00.00	1,1			8	240	
	06.00	0,2	2,4	0,1	11	250	0
	12.00	2,1			12	240	
	18.00	2,1	3,1	0,1	10	250	0

WEEK 25

Date	Time	Temp. (ºC)	Temp.max (ºC)	Temp.min (ºC)	Windspeed (knot)	Wind direction (º)	Precipitation (mm)
15.06.98	00.00	1,1			10	230	
	06.00	0,3	2,3	-0,7	6	270	0,1
	12.00	1,9			14	240	
	18.00	1,1	3,1	-0,0	17	240	0
16.06.98	00.00	1,0			19	230	
	06.00	1,9	1,9	0,3	15	230	0,1
	12.00	1,3			19	240	
	18.00	2,2	2,7	0,8	17	230	0,1
17.06.98	00.00	1,9			15	220	
	06.00	1,3	2,8	0,8	18	240	0,1
	12.00	2,0			12	240	
	18.00	1,7	3,3	1,1	10	260	0
18.06.98	00.00	0,3			5	260	
	06.00	1,6	2,7	0,2	6	250	0
	12.00	2,6			4	260	
	18.00	2,7	3,4	1,4	8	250	0
19.06.98	00.00	2,6			10	240	
	06.00	2,3	3,1	1,5	10	250	0
	12.00	2,1			13	250	
	18.00	2,5	3,5	1,6	12	240	0
20.06.98	00.00	0,8			9	240	
	06.00	0,6	2,9	-0,0	10	240	0
	12.00	1,8			9	260	
	18.00	2,6	3,2	0,6	9	250	0
21.06.98	00.00	2,6			7	250	
	06.00	2,6	3,1	2,1	5	280	0
	12.00	2,7			3	290	
	18.00	2,9	3,8	2,1	2	350	0

WEEK 26

Date	Time	Temp. (ºC)	Temp.max (ºC)	Temp.min (ºC)	Windspeed (knot)	Wind direction (º)	Precipitation (mm)
22.06.98	00.00	2,5			2	320	
	06.00	1,9	3,2	1,8	1	270	
	12.00	4,4			5	360	
	18.00	5,1	6,1	1,5	5	260	
23.06.98	00.00	2,4			12	110	
	06.00	4,3	5,9	1,9	7	100	
	12.00	5,4			9	250	
	18.00	5,2	3,3	6,9	6	270	
24.06.98	00.00	3,1			3	320	
	06.00	4,7	5,7	2,2	10	260	
	12.00	5,6			10	260	
	18.00	6,2	7,0	4,1	5	260	
25.06.98	00.00	5,4			2	330	
	06.00	7,4	8,5	4,0	5	260	
	12.00	6,9			6	280	
	18.00	8,6	5,2	9,1	4	260	
26.06.98	00.00	9,6			3	260	
	06.00	9,0	11,4	6,3	5	280	
	12.00	8,3			6	260	
	18.00	6,8	9,0	6,3	5	280	
27.06.98	00.00	6,0			1	290	
	06.00	6,9	7,1	5,8	4	270	
	12.00	9,0			11	260	
	18.00	8,3	9,8	6,6	5	290	
28.06.98	00.00	7,8			4	060	
	06.00	6,9	8,9	6,8	11	250	
	12.00	8,0			14	250	
	18.00	8,5	6,7	9,5	11	250	

Appendix B

Weather-maps over Spitsbergen

Weather-maps showing 6 typical examples of the dominating weather systems, with strong winds bringing in precipitation from east over Spitsbergen, from late February to mid April 1999 (provided by Vervarslinga på Vestlandet). Note the weather station at central Spitsbergen showing wind direction from east and force from 15-25 knots from low-pressures moving from the Norwegian Sea and northwards into the Barents Sea on all examples.

Legend:

Friday 26.02.99 09Z

Spitsbergen

Monday 15.03.99 00Z

Spitsbergen

Monday 22.03.99 12Z

Spitsbergen

Wednesday 31.03.99 09Z

Spitsbergen

Saturday 17.04.99 00Z

Spitsbergen

Saturday 17.04.99 06Z

Spitsbergen